AD-A232 695

:UMENTATION PAGE

Form Approved
OMB No. 0704-0188

1a. REPORT SECURITY CLASSIFICATION
Unclassified

1b. RESTRICTIVE MARKINGS

2a. SECURITY CLASSIFICATION AUTHORITY
Unclassified

3. DISTRIBUTION/AVAILABILITY OF REPORT
Unlimited

2b. DECLASSIFICATION/DOWNGRADING SCHEDULE

4. PERFORMING ORGANIZATION REPORT NUMBER(S)
10

5. MONITORING ORGANIZATION REPORT NUMBER(S)
AFOSR-TR- 91 0151

6a. NAME OF PERFORMING ORGANIZATION
California Institute of Technology
Pasadena, CA 91125

6b. OFFICE SYMBOL (If applicable)

7a. NAME OF MONITORING ORGANIZATION
Air Force Office of Scientific Research

6c. ADDRESS (City, State, and ZIP Code)
MS 128-95
Pasadena, CA 91125

7b. ADDRESS (City, State, and ZIP Code)
Building 410
Bolling AFB, DC 20332=6448

8a. NAME OF FUNDING/SPONSORING ORGANIZATION
AFOSR

8b. OFFICE SYMBOL (If applicable)
NE

9. PROCUREMENT INSTRUMENT IDENTIFICATION NUMBER
AFOSR-86-0306

8c. ADDRESS (City, State, and ZIP Code)
Building 410
Bolling AFB, DC 20322-6448

10. SOURCE OF FUNDING NUMBERS

PROGRAM ELEMENT NO.	PROJECT NO.	TASK NO	WORK UNIT ACCESSION NO.
61102F	2305	B1	

11. TITLE (Include Security Classification)
In BASED III-V MICROSTRUCTURES WITH NOVEL ELECTRONIC PROPERTIES (UNCLASSIFIED)

12. PERSONAL AUTHOR(S)
McGill, T. C. Jr.

13a. TYPE OF REPORT	13b. TIME COVERED	14. DATE OF REPORT (Year, Month, Day)	15. PAGE COUNT
Final	FROM 9/15/86 TO 2/14/90	10/30/90	

16. SUPPLEMENTARY NOTATION

17. COSATI CODES			18. SUBJECT TERMS (Continue on reverse if necessary and identify by block number)
FIELD	GROUP	SUB-GROUP	Microstructures, Tunnel Devices, Indium and Antimony based Molecular Beam Epitaxy (MBE)

19. ABSTRACT (Continue on reverse if necessary and identify by block number)

This program addresses the development of microstructures for high density and high speed electronics. The molecular beam epitaxy technology for InAs and GaSb were developed for growth in GaAs substrates. Three new single barrier negative resistance devices were demonstrated. Double barrier negative resistance devices based on InAs/AlSb/InAs/AlSb/InAs heterostructures were fabricated. These currently hold all the power and frequency records.

20. DISTRIBUTION/AVAILABILITY OF ABSTRACT
☒ UNCLASSIFIED/UNLIMITED ☐ SAME AS RPT. ☐ DTIC USERS

21. ABSTRACT SECURITY CLASSIFICATION
UNCLASSIFIED

22a. NAME OF RESPONSIBLE INDIVIDUAL
Major Gernot S. Pomrenke, Ph.D.

22b. TELEPHONE (Include Area Code)
202/767-4931

22c. OFFICE SYMBOL
NE

DD Form 1473, JUN 86 Previous editions are obsolete.

SECURITY CLASSIFICATION OF THIS PAGE

FINAL REPORT ON AFOSR GRANT NO. 86-0306

In BASED III-V MICROSTRUCTURES WITH NOVEL ELECTRONIC PROPERTIES

By T. C. McGill

T. J. Watson Laboratory of Applied Physics

California Institute of Technology

Pasadena, California 91125

(818) 356-4849

I. INTRODUCTION

This research grant was aimed at exploring some new possibilities for electronic devices based on indium and later on antimony. Recently it has been widely recognized that the future digital and high speed electronic systems will have to exploit device technologies which are substantially different from the current transistor technologies. It is widely held that in the mid to early parts of the next decade the strategy of continuing to shrink current transistor technologies to ever smaller dimensions will fail. At this point new device concepts will have to take over to allow a continuation of the electronics revolution that we have become addicted to.

In the military, it is particularly important to have high frequency solid state sources. Some of the device concepts explored under this program have led to the world's records in high frequency, high power solid state sources.

The effort encompassed by this program included the development of an indium and antimony MBE technology, the exploration of single barrier tunnel devices, and the exploration and development of double barrier tunnel devices in a material system which is now widely acclaimed as the optimum for such structures. As with all research programs in universities, one of the major outputs of the activity has been the training of students. Each of these topics is covered in sections of the rest of this report.

II. MAJOR RESULTS

A. Materials Development Program

As with all device technology programs, they are only as good as the materials program that underlies them. When we started our In and Sb program there was little information on MBE growth of In and Sb based structures. While GaAs/AlAs MBE had arrived at a high level of sophistication, little effort had been aimed at developing a materials growth technology that would be appropriate for In and Sb. The first part of this program was aimed at developing such a technology. Notably, we expended a great deal of effort in attempting to learn to grow In and Sb based systems on substrates other an InAs and GaAs. A substrate technology was developed in which the widely available GaAs substrates were used as a basis on which a superlattice of InAs/GaAs or GaSb/GaAse was grown. On this structure a thick layer of either GaAs or InAs was then grown to provide high quality material for the fabrication and devices on a relatively inexpensive and widely available substrate. Some of the results of these activities are reported in the paper in Appendix A-1.

B. Single Barrier Tunnel Devices

The work to date when we started this program had been on so-called double barrier resonant tunneling devices. In these device structures, the negative resistance phenomena is produced by moving the electron distribution from the contact through the resonance produced in the well between the double barriers. This device approach has a number of disadvantages: notably the need for careful control of the well width and possible frequency limitations due to the lifetime of the electrons in the resonance in the well. Our group at Caltech invented a new tunnel device based on a single barrier. For particular values of the band offsets, it was predicted that negative resistance could be obtained from a single barrier. The advantages of such device structures are that the negative resistance is not controlled by a quantum well thickness and the lack of a resonance should increase the frequency of operation. Under this program this device concept was demonstrated in two material systems. The first was single barrier structures based on HgTe/CdTe/HgTe device structures. In Appendix A-2, we have included the paper reporting this first observation of the negative resistance.

Efforts in our own laboratory resulted in the fabrication of a III-V based single barrier negative resistance device. In the paper included in Appendix A-3, we report the observation of negative resistance in single barrier tunnel devices based on InAs/GaAlSb/InAs single barrier tunnel devices. At the present time we hold the record for peak to valley current ratios in these structures.

Finally, in the area of single barrier tunnel structures, we reported the first observation of single barrier tunneling in a structure based on tunneling

from the conduction band of InAs through the valence band of GaSb. This novel tunnel device works on a quite different principle than that for the other two single barrier structures since its negative resistance is produced by tunneling through a resonance produced in the GaSb valence band due to the discontinuities in the band structure at the InAs/GaSb interface. This device structure has the potential of producing much higher peak currents than that observed in the single barrier negative resistance devices discussed above. The results of this work are included in the paper attached in Appendix A-4.

C. Indium and Antimony Based Double Barrier Negative Resistance Devices

The traditional system of choice for double barrier negative resistance devices has been GaAs/AlAs. While some investigators have improved the performance of the standard device structure by the addition of In, our work has pioneered the way to what is now widely regarded as the optimum system for making double barrier negative resistance devices. Notably, InAs is the material of choice for the two cladding layers. Indium arsenide has a high electron mobility and easily makes a high quality ohmic contract for electrons. When used in the cladding layer InAs can lead to extremely small series resistance between the outside world and the negative resistance device. Aluminum antimonide is a lattice match material with InAs. Further, it has the property that the barrier for electrons is quite high and pecularities of the band structure lead to the potential for small leakage currents. In our laboratory we fabricated the first InAs/AlSbInAs/AlSbInAs double barrier structures. These structures indicated the largest peak to valley ratios observed with very high peak current densities. The basic work

on these systems is included in the papers attached in Appendix A-4 and A-5. Subsequent work on samples fabricated under this program were investigated at Lincoln Laboratories for their high frequency capabilities. At the present time these device structures hold the world's records for power and frequency. Power levels as high as 90 W/cm^2 at 360GHz and frequencies as high as 712 GHz have been measured. Projections indicate that these device structures are capable of oscillating at 1.4 THz.

D. Students

One of the major results of any funding of university research programs is the training of graduate students. With the funding provided by this program a number of graduate students were trained, notably David H. Chow and J. R. Soderstrom. These two students are now leading MBE device authorities. David Chow is leading the effort at Hughes Research Laboratories and exploring antinimides for infrared superlattices. Jan Soderstrom is continuing his academic studies at Chalmers University where he has transported the antinimide based technology developed at Caltech. Also supported under this program were Michael K. Jackson, who has received his Ph.D. and is currently a research fellow at the Ecole Polytechnique in France. Two other students supported by the Air Force during this time were Mark Phillips and Todd Rossi.

III. SUMMARY

This research program was very successful in its objectives to explore indium and later antimony based III-V's for novel electronic device phenomena. This program successfully developed a materials technology

and produced a number of device structures which potentially might find applications in digital as well as high frequency applications.

Apendix A-1. MBE Growth of InAs/GaSb Epitaxial Layers and GaAs Substrates. J. R. Soderstrom, D. H. Chow and T. C. McGill.

MBE-GROWTH OF InAs AND GaSb EPITAXIAL LAYERS ON GaAs SUBSTRATES

J. R. Söderström*, D.H. Chow and T.C. McGill
T.J. Watson, Sr., Laboratory of Applied Physics, California Institute of Technology, Pasadena, CA 91125
* On leave from: Chalmers University of Technology, Phys. Dept., S-412 96 Göteborg, Sweden

ABSTRACT

We have grown a number of InAs and GaSb bulk layers on GaAs substrates and studied the properties of the semiconductor films as a function of the various growth parameters. Preliminary results from GaSb growth are presented in addition to an extensive study of InAs growth. The films were characterized during growth by RHEED. RHEED-oscillations were observed during both InAs and GaSb growths. Hall effect measurements yielded peak electron mobilities for InAs of 18,900 cm^2/Vs at 300 K and 35,000 cm^2/Vs at 77 K. For GaSb the as grown layers were found to be p-type with a carrier concentration of $9x10^{15}cm^{-3}$ and a hole mobility of 910 cm^2/Vs at 300 K.

INTRODUCTION

The nearly lattice matched semiconductor materials InAs, GaSb and AlSb are promising candidates for several interesting heterostructures. Many of the devices that have been made in the GaAs/AlAs system also can be made with these materials, perhaps with even better performance. For example InAs/AlSb/InAs/AlSb/InAs double barrier tunnel devices are expected to have higher peak-to-valley current ratios and smaller series resistance[1,2]. Furthermore, InAs/AlGaSb heterostructures can be used for novel devices such as single barrier tunnel structures[3] and infrared superlattice detectors[4]. Thus the growths of high quality epitaxial InAs and GaSb films are important material problems.

Molecular beam epitaxy (MBE) is a promising method for InAs-growth and has been used in most previous studies[5-9]. Since InAs substrates are expensive and of relatively poor quality (high impurity concentration and dislocation densities) GaAs is preferred as substrate material. The lattice mismatch between the two materials (7.2%) makes epitaxy complicated since dislocations develop after the first few monolayers have been grown. To be able to grow material with bulk-like properties (μ=35000 cm^2/Vs at 300 K) it is important to find a way of preventing these dislocations from penetrating all the way through the epitaxial film. An InGaAs/GaAs superlattice in the GaAs(bulk)/InAs(bulk) interface has proven important for high quality films[5]. In this study we have grown several InAs films on GaAs substrates with one or two superlattices at the interface. Substrate temperatures and growth rates were varied and the samples were investigated with Hall measurements at 293 K and 77 K. RHEED patterns were studied and RHEED oscillations were observed. X-ray measurements for checking the crystal quality were made on one of the samples.

The MBE growth of GaSb on GaAs has similarities to the InAs growth (7.8 % lattice mismatch)[11,12]. As in the case of InAs growth a superlattice at the GaAs(bulk)/GaSb(bulk) interface should help to reduce the number of dislocations. We expect the interfaces to be less abrupt since under growth conditions there is an excess anion flux and the switch from As to Sb cannot occur instantaneously. Thus, a short period GaAs/GaSb superlattice at the interface is difficult to achieve. The InGaAs/GaAs superlattice (the same as for InAs growth), on the other hand, would serve the same purpose and is easier to grow since only the group III fluxes are changed. The GaSb samples were investigated with Hall measurements at 300 K. During growth the RHEED pattern was studied to find the optimum substrate temperature and Sb/Ga ratio. We also observed RHEED oscillations during the GaSb growth (the first reported).

In the next section we provide the details of the procedures used in growth. The results of characterizations of the grown films are presented in the following section. Finally we present our major conclusions in the last section.

EXPERIMENTAL METHOD

The InAs and GaSb samples were grown in a Perkin-Elmer 430 MBE system. Substrate

temperatures were measured both with a thermocouple touching the back of the molybdenum block and a pyrometer. The temperature readings were calibrated against the desorption temperature of the native oxide of GaAs (590-600°C). The oxide desorption was observed by studying the RHEED pattern. We estimate the accuracy of our temperature measurements to ±10°C. Unlike most previous studies[6-9,11,12] we used an As-cracker and an Sb-cracker for evaporating the group V materials. This results in As_2 and Sb_2 dimers instead of the As_4 and Sb_4 tetramers that evaporate from elemental sources.

All samples consisted of a 5000 Å GaAs buffer layer, an InGaAs/GaAs superlattice interface layer and a thick InAs or GaSb layer. The GaAs buffer layer was grown at 600°C. During a five minute interrupt after this layer, the substrate temperature was lowered to 525°C, which was the temperature during the superlattice growth. After this the temperature was ramped to 545°C for GaSb growth and to the values listed in table I for the InAs growth.

In the InAs case, a 2 µm thick film was grown on top of the interface layer. Two different interface layers were used. Samples #118 to #122 had a five period $In_{0.7}Ga_{0.3}As$/GaAs (2 ML/2 ML) superlattice interface layer. Samples #123, #126 and #132 had the same superlattice plus an additional five period InAs/$In_{0.7}Ga_{0.3}As$ (100 Å/ 6 Å) superlattice grown directly after the first. Table I lists the growth parameters used for the InAs layers. The two different interface structures are labelled with "1 SL" or "2 SL", indicating whether one or two superlattices were used. Beam fluxes were kept the same for all samples except for sample #122 which was grown at a lower growth rate and had half the In-flux compared to the other samples. The actual As/In ratio is difficult to estimate as the measured fluxes depend on growth chamber geometries. However, for GaAs we were able to calibrate the fluxes to the relatively well known[12] transition between the Arsenic (2x4) and the Gallium (4x2) stabilized surface reconstruction. By comparing the InAs and GaAs growth rates we estimate our As_2/In ratio to be in the range 10 to 20 (sample #122 twice as much).

Two GaSb films were grown on the same type of superlattice interface layer as used for some of the InAs samples (i.e. a five period $In_{0.7}Ga_{0.3}As$/GaAs , 2 ML/2 ML) to accommodate the strain in the interface. The superlattice was again grown at a substrate temperature of 525°C. The first 500 Å of GaSb growth was also grown at this temperature after which the temperature was raised to 545°C. However, sample #155 was used for RHEED-oscillation experiments and the substrate temperature was for a short time ramped down to 450°C and then back to 545°C again, as will be discussed later. The growth rate was 0.6 µm/h and the GaSb film thickness for the two samples #155 and #159 were 1.5 µm and 0.8 µm, respectively.

The RHEED-pattern was monitored for all samples using a RHEED gun working at 8 kV high voltage and 1 mA emission current. RHEED oscillations were measured for both InAs and GaSb using a home-built setup. Hall measurements were performed at 300 K and 77 K using the conventional Van der Pauw technique with samples grown on semi-insulating GaAs substrates.

Table I

The result of the Hall measurements at 300 K and 77 K listed together with the growth parameters used for each sample. The notation for interface structure is explained in the text. The surface reconstructions (2x4) and (4x2) corresponds to arsenic and indium stabilized surfaces respectively. The notation "transition" indicates that the sample was grown in the transition region between arsenic and indium stabilized growth.

					300 K		77 K	
Sample #	Substrate temp. (°C)	Interface structure	Surface reconstr.	Growth rate (µm/h)	μ_h (cm^2/Vs)	electron conc. (10^{16} cm^{-3})	μ_h (cm^2/Vs)	electron conc. (10^{16} cm^{-3})
118	525-530	1 SL	2x4	1.0	16600	4.5	28200	4.1
119	525-530	1 SL	2x4	1.0	18900	3.8	23000	3.4
120	490-495	1 SL	2x4	1.0	13400	4.6	14500	4.2
121	540-550	1 SL	4x2	1.0	13300	1.1	35500	0.6
122	525-530	1 SL	2x4	0.5	15300	3.4	22900	2.7
123	525-530	2 SL	2x4	1.0	15400	3.0	24200	2.2
126	530-535	2 SL	Transition	1.0	13900	1.7	23600	1.0
132	535-540	2 SL	4x2	1.0	12000	1.6	35100	0.9

RESULTS AND DISCUSSION

InAs Mobilities

The results of the Hall measurements are presented in Table I. The highest mobilities at 300 K (18900 cm^2/Vs) and 77 K (35500 cm^2/Vs) were obtained for samples #119 and #121, respectively. Samples #118 and #119 were grown under identical conditions but gave somewhat different results. Sample #118 was the first sample grown after the system had been baked and therefore had a higher background doping. The interface structure that seems to give the best result is the single superlattice structure ("1 SL") as can be seen by comparing the results of samples #119 and #123, which were grown under identical conditions except for the interface structure. The additional long-period superlattice in #123 decreases the mobility indicating a degradation of crystal quality.

The substrate temperature and the surface reconstruction have a significant influence on the mobilities and carrier concentrations.We observe that samples grown under As-stabilized conditions (i.e. substrate temp.<530°C) have a higher room temperature mobility than samples grown under otherwise similar conditions but with a In-stabilized surface (compare for example sample #119 with #121 and sample #123 with #132). We suspect the difference to be due to the larger number of dislocations in the latter case. On the other hand In-stabilized growths have a higher mobility at 77 K, where impurity scattering becomes dominant. We attribute this effect to a lower background doping level. Sample #120 was grown at As-stabilized conditions but at a lower substrate temperature resulting in a fairly high background doping and a lower room temperature mobility than sample #119. Sample #122 was grown at a lower growth rate and consequently higher As/In ratio. This sample had a lower mobility than #119 even though the background doping level was lower. This suggests that the excess arsenic results in electrically inactive impurities that decreases the mobility.

All samples grown at As-stabilized conditions had smooth mirror-like surfaces with morphology as seen under optical microscope almost as good as GaAs epitaxial layers. Samples grown under In-stabilized conditions had a rough, hazy surface. These results are contradictory to most previous reports[13,14] in which As_4 tetramers were used, and in agreement with Kalan et al.[5] who also used As_2. The use of As_2 dimers appears to markedly change the optimum growth conditions. The possibility to grow high quality crystals under As-rich conditions makes it easier to reproduce the results since high quality crystals can be grown in a much larger substrate temperature interval than in the case of In-rich growth.

InAs RHEED-patterns and -oscillations

Figure 1 displays the RHEED-pattern along the [110] azimuth during the growth of sample #132. Figure 1a shows the pattern prior to the superlattice growth recognized as the well known GaAs 2-fold pattern. In figure 1b the short period superlattice has been grown (5 periods $In_{0.7}Ga_{0.3}As$/GaAs 2ML/2ML) plus two monolayers of pure InAs. The pattern is somewhat spotty indicating that the growth is not purely two-dimensional, with flat islands of InGaAs beginning to appear. Still this pattern is much better than that obtained when InAs is grown directly on GaAs[9]. It is also interesting to note that even though the pattern is a bit spotty it is still 2-fold so that our surface reconstruction is the same throughout the growth. After 1500 Å of InAs-growth the pattern looks as in figure 1c which is a nice streaky 2-fold pattern.

After 5000 Å of InAs-growth the growth was interrupted for about a minute and then restarted while monitoring intensity oscillations in the RHEED pattern. The result of this experiment is shown in figure 2, where a large number (~20) of RHEED-oscillations can be seen.

InAs X-ray diffraction

Sample #123 was investigated with X-ray crystal diffraction. The InAs layer gave a peak at $2\Theta=29.3°\pm0.2°$ corresponding to a lattice constant of 6.08 Å ±0.04 Å. This is close to the bulk lattice constant for InAs (6.06 Å) and indicates that the major part of the InAs epilayer is free-standing. The half-width of the InAs-peak is $\Delta(2\Theta)=0.09°$. Since the x-ray data is averaging over the entire film thickness it is likely that most of the broadening comes from the InAs close to the GaAs substrate where the strain is large. Thus we expect that the quality of the top of the layer is better than what the x-ray data shows.

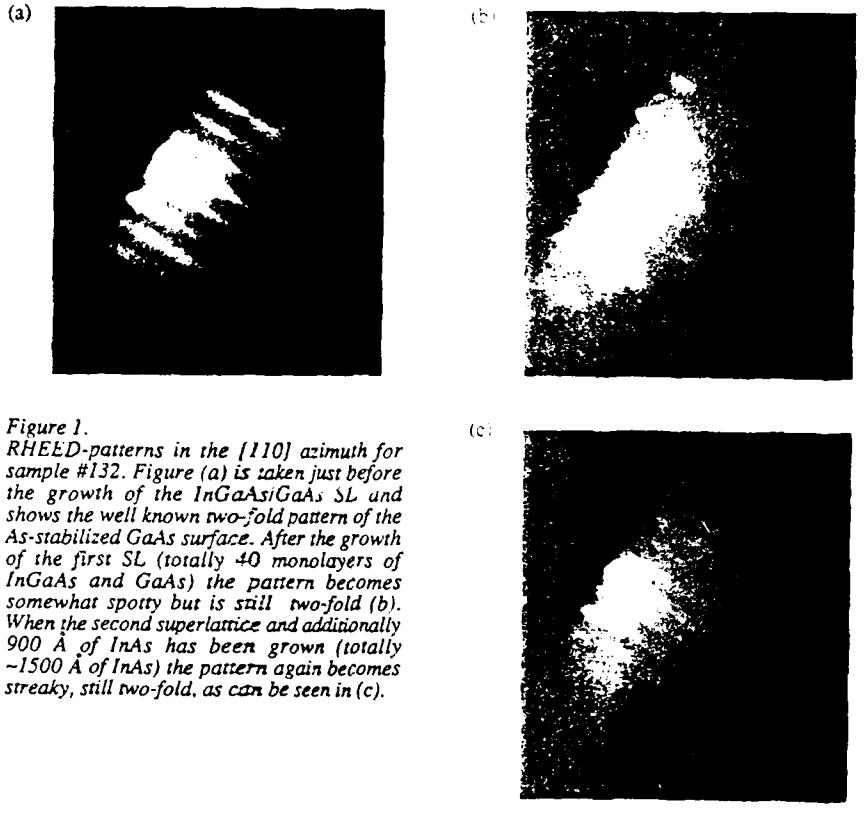

Figure 1.
RHEED-patterns in the [110] azimuth for sample #132. Figure (a) is taken just before the growth of the InGaAs/GaAs SL and shows the well known two-fold pattern of the As-stabilized GaAs surface. After the growth of the first SL (totally 40 monolayers of InGaAs and GaAs) the pattern becomes somewhat spotty but is still two-fold (b). When the second superlattice and additionally 900 Å of InAs has been grown (totally ~1500 Å of InAs) the pattern again becomes streaky, still two-fold, as can be seen in (c).

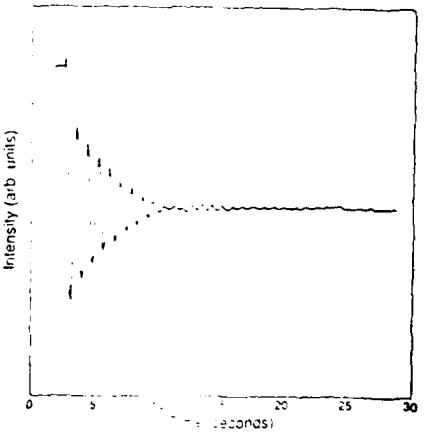

Figure 2.
RHEED intensity oscillations after 5000 Å of InAs growth and a one minute growth interrupt. About twenty oscillations can be seen. The growth rate as calculated from these oscillations is 3.17 Å/s.

GaSb mobilities and RHEED-oscillations

Sample #159 had a shiny surface and a surface morphology as seen under an optical microscope almost as good as GaAs films. Sample #155 on the other hand had a somewhat hazy surface and looked rough and textured under the microscope. The reason for this difference is probably due to the fact that sample#155 was used for RHEED-oscillations experiment and the temperature was for a short time ramped down to 450°C. Even though 1 μm of GaSb was grown at 545°C following this experiment the surface did not recover. This can also be seen from the Hall measurements where sample #159 has better mobility than sample #155. The mobilities and carrier concentrations at 300 K are shown in Table II (no measurements at 77 K were made due to problems with the Hall setup). The background doping is p-type as observed in previous studies[10] with a hole concentration of 9×10^{15} cm^{-3} for sample #159. The hole mobility for this sample is as high as 910 cm^2/Vs which is among the best reported for MBE-grown material[10]. This should be compared to bulk grown GaSb crystals which have hole mobilities of 1400 cm^2/Vs.

Table II
The mobilities and carrier concentration (holes) at 300 K for the GaSb samples.

Sample #	μ_h (cm^2/Vs)	p (10^{16} cm^{-3})
155	660	5.0
159	910	0.9

Figure 3 displays the RHEED-pattern along the [1 -1 0] azimuth during GaSb growth. We can see a three-fold pattern, which together with the observed one-fold pattern in the [110] direction (not shown), indicates that we have a (1x3) or c(2x6) surface reconstruction. Figure 4 shows the results of the RHEED-oscillation experiment. At 550°C (the substrate temperature we consider as the best for GaSb growth), no oscillations could be seen. However, as the temperature is lowered to 510°C some oscillations can be observed. At 450°C relatively intense oscillations are seen. The fact that oscillations cannot be seen at 550°C but are observed at lower temperatures indicates that at 550°C the growth occurs at step edges rather than by forming islands on the surface as has been discussed in previous studies of GaAs growth[15]. The surface mobility of the atoms at 550°C is high enough for them to have time to move to a step edge before being incorporated in the lattice. The combined RHEED oscillation and Hall measurement results indicate that the existence of RHEED oscillations does not necessarily mean that a high quality film is grown.

Figure 3.
The RHEED-pattern in the [1-10] azimuth for sample #155. The three-fold pattern is the image of the 1x3 surface reconstruction of the GaSb surface.

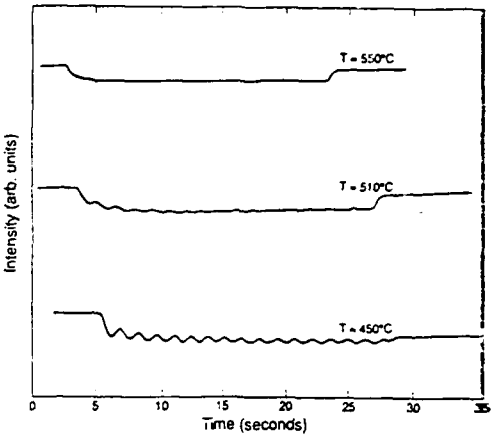

Figure 4.
RHEED intensity oscillations during GaSb growth (sample #155) after a one minute growth interrupt. At 550°C no oscillations can be seen. However, as the temperature decreases, RHEED oscillations start to appear. Thus at 550°C the crystal growth occurs at step edges while at the two lower temperatures the GaSb molecules form two-dimensional islands on the surface (which is the condition under which RHEED oscillations can be observed).

CONCLUSIONS

The results of the InAs growths indicate that for maximum room temperature mobility and good surface morphology the crystal should be grown under the 2x4 As-stabilized surface reconstruction, as close to the transition region as possible (i.e. with minimum excess arsenic to maintain a As-stabilized surface). We have also observed intense RHEED-oscillations during InAs-growth which to our knowledge are the best ever reported[16].

In this study we find optimal GaSb crystal quality at substrate temperatures around 545°C, while the best RHEED-oscillations are seen at much lower temperatures. To our knowledge this is the first report of RHEED-oscillations during GaSb growth.

ACKNOWLEDGEMENTS

The authors wish to thank R.J. Huenstein and R.H. Miles of Hughes Research Laboratories for Hall measurement and X-ray diffraction measurements on one of the InAs samples, respectively. This work was sponsored by Air Force Office of Scientific Research under the grant # 86-0306. One of us (DHC) received financial support from TRW.

REFERENCES

1. L.F. Luo, R. Beresford and W.I. Wang, Appl. Phys. Lett. 53, 2320 (1988)
2. J.R. Soderstrom, D.H. Chow and T.C. McGill, (to be published)
3. H. Munekata, T.P. Smith, III and L.L. Chang, J. Vac. Sci. Tech. B, March/April (1989).
4. D.L. Smith and C. Maihiot, J. Appl. Phys. 62, 2545 (1987).
5. S. Kalem, J.-I. Chyi and H. Morkoç, Appl. Phys. Lett. 53, 1648 (1988).
6. R.A.A Kubiak, E.H.C. Parker and S. Newstead, Appl. Phys. A35, 61 (1984).
7. B.T. Meggit, E.H.C. Parker, R.M. King and J.D. Grange, J. Cryst. Growth 50, 538 (1980).
8. C.-A. Chang, C.M. Serrano, L.L. Chang and L.Esaki, J. Vac. Sci. Tech. 17, 603 (1980).
9. M. Yano, M. Nogami, Y. Matsushima and M. Kimata, Jap. J. Appl. Phys. 16, 2133 (1977).
10. M. Lee, D.J. Nicholas, K.E. Singer and B. Hamilton, J.Appl. Phys. 59, 2895 (1986).
11. M. Yano, Y. Suzuki, T. Ishii, Y. Matsushima and M. Kimata, Jap. J. Appl. Phys. 17, 2091 (1978).
12. A.Y. Cho, Thin Solid Films, 100, 291 (1983).
13. W.J. Shaffer, M.D. Lind, S.P. Kowalczyk and R.W. Grant, J. Vac. Sci. Tech. B1, 688 (1983).
14. J.D. Grange, E.H.C. Parker and R.M. King, J. Phys. D12, 1601 (1979).
15. P.J. Dobson, B.A. Joyce and J.H. Neave, J. Cryst. Growth 81, 1 (1987).
16. B.F. Lewis, R. Fernandfez, A. Madhukar and F.J. Grunthaner, J. Vac. Sci. Tech. B4, 560 (1986).

Appendix A-2. Observation of Negative Differential Resistance for a Single Barrier Heterostructure. D. H. Chow and T. C. McGill, I. K. Sue, J. P. Forray and C. W. Nee.

Observation of negative differential resistance from a single barrier heterostructure

D. H. Chow and T. C. McGill
T. J. Watson, Sr., Laboratory of Applied Physics, California Institute of Technology, Pasadena, California 91125

I. K. Sou and J. P. Faurie
Department of Physics, University of Illinois at Chicago, Chicago, Illinois 60680

C. W. Nieh
Keck Laboratory of Materials Engineering, California Institute of Technology, Pasadena, California 91125

(Received 9 October 1987; accepted for publication 29 October 1987)

We report the first experimental observation of negative differential resistance (NDR) due to electron tunneling in a single barrier heterostructure. The largest peak-to-valley current ratio attained is slightly greater than 2:1. The single barrier structure studied here consists of a thin CdTe layer sandwiched between two $Hg_{0.78}Cd_{0.22}Te$ electrodes. In this particular material system, NDR can only be achieved at low temperatures ($T = 4.2$ K) due to the dominance of thermionic hole currents at high temperatures. The observation of NDR in this system suggests that the low-temperature valence-band discontinuity at the HgTe-CdTe interface is small (less than 100 mV). Room-temperature operation of single barrier NDR structures may be possible in other semiconductor systems.

It has been proposed that a few specific semiconducting materials may be suitable for fabricating single barrier heterostructures which display negative differential resistances (NDR's) in their current-voltage (I-V) characteristics.[1-3] In these devices, a thin layer of one semiconductor forms a quantum barrier between two thick cladding layers of another semiconductor. Charge transport in such a structure is achieved via tunneling of electrons in the cladding layers through the quantum barrier. Therefore, it is reasonable to suggest that these structures will have good high-speed properties. In fact, single barrier structures may have better high-frequency response and are easier to fabricate than quantum well (double barrier) devices, which produce NDR due to resonant electron tunneling. A single barrier NDR heterostructure might have applications in high-frequency microwave oscillators, amplifiers, and mixers. In this letter, we report the first experimental realization of such a structure.

The device used in this study consisted of a thin CdTe layer sandwiched between two $Hg_{0.78}Cd_{0.22}Te$ electrodes, doped n-type. The alloy $Hg_{1-x}Cd_xTe$ has been used as an infrared (IR) detector material since the 1960s.[4] A great deal of attention has been focused upon the high quality layered growth of HgTe, CdTe, and $Hg_{1-x}Cd_xTe$, largely due to the potential applications of the HgTe-CdTe superlattice as an IR material.[5-9] Recently, room temperature NDR has been observed in the I-V curves of double barrier heterostructures grown from HgTe and $Hg_{1-x}Cd_xTe$.[10,11] $Hg_{0.78}Cd_{0.22}Te$ and CdTe were selected for the single barrier heterostructure because their band alignments satisfy the requirement for observing NDR.[3] Tunneling electrons which originate in the $Hg_{0.78}Cd_{0.22}Te$ electrodes lie much closer in energy to the valence-band edge in CdTe than to the conduction-band edge. Such a structure can produce NDR because the electron tunneling probability is reduced as the valence-band edge in the barrier is pushed to lower energies (away from the electron energies) by an increasing applied voltage. This situation is depicted in Fig. 1, which is a calculated energy-band diagram for the single barrier heterostructure under an applied bias of 50 mV. The diagram was calculated by solving Poisson's equation self-consistently via the method of Bonnefoi *et al.*[12]

In addition to the appropriate band alignments, there are several conditions which must be satisfied in order to observe NDR from a single barrier heterostructure. The most important of these is that the total current must be dominated by elastic electron tunneling. This is not the case

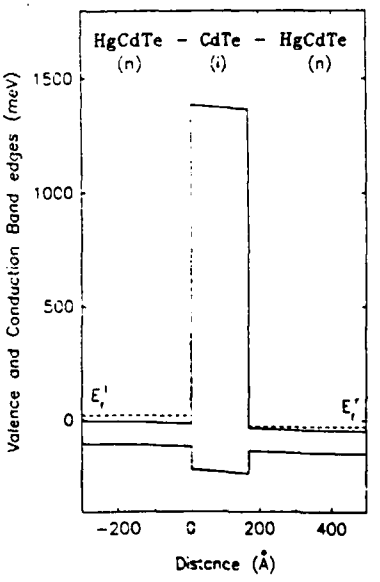

FIG. 1. Calculated band diagram for the $Hg_{0.78}Cd_{0.22}Te$-CdTe-$Hg_{0.78}Cd_{0.22}Te$ single barrier heterostructure, under an applied voltage of 50 mV. The upper (lower) solid line represents the conduction- (valence-) band edge as a function of distance in the direction of growth. The dashed line represents the Fermi energy in each of the electrodes, which are doped n type at 3.6×10^{16} cm^{-3}. The CdTe barrier is 170 Å thick. The CdTe valence-band edge is pushed away from tunneling electron energies as the applied voltage is increased.

 0003-6951/88/010054-03$01.00

at high temperatures for the $Hg_{0.78}Cd_{0.22}Te$-CdTe heterostructure studied here, because of thermionic hole currents across the CdTe layer.[13] It is important to note that thermionic hole emission is not prohibited by the *n*-type doping of the electrodes, because the band gap in the electrodes is very small (<200 meV). All measurements reported here are taken at low temperature (4.2 K) to eliminate these thermionic currents. Another condition which is necessary for obtaining NDR is that a reasonably large fraction of the total applied voltage must be dropped across the barrier, instead of across the cladding layers. For example, the band diagram in Fig. 1 depicts a situation in which roughly 40% of the total bias appears across the CdTe layer. The remainder of the voltage is lost in creating depletion and accumulation regions in the electrodes. The theoretical calculations for this device discussed in Ref. 3 do not include this effect. *I-V* simulations which incorporate band bending have been developed recently.[12] These simulations indicate that peak-to-valley current ratios can be expected to be drastically reduced by voltage drops in the electrodes. The structure depicted in Fig. 1 is predicted to have a maximum peak-to-valley current ratio of 3:1, depending upon the valence-band offset at the HgTe-CdTe interface. A larger barrier voltage drop can be obtained by increasing the thickness of the CdTe layer.[12] However, this reduces the overall elastic tunneling current through the structure, making it more likely that other transport mechanisms, such as inelastic or impurity-assisted tunneling, will dominate. Calculations indicate that the quantum barrier must drop at least 25% (roughly) of the total voltage in order to observe NDR.

The sample studied here was grown by molecular beam epitaxy (MBE) on a GaAs substrate in a Riber 2300 system. The $Hg_{0.78}Cd_{0.22}Te$ electrodes were doped *n*-type with In, to a carrier concentration of 3.6×10^{16} cm^{-3}. The top (bottom) electrode was grown 0.5 (3.0) μm thick. Growth of the bottom electrode was preceded by a 2.5-μm CdTe buffer layer. Transmission electron microscopy (TEM) yielded measurements of the CdTe barrier thickness ranging from 170 to 240 Å. A detailed description of the procedure used to prepare the sample for electrical measurements will be given elsewhere.[13] Mesas were fabricated in the sample by wet etching with Br_2:HBr:H_2O in a 0.005:1:3 ratio. Au was used to make ohmic contacts to both the tops of the mesas and the etched $Hg_{0.78}Cd_{0.22}Te$ surface, forming a set of isolated two terminal devices. In order to make electrical measurements at liquid helium temperatures, it was necessary to attach thin (20 μm) Au wires to the devices. This was accomplished by using a conductive epoxy which could be cured at room temperature (Acme, E-Solder No. 3021). The bonding technique was both tedious and time consuming, and resulted in bonds which were not particularly resilient at low temperatures. Consequently, only a few devices have been studied.

Figure 2 is an experimental *I-V* curve, taken in reverse bias (negative voltage on the top electrode) from a 37-μm-diam device at 4.2 K. The curve displays negative differential resistance, with a peak current density of 0.51 mA/cm^2 at 109 mV. The peak-to-valley current ratio is slightly greater than 2:1, in reasonable agreement with the previously discussed simulations. However, the calculations also indicate that NDR should be displayed over the voltage range 50–100 mV (roughly), in contrast to the 109–139 mV range observed in Fig. 2. The forward bias (positive voltage on the top electrode) *I-V* curve from this device is shown in Fig. 3. The curve displays two distinct NDR regions, with peak current densities of 0.010 mA/cm^2 at 57 mV and 0.039 mA/cm^2 at 109 mV. This bimodal characteristic is not predicted by our straightforward electron tunneling model. It is possible that nonuniformity in the portion of the sample covered by this device is responsible for the observed behavior. Another possible explanation is the presence of interface states at energies which lie within the $Hg_{0.78}Cd_{0.22}Te$ band gap. Other devices tested at 4.2 K gave a variety of results. One device showed forward bias NDR at approximately the same position as the lower voltage region in Fig. 3, with a peak-to-valley current ratio of 1.4:1. This device also displayed inflections (d^2I/dV^2 changed from positive to negative) at approximately the same voltages as the second peak in Fig. 3 and the peak in Fig. 2. Two other devices showed inflections in both bias directions, but did not have NDR. Finally, three devices did not display any inflections or NDR. The variations in the *I-V* behavior of different devices may have been caused by nonuniformity in the sample or by the poor resiliency of the conductive epoxy bonds at low temperatures.

The asymmetry between the forward and reverse bias *I-*

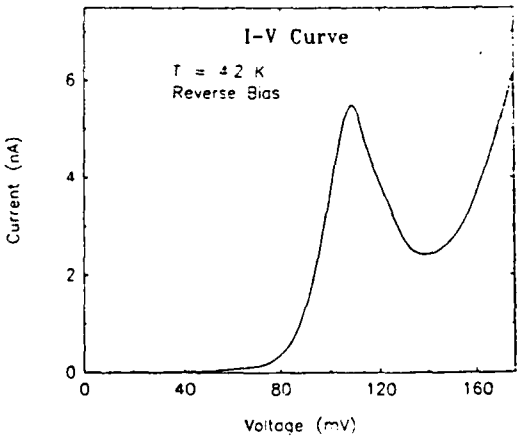

FIG. 2. Reverse bias *I-V* curve (negative voltage on the top electrode) taken at 4.2 K. The curve displays negative differential resistance over the voltage range 109–139 mV. The peak-to-valley current ratio is slightly greater than 2:1.

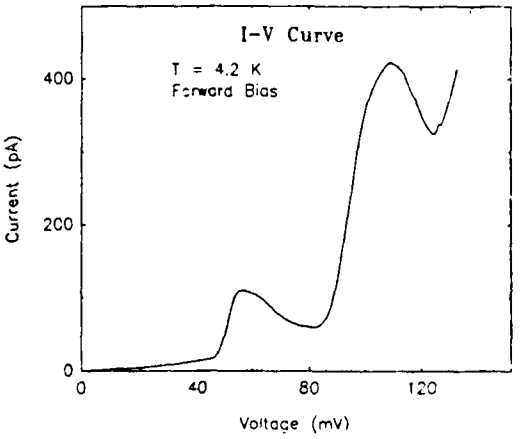

FIG. 3. Forward bias *I-V* curve (positive voltage on the top electrode) taken at 4.2 K. Two distinct NDR regions are observed. The lower (higher) bias region has a peak-to-valley current ratio of 1.8:1 (1.3:1).

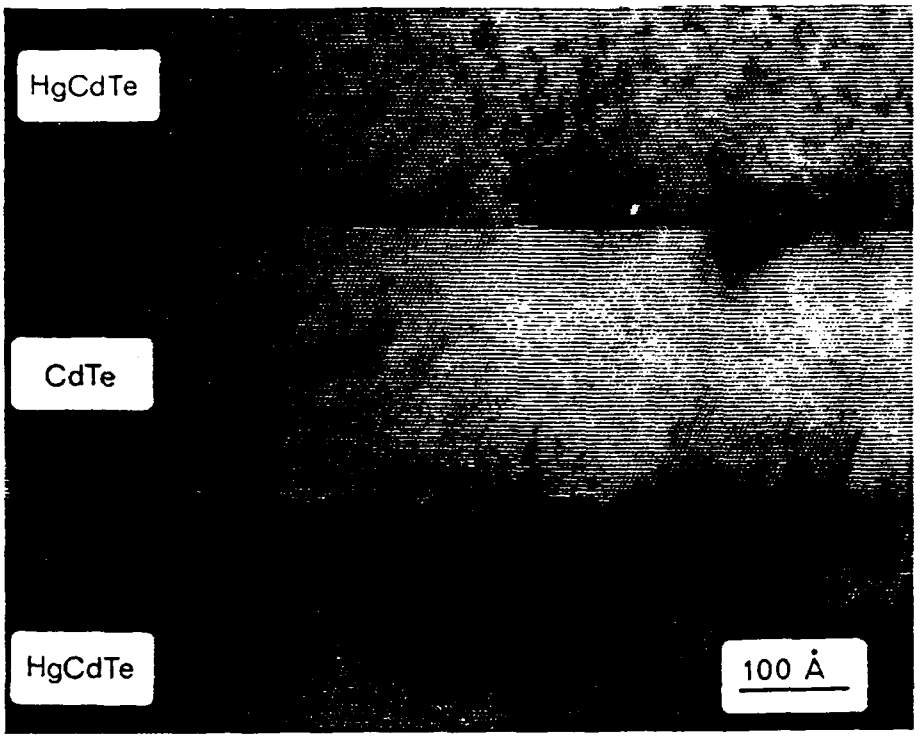

FIG. 4. High-resolution TEM photograph of the active region of the sample. A twin boundary is seen at the interface between the top $Hg_{0.78}Cd_{0.22}Te$ electrode and the CdTe barrier layer.

V curves from the single barrier heterostructure at 4.2 K may be caused by an asymmetry between the interfaces on either side of the CdTe barrier. Figure 4 is a high-resolution TEM photograph of the active region of the sample. A twin boundary is seen at the interface between the top $Hg_{0.78}Cd_{0.22}Te$ electrode and the CdTe barrier. In contrast, the interface between the barrier and the bottom $Hg_{0.78}Cd_{0.22}Te$ layer shows no evidence of twinning. The two types of interfaces are similar to the type A and B orientations which have been observed for $NiSi_2$ on Si.[14] In both cases, the [111] growth direction gives rise to the two possible orientations. The $NiSi_2$:Si barrier height was shown to vary by greater than 100 mV, depending upon which type of interface was grown.[14,15] However, no evidence of asymmetric barrier heights was found in high-temperature I-V studies of the heterostructure discussed here.[13]

In this letter, we have reported the first experimental observation of negative differential resistance from a single barrier heterostructure. Because of the choice of $Hg_{0.78}Cd_{0.22}Te$ and CdTe as materials for this study, thermionic hole currents prevented the observation of electron tunneling effects at room temperature. I-V measurements at 4.2 K showed NDR in some devices, but not in others. The variety of results obtained from different devices may be due to nonuniformity in the sample, or to the unreliability of the low-temperature bonding technique used. It should be noted that the observation of NDR implies that the valence-band offset at the HgTe-CdTe interface is small (less than 100 mV) at 4.2 K. Single barrier NDR devices may have high-speed applications, but it seems likely that room-temperature operation will be highly desirable. In this respect, it may be advantageous to try fabricating these devices with materials which do not have large thermionic currents at room temperature. One notable example is the InAs-GaSb (or perhaps InGaAs-GaAsSb) system.[1] It is also possible that heterostructures grown from combinations of III-V and II-VI semiconductors will be achievable, creating a number of systems which have the appropriate band alignment properties.

The authors wish to acknowledge useful discussions with J. O. McCaldin, A. R. Bonnefoi, T. K. Woodward, and M. B. Johnson. This work was supported by the Air Force Office of Scientific Research under contract No. AFOSR-86-0306, the Defense Advanced Research Projects Agency under contract Nos. N00014-86-K-0841 and F49620-87-C-0021, and the National Science Foundation under grant No. NMR8421119. One of us (D.H.C.) received financial support from International Business Machines Corporation.

[1] G. A. Sai-Halasz, R. Tsu, and L. Esaki, Appl. Phys. Lett. **30**, 651 (1977).
[2] J. Heremans, D. L. Partin, P. D. Dresselhaus, and B. Lax, Appl. Phys. Lett. **48**, 644 (1986).
[3] D. A. Chow and T. C. McGill, Appl. Phys. Lett. **48**, 1485 (1986).
[4] J. Ameurlaine, J. Coester, and H. Hofheimer, Opt. Spectra, 27 (October, 1973).
[5] J. N. Schulman and T. C. McGill, Appl. Phys. Lett. **34**, 663 (1979).
[6] C. E. Jones, J. N. Casselman, J. P. Faurie, S. Perkowitz, and J. N. Schulman, Appl. Phys. Lett. **47**, 140 (1985).
[7] S. R. Hetzler, J. P. Baukus, A. T. Hunter, J. P. Faurie, P. P. Chow, and T. C. McGill, Appl. Phys. Lett. **47**, 260 (1985).
[8] J. P. Faurie, IEEE J. Quantum Electron. **QE-22**, 1656 (1986).
[9] D. J. Leopold, M. L. Wroge, and J. G. Broerman, Appl. Phys. Lett. **50**, 924 (1987).
[10] J. N. Schulman and C. L. Anderson, Appl. Phys. Lett. **48**, 1684 (1986).
[11] M. A. Reed, R. J. Koestner, and M. W. Goodwin, Appl. Phys. Lett. **49**, 1293 (1986).
[12] A. R. Bonnefoi, D. H. Chow, and T. C. McGill, J. Appl. Phys. **62**, 3836 (1987).
[13] D. A. Chow, J. O. McCaldin, A. R. Bonnefoi, T. C. McGill, J. P. Faurie, and I. K. Sou (unpublished).
[14] R. T. Tung, Phys. Rev. Lett. **52**, 461 (1984).
[15] R. J. Hauenstein, T. E. Schlesinger, T. C. McGill, B. D. Hunt, and L. J. Schowalter, Appl. Phys. Lett. **47**, 853 (1985).

Appendix A-3. Demonstration of Large Peak to Valley Current Ratios in InAs/AlGaSb/InAs Single Barrier Heterostructures. J. R. Soderstrom, D. H. Chow and T. C. McGill.

Demonstration of large peak-to-valley current ratios in InAs/AlGaSb/InAs single-barrier heterostructures

J. R. Söderström,[a] D. H. Chow, and T. C. McGill
T. J. Watson, Sr., Laboratory of Applied Physics, California Institute of Technology, Pasadena, California 91125

(Received 24 April 1989; accepted for publication 19 July 1989)

We report large peak-to-valley current ratios in InAs/$Al_x Ga_{1-x}$Sb/InAs single-barrier tunnel structures. The mechanism for single-barrier negative differential resistance (NDR) has been proposed and demonstrated recently. A peak-to-valley current ratio of 3.4 (1.2) at 77 K (295 K), which is substantially larger than what has been previously reported, was observed in a 200-Å-thick $Al_{0.42}Ga_{0.58}Sb$ barrier. A comparison with a calculated current-voltage curve yields good agreement in terms of peak current and the slope of the NDR region. The single-barrier structure is a candidate for high-speed devices because of expected short tunneling times and a wide NDR region.

Double-barrier tunnel devices with negative differential resistance (NDR) have been the subject of great interest for several years.[1,2] New devices such as field-effect transistors with NDR,[3] the Stark effect transistor,[4,5] the resonant hot-electron transistor,[6] and devices for multiple level logic[7,8] are based on the double-barrier structure. High-speed devices such as oscillators and detectors for the THz range have also been made.[9] These devices are all based on the NDR in the current-voltage (I-V) characteristic of the tunnel structure.

Recently we proposed a new tunnel device in which NDR occurs in a single-barrier structure.[10,11] The NDR in this structure occurs because of the alignment of the bands in the barrier and contact layers and has a completely different origin than in the double-barrier case. A number of material systems have the required band structures and offsets to display this effect, including HgCdTe/CdTe, InAs/AlGaSb, and perhaps InAs/ZnTe.

Single-barrier structures are interesting for devices for several reasons. In double barrier structures the electrons tunnel through a quantum state with a width that will govern the tunneling time. In single barrier structures the electrons are not captured in such a quantum state which could yield faster tunneling times (good for high-speed operations). The NDR region is predicted to be much wider on the voltage scale than in the case of double barriers. This is of importance for high-frequency oscillators where the output power is governed by the product $\Delta I \times \Delta V$, where ΔI and ΔV are the width of the NDR region on the current and voltage scale, respectively.

The single-barrier NDR has experimentally been demonstrated by a few groups. The first observation was made in 1987 by Chow *et al.* in a single-barrier HgCdTe heterostructure.[12] In 1988 Munekata *et al.* observed NDR in an InAs/$Al_{0.4}Ga_{0.6}Sb$/InAs (200 Å barrier) structure.[13] A peak-to-valley current ratio (P/V ratio) of ~1.1 was obtained at 77 K. Recently Beresford *et al.* reported room-temperature NDR in an InAs/$Al_{2.5}Ga_{0.5}Sb$/InAs (150 Å barrier) structure.[14]

In this study we have investigated NDR in InAs/$Al_x Ga_{1-x}$Sb/InAs single-barrier structures with 200-Å-thick barriers. P/V ratios as high as 1.2 and 3.4 at room temperature and 77 K, respectively, have been observed for an aluminum concentration of 42%. The 77 K value of 3.4 is substantially larger than what has previously been reported for any single-barrier structure. We also report a wide NDR region (~140 meV). Six single-barrier samples were grown with aluminum concentrations in the barrier ranging from 38% to 48%. Four of the samples yielded NDR. We have compared our results to a simple theoretical calculation.

A qualitative understanding of the single-barrier NDR can be obtained by considering the positions of the conduction- and valence-band edges under applied bias as shown in Fig. 1. From the Wentzel–Kramers–Brillouin approximation theory we know that an electron traveling in the z direction has a probability of tunneling through the barrier given by the transmission coefficient

$$T \propto \exp\left(-2\int_0^w K\,dz\right),$$

where K is the imaginary wave vector (or the decay constant) in the band gap of the barrier and w is the thickness of the barrier. K can be obtained from a two-band model, $k\cdot p$ theory calculation.[15] The important thing about the two-band model is that it accounts for the reduction of the decay constant for energies closer to the valence band, re-

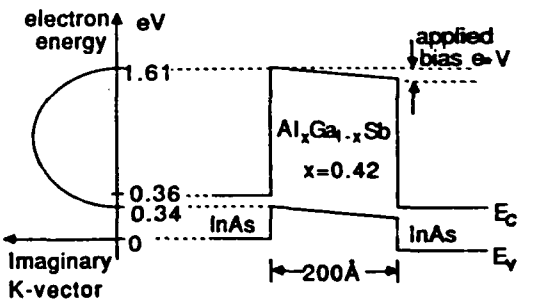

FIG. 1. Band-edge diagram (Γ point) for the single-barrier structure under applied bias. The imaginary wave vector in the barrier layer is plotted as function of the electron energy. NDR occurs due to the enhanced tunneling probability for electrons close to the valence band of the barrier layer.

[a] On leave from Chalmers University of Technology, Department of Physics, S-412 96 Göteborg, Sweden.

 0003-6951/89/391348-03$01.00

sulting in a maximum of K at (or close to) midgap of the barrier layer as shown in the left-hand side of Fig. 1. The requirement for getting NDR in a single-barrier structure is that the tunneling electrons (at low voltages) are injected close to the valence band of the barrier layer where the decay constant is small. As the voltage increases the electrons tunnel at higher average energies in the barrier, resulting in larger K, smaller transmission coefficient and hence a lower current. It should be emphasized that this effect can be seen only in single-barrier structures where the electrons tunnel below midgap (or below the maximum of the imaginary wave vector) of the barrier. This explains why GaAs/AlGaAs single-barrier structures do not display this effect.

The samples were grown in a Perkin–Elmer 430 molecular beam epitaxy (MBE) system. An As cracker and an Sb cracker were used to produce dimers instead of tetramers in the molecular beams. Details of bulk growth parameters for InAs and GaSb can be found elsewhere.[16] Calibrations of growth rates and x values were done with reflection high-energy electron diffraction (RHEED) oscillations and bulk film thickness measurements.

The single-barrier structures were grown on GaAs (100) substrates. Due to the large lattice mismatch (7.2%) between the substrate and the epilayer, a thick buffer layer was grown. The buffer layer consisted of 5000 Å GaAs grown at 600 °C, a five-period $In_{0.7}Ga_{0.3}As$/GaAs (2 monolayers/2 monolayers) superlattice grown at 500–520 °C, and 1.5 μm InAs (heavily Si doped) grown at 500 °C. The superlattice at the GaAs/InAs interface reduces the number of strain-induced dislocations which penetrate into the InAs layer.[16,17] The single-barrier structures were grown at 500 °C on top of the buffer layers. Each structure consisted of a 200 Å undoped $Al_xGa_{1-x}Sb$ ($38\% \leqslant x \leqslant 48\%$) barrier sandwiched between 100 Å undoped InAs spacer layers and 500 Å lightly doped ($n = 2\times10^{16}$ cm^{-3}) InAs spacer layers. The two-step spacer layer technique is used to reduce the number of Si donors in the barrier region and has previously been used for double-barrier structures.[18] Finally a 2500-Å-thick heavily doped ($n = 2\times10^{18}$ cm^{-3}) InAs cap layer was grown.

Mesa structures with varying areas (down to 100 μm^2) were prepared using standard photolithography and liftoff techniques. The evaporated Au/Ge contacts served as masks during etching in H_2SO_4:H_2O_2:H_2O (1:8:80) for 90 s, which resulted in $\sim$0.7 μm high mesas. Au/Ge deposited on the etched InAs buffer layer was used as the back contact. No annealing was necessary since Au/Ge forms an ohmic contact to InAs. The mesas were probed with a thin gold wire to establish electrical contact to the devices.

Figure 2 shows an experimentally obtained current density versus voltage (J-V) characteristic for a single-barrier structure with a 200-Å-thick $Al_{0.42}Ga_{0.58}Sb$ barrier. NDR can be seen at room temperature and 77 K for both positive and negative bias. The remainder of the discussion focuses on the reverse bias peak (i.e., electrons injected from the top mesa contact) since it gave the best result. The P/V ratios are as high as 1.2 and 3.4 at room temperature and 77 K, respectively. The 77 K value is the largest P/V ratio ever reported for single-barrier structures. The peak current densities are 30 A/cm^2 at 295 K and 22 A/cm^2 at 77 K. The width of the NDR region at 77 K is about 140 mV.

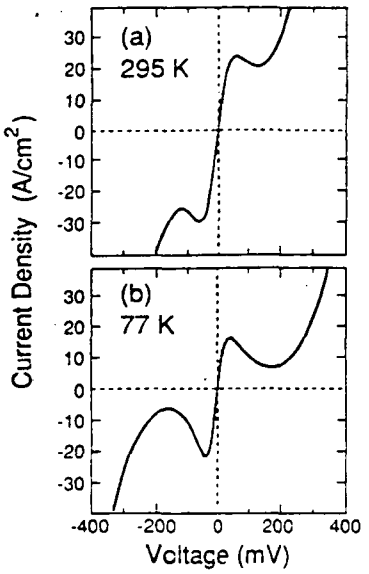

FIG. 2. Experimental J-V characteristic at (a) room temperature and (b) 77 K for a 200-Å-thick $Al_{0.42}Ga_{0.58}Sb$ single-barrier enclosed by InAs. The device size is 10×10 μm^2. The P/V ratios (in reverse bias) are as high as 1.2 and 3.4 at 295 and 77 K, respectively.

Figure 3 shows the calculated J-V curve for the same structure. Details of the calculations have been reported earlier.[19] A peak at $\sim$15 mV followed by a wide region of NDR can be seen. The peak current density is $\sim$20 A/cm^2 which is only slightly smaller than the measured value. The measured peak voltage is about twice as large as the calculated peak voltage which could be atrributed to series resistance in the circuit which has not been accounted for in the calculation. The slope of the NDR region is about 200 Ω^{-1} cm^{-2} which is close to the 350 Ω^{-1} cm^{-2} value that was obtained from the theoretical curve.

Obviously the calculated and experimental curves are in good agreement in several respects. This is in contrast to

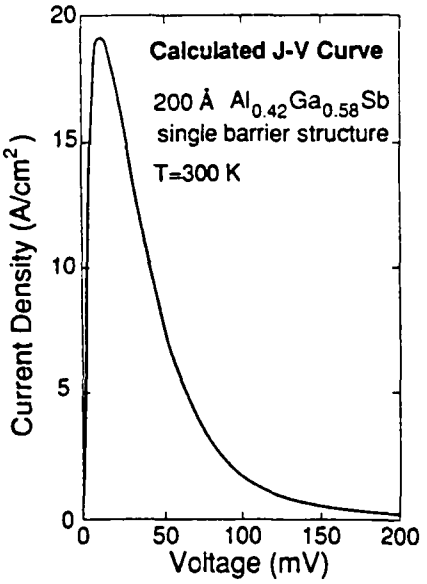

FIG. 3. Calculated J-V curve at 300 K for the single-barrier structure.

previous studies. The computer program does not account for any other current transport mechanism than elastic tunneling of electrons. We will briefly discuss possible additional current transport mechanisms that could account for the measured excess valley current. Since the barrier in the conduction band is high (1.3 eV), thermionic currents over the barrier will only give a small current contribution at low voltages. However, at higher voltages the potential drop over the undoped layer on the emitter side will result in electrons being ballistically injected close to or above the top of the barrier, producing a larger current. In the valence band, thermally excited holes are present (due to the small band gap of InAs) which do not experience any barrier and give rise to a hole current. Furthermore, electrons occupying valence-band states will start to tunnel over to states in the conduction band when the voltage over the barrier aligns the energy of these states. Other possible current mechanisms include inelastic tunneling processes and currents on the mesa surface. The calculated J-V curve indicates that much better P/V ratios can be obtained if the excess currents can be reduced. We are presently working to achieve this goal.

NDR was observed in three more samples with the aluminum concentrations of 44, 40, and 38%. P/V ratios in these samples were smaller than 1.5. At an aluminum concentration of 38% the single-barrier structure may be semimetallic according to reported values of band gaps and offsets.[20,21] The fact that NDR is observed anyway can be explained either by an error in the growth rate calibration or by error in the band offsets. Even if the calibration and the offset values are correct we might still be able to explain the NDR due to the fact that when a bias is applied to the semimetallic structure the barrier region gets skewed and the valence-band state of the barrier layer gets quantized. These states will no longer extend out in the InAs conduction band and the incoming electrons will experience a barrier exactly as in the case of higher x values.

The samples with 44% and 46% aluminum concentration have some interesting features. The 46% sample shows no NDR at any temperature. However, a room-temperature inflection in the I-V curve can clearly be seen. This inflection disappears as the temperature is lowered, and at 77 K the curve is exponential as in the case of thermionic emission currents over a barrier. We attribute this effect to an increase in the energy difference between the conduction band of the contact layer and the valence band of the barrier (due to the increase of the InAs and AlGaSb band gaps). Thus, the tunneling probability is reduced at 77 K. The same argument holds for the behavior of the 44% sample in which no NDR is observed at 77 K. As the temperature is increased to ~180 K a NDR region with a ratio P/V of 1.1 appears. As the temperature is increased even further, the NDR disappears due to thermionic currents.

To summarize, we have observed NDR in InAs/AlGaSb/InAs single-barrier structures with substantially larger P/V ratios than previously reported. The measured J-V curve is in close agreement with the theoretically obtained curve in terms of peak current density, peak voltage, and the slope of the NDR region. The result of the calculation also shows that much larger P/V ratios can be obtained if the excess currents can be controlled. Other experiments to examine the physics of these structures are in progress.

We acknowledge the support of the Air Force Office of Scientific Research under grant No. 86-0306. Two of us (JRS and DHC) are thankful for financial support from the Sweden–America Foundation and TRW, respectively.

[1] L. L. Chang, L. Esaki, and R. Tsu, Appl. Phys. Lett. **24**, 593 (1974).
[2] J. R. Söderström and T. G. Andersson, Superlatt. Microstruct. **5**, 109 (1989).
[3] T. K. Woodward, T. C. McGill, H. F. Chung, and R. D. Burnham, Appl. Phys. Lett. **51**, 1542 (1987).
[4] A. R. Bonnefoi, D. H. Chow, And T. C. McGill, Appl. Phys. Lett. **47**, 888 (1985).
[5] F. Beltram, F. Capasso, S. Luryi, S. N. G. Chu, A. Y. Cho, and D. L. Sivco, Appl. Phys. Lett. **53**, 219 (1988).
[6] T. Futatsugi, Y. Yamaguchi, K. Imamura, S. Muto, N. Yokoyama, A. Shibatomi, Jpn. J. Appl. Phys. **26**, L131 (1987).
[7] S. Sen, F. Capasso, A. Y. Cho, and D. Sivco, IEEE Trans. Electron Devices **34**, 2185 (1987).
[8] J. R. Söderström and T. G. Andersson, IEEE Electron Device Lett. **9**, 200 (1988).
[9] T. C. L. G. Sollner, W. D. Goodhue, P. E. Tannenwald, C. D. Parker, and D. D. Peck, Appl. Phys. Lett. **43**, 588 (1983).
[10] D. H. Chow and T. C. McGill, Appl. Phys. Lett. **48**, 1485 (1986).
[11] G. A. Sai-Halasz, R. Tsu, and L. Esaki, Appl. Phys. Lett. **30**, 651 (1977).
[12] D. H. Chow, T. C. McGill, I. K. Sou, J. P. Faurie, and C. W. Nieh, Appl. Phys. Lett. **52**, 54 (1988).
[13] H. Munekata, T. P. Smith III, and L. L. Chang, J. Vac. Sci. Technol. B **7**, 324 (1989).
[14] R. Beresford, L. F. Luo, W. I. Wang, Appl. Phys. Lett. **54**, 1899 (1989).
[15] E. O. Kane, *Physics of III-V compounds* (Academic, New York, 1966), Vol. 1, Chap. 3, pp. 75–100.
[16] J. R. Söderström, D. H. Chow, and T. C. McGill, *Proceedings of the MRS 1989 Spring Meeting, San Diego* (Materials Research Society, Pittsburgh, in press).
[17] S. Kalem, J. I. Chyi, and H. Morkoç, Appl. Phys. Lett. **53**, 1648 (1988).
[18] C. I. Huang, M. J. Paulus, C. C. Bozada, S. C. Dudley, K. R. Evans, C. E. Stutz, R. L. Jones, and M. E. Cheney, Appl. Phys. Lett. **51**, 121 (1987).
[19] A. R. Bonnefoi, D. H. Chow, and T. C. McGill, J. Appl. Phys. **62**, 3836 (1987).
[20] G. J. Gulatieri, G. P. Schwarz, R. G. Nuzzo, and W. A. Sunder, Appl. Phys. Lett. **49**, 1073 (1986).
[21] G. J. Gulatieri, G. P. Schwarz, R. G. Nuzzo, R. J. Malik, and J. F. Walker, J. Appl. Phys. **61**, 5337 (1987).

Appendix A-4. Observation of Negative Differential Resistance in Broken Gap Interband Tunnel Structures. D. A. Collins, D. H. Chow and T. C. McGill.

Observation of Negative Differential Resistance in a Broken-Gap Resonant Interband Tunneling Structure.

D.A. Collins, D.H. Chow and T.C. McGill
T. J. Watson, Sr., Laboratory of Applied Physics
California Institute of Technology
Pasadena, California 91125

RECEIVED
Editor's Office
NOV 27 1989
Applied Physics Letters

ABSTRACT

We report the experimental observation of negative differential resistance (NDR) in an InAs/GaSb/InAs heterostructure. The NDR is readily observable at room temperature with peak-to-valley current ratios of ~1.6-2 and peak current densities greater than 10^4 A/cm^2. These materials have type II staggered band alignments, hence the electrons do not tunnel through a classically forbidden region as they traverse the device. The resonance giving rise to the NDR is due solely to the coupling of conduction band states and valence band states in adjacent layers of the device. This unique feature raises the possibility of high-speed switching or high-frequency oscillator circuits.

Recently, there has been a great deal of investigation into heterostructures in which coupling of conduction band states in one material with valence band states in an adjacent layer of another material is crucial to the performance of the device. In 1977 Sai-Halasz *et al.*[1] proposed that negative differential resistance (NDR) could be realized for single barrier structures if the conduction band edge in the emitter electrode is close to valence band edge in the barrier material. They reasoned that if the coupling between conduction band states in the emitter and valence band states in the barrier material was large enough then there would be an enhancement of the tunneling current for electrons tunneling near the valence band edge of the barrier material. As the bias across the structure is increased the electrons impinge on the barrier at energies farther from the barrier material's valence band edge and as a result, the interaction between the conduction band states and valence band states in the adjacent layers will decrease giving rise to NDR. Such single barrier structures in which NDR is due to the coupling of conduction band states in one material with valence band states in an adjacent layer of another material have been demonstrated in two material systems: HgCdTe/CdTe[2] and AlGaSb/InAs.[3,4,5] More recently, resonant devices in which conduction band electrons tunnel into quasibound valence band states of neighboring materials have been proposed[6] and demonstrated[7,8] in InAs/AlSb/GaSb/AlSb/InAs heterostructures. These devices in particular demonstrate that strong coupling can exist between valence band and conduction band states.

In this letter we report NDR from a recently proposed broken-gap resonant interband tunneling (BRIT) structure.[9] The two structures grown consisted of thin, undoped GaSb layers sandwiched between heavily doped InAs cladding layers. The central layers were 150 Å and 300 Å thick (with an uncertainty in the GaSb layer thickness of ~2%.) Both BRITs showed NDR at room temperature with peak-to-valley current (PVC) ratios ranging from 1.6:1 to 2:1 and peak current densities greater than 10^4 A/cm^2 in both devices.

Fig. 1 shows the band edge diagram for the structure along the growth direction. This diagram can be misleading in that it implies that it is possible to have ohmic conduction

of electrons originating in the InAs cladding layer across the GaSb layer as long as the electron's energy is less than that of the valence band edge of GaSb. However, because the electronic wavefunctions in the InAs conduction band and the GaSb valence band are very different the charge carriers are partially confined in the GaSb. These quasibound states in the GaSb valence band give rise to resonances in the transmission probability as a function of the electron energy and hence NDR.

A layer diagram of the structures is given in Fig. 2. The samples studied were grown on GaAs [100] substrates in a Perkin-Elmer 430 molecular beam epitaxy system. A buffer layer of 1500 Å of GaAs was grown on the substrate at 600 °C in order to smooth the growth surface. The growth temperature was then lowered to 520 °C and a five period InGaAs/GaAs superlattice with 2 monolayer thick layers was grown in order to reduce the number of threading dislocations in the InAs buffer layer caused by the lattice mismatch between the two materials.[10,11] The substrate temperature was then lowered to 480 °C and held at this value for the rest of the growth. The growth rates for the InAs and GaSb were 1.0 μm/hr and 0.5 μm/hr, respectively. The InAs was heavily Si-doped n-type. Undoped spacer layers 50 Å thick were grown on both sides of the GaSb layer in order to inhibit the diffusion of silicon into the undoped well region. Device mesas (with a surface area of 10^{-6} cm^2) were fabricated using photolithography and a wet etch. The etch was stopped in the InAs layer closest to the substrate and two Au wires were used to probe the mesas at 300 K.

Representative I-V curves taken at 300 K for the two structures are shown in Fig. 3 and Fig. 4 for the devices with 150 Å and 300 Å GaSb wells, respectively. The peak current densities in forward bias are (2.65±.18)x10^4 A/cm^2 and (1.06±.08)x10^4 A/cm^2 for the 150 Å and 300 Å GaSb wells, respectively. The above values for the peak current density are the mean and standard deviation for 25 randomly chosen devices. These current densities are comparable to those obtained for AlGaAs/GaAs and AlGaSb/InAs heterostructures, hence they hold promise for use in applications that require large current densities such as

high-frequency oscillators.

We should note that there is an unpublished report of NDR in a BRIT structure grown by atmospheric MOCVD.[12] In this letter we conclusively demonstrate that large peak current densities and reasonable PVC ratios can be obtained from BRIT's at room temperature.

In summary we have demonstrated a broken-gap resonant interband tunneling device. Unlike conventional tunneling devices that show NDR, the charge carriers in BRIT devices do not tunnel through any classically forbidden regions hence, the observed NDR is due to the imperfect overlap of the InAs conduction band wavefunctions and the GaSb conduction band wavefunctions. The structures show NDR at room temperature with current densities greater than 10^4 A/cm^2. These current densities are comparable to those reported in AlGaAs/GaAs double barrier tunneling diodes. Further, a recent calculation[9] has estimated that the intrinsic lifetime of the quasi-bound state for a similar structure to be 50 fs which suggests that BRIT structures could be useful in high-frequency oscillator and high-speed switching circuits.

The authors would like to thank J.R. Söderström, M.K. Jackson, E.T. Yu, Y. Rajakarunanayake, D.Z.-Y. Ting and M. Hudson for helpful discussions. This work was supported by the Office of Naval Research under contract No. N00014-89-J-1141 and by the Air Force Office of Scientific Research under contract No. AFOSR-86-0306.

REFERENCES

[1]G.A. Sai-Halasz, R. Tsu and L. Esaki, Appl. Phys. Lett. **30**, 651 (1977).

[2]D.H. Chow, T.C. McGill, I.K. Sou, J.P. Faurie and C.W. Nieh, Appl. Phys. Lett. **52**, 54 (1988).

[3]R. Beresford, L.F. Luo and W.I. Wang, Appl. Phys. Lett. **54**, 1899 (1988).

[4]J.R. Söderström, D.H. Chow and T.C. McGill, Appl. Phys. Lett. **55**, 1348 (1989).

[5]H. Munekata, T.P. Smith III and L.L. Chang, J. Vac. Sci. Technol. B **7**, 324 (1989).

[6]M. Sweeny and J. Xu, Appl. Phys. Lett. **53**, 60 (1989).

[7]J.R. Söderström, D.H. Chow and T.C. McGill, Appl. Phys. Lett. **55**, 1094 (1989).

[8]L.F. Luo, R.Beresford, and W.I. Wang, Appl. Phys. Lett. **55**, 2023 (1989).

[9]J.R. Söderström, E.T. Yu, M.K. Jackson, Y. Rajakarunanayake and T. C. McGill, unpublished.

[10]S. Kalem, J.-I. Chyi and H. Morkoç, Appl. Phys. Lett. **53**, 1648 (1988).

[11]J.R. Söderström, D.H. Chow and T.C. McGill, Proceedings of the MRS 1989 Spring Meeting, San Diego (Material Research Society, Pittsburgh, in press).

[12]K. Taira, I. Hase and H. Kawai, The 7th International Workshop on Future Electron Devices Superlattice and Quantum Functional Devices, Oct. 2-4, 1989, Toba, Japan.

FIGURE CAPTIONS

FIG. 1. Band edge diagram for the structures grown.

FIG. 2. Layer diagram for the structures grown. The layer thicknesses are not drawn to scale.

FIG. 3. I-V curves for the device with a 150 Å GaSb well taken at 300 K.

FIG. 4. I-V curves for the device with a 300 Å GaSb well taken at 300 K.

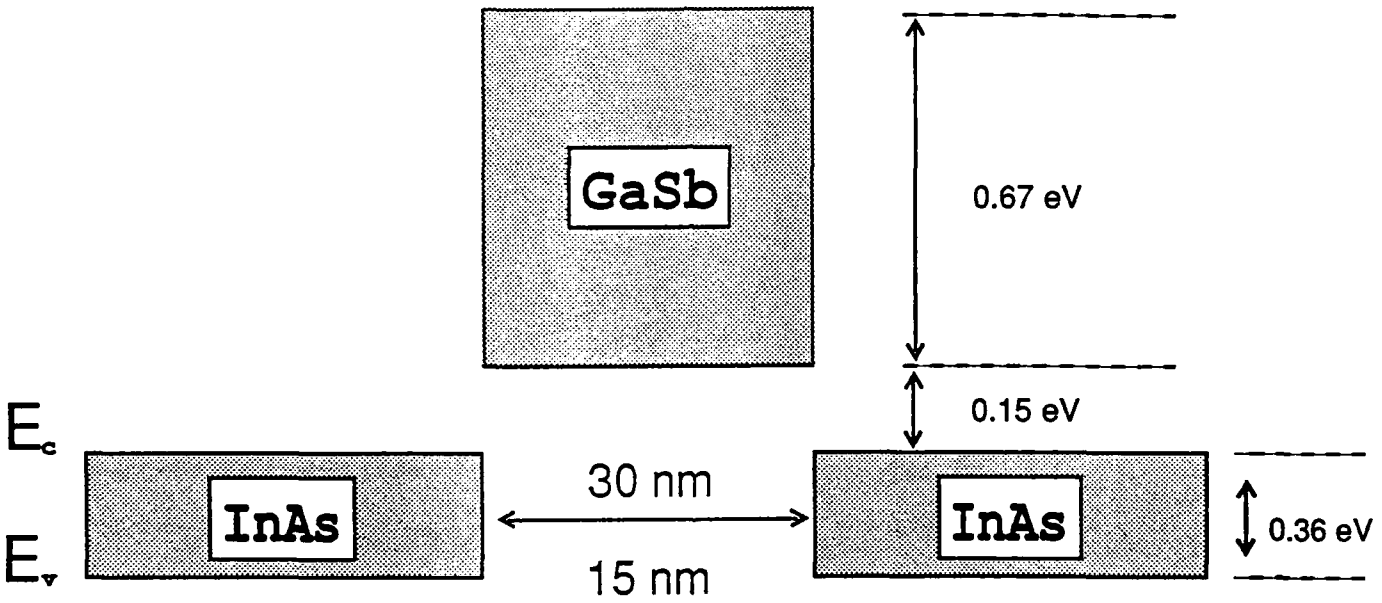

Fig. 1g4

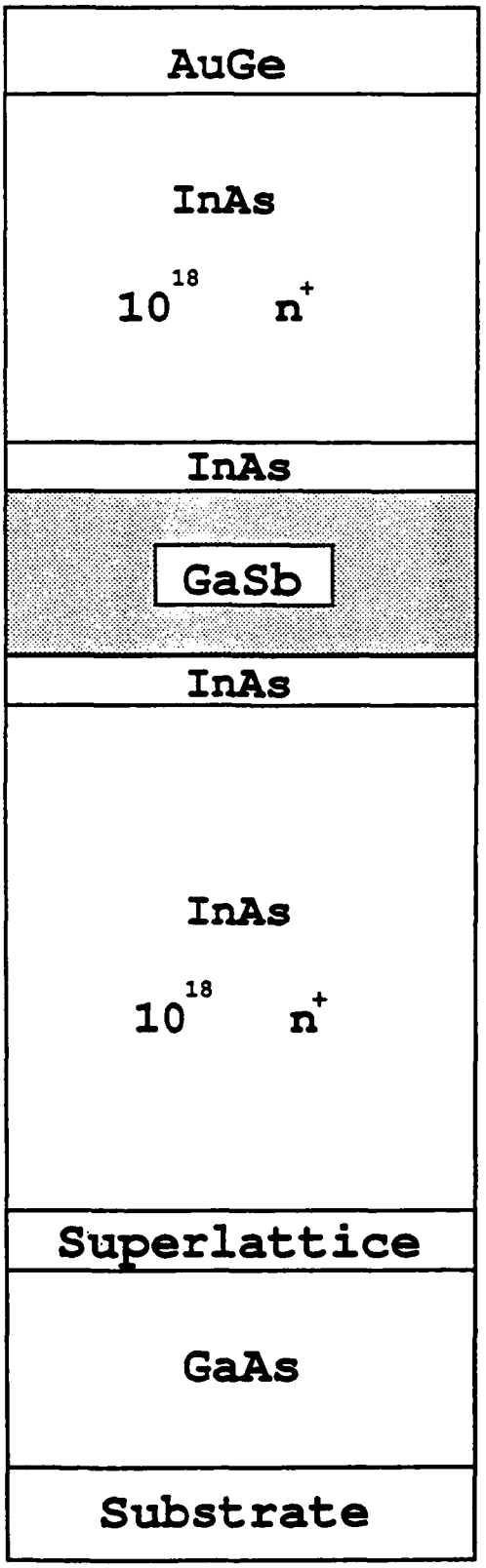

Fig. 2y
Collins et el

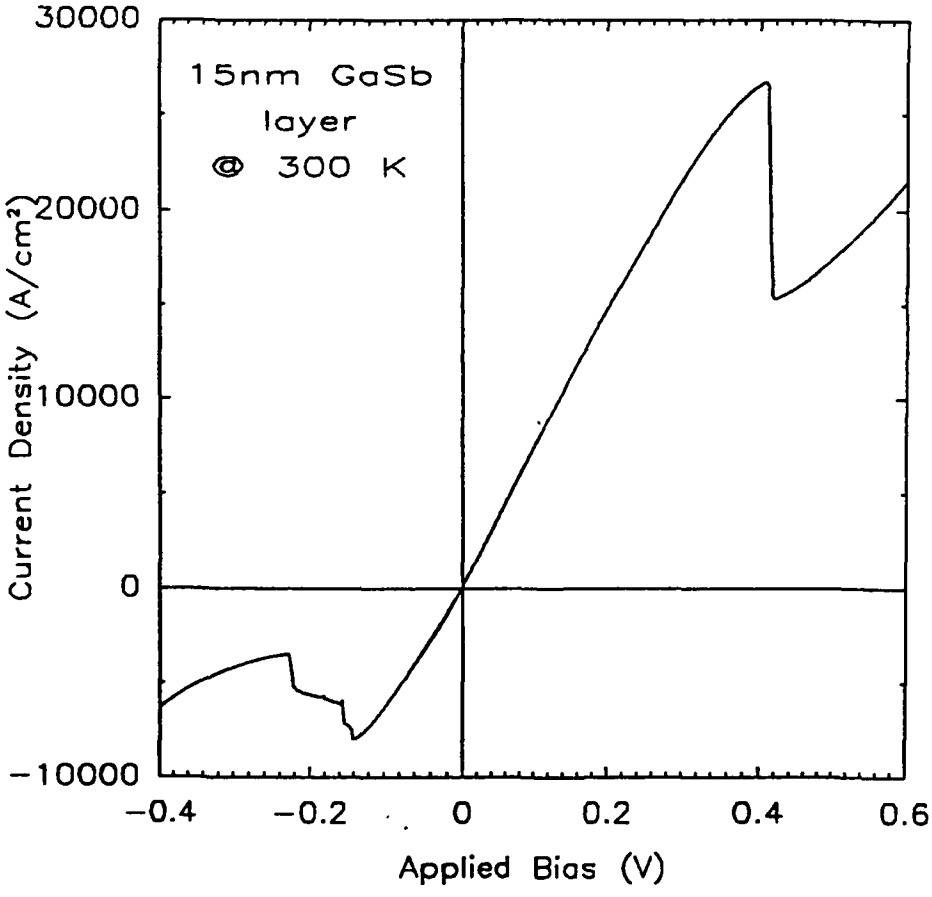

Fig. 3, 4
Collins et el

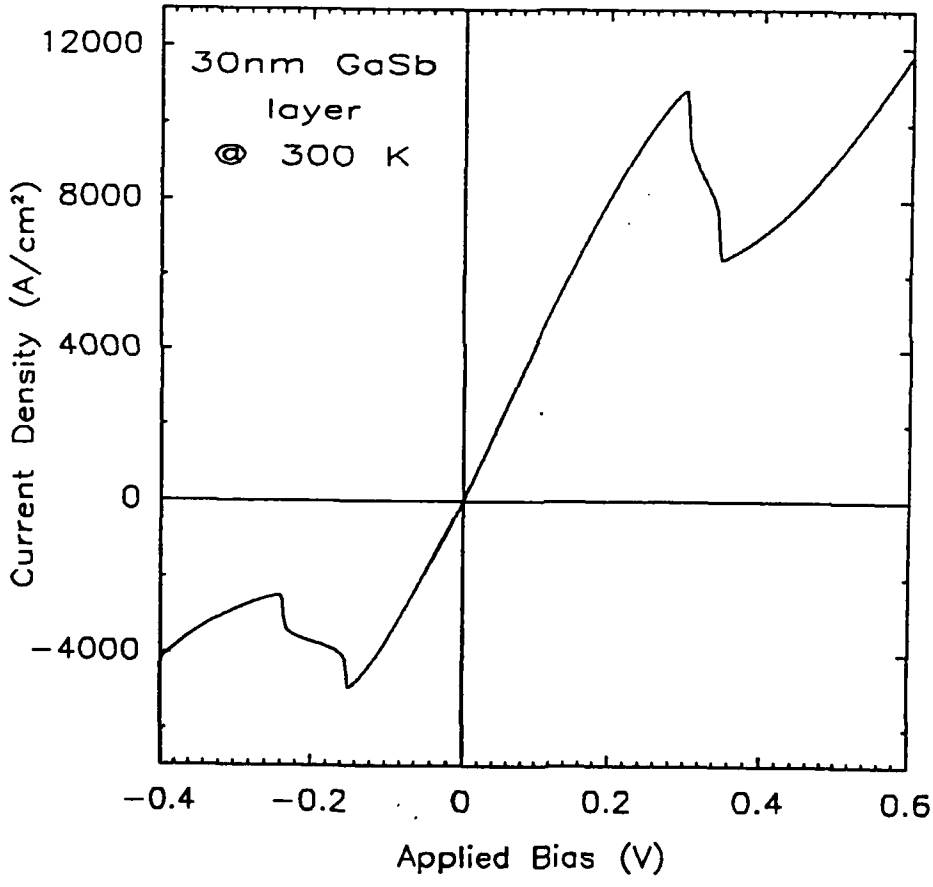

Fig. 4,4
Collins et el

Appendix A-5. Observation of Large Peak to Valley Current Ratios and Large Peak Current Densities in AlSb/InAs/AlSb Double Barrier Tunnel Structures. J. R. Soderstrom, D. H. Chow and T. C. McGill.

Observation of large peak-to-valley current ratios and large peak current densities in AlSb/InAs/AlSb double-barrier tunnel structures

J. R. Söderström,[a] D. H. Chow, and T. C. McGill
T. J. Watson, Sr., Laboratory of Applied Physics, California Institute of Technology, Pasadena, California 91125

(Received 1 May 1989; accepted for publication 1 August 1989)

We report improved peak-to-valley current ratios and peak current densities in InAs/AlSb double-barrier, negative differential resistance tunnel structures. Our peak-to-valley current ratios are 2.9 at room temperature and 10 at liquid-nitrogen temperatures. Furthermore, we have observed peak current densities of 1.7×10^5 A/cm^2. These figures of merit are substantially better than previously reported values. The improvements are obtained by adding spacer layers near the barriers, thinner well regions, and thinner barriers.

Double-barrier tunnel devices have been a subject of great interest for several years.[1-3] These device structures offer the possibility of making new devices, exploring interesting device physics, and the possibility of making high-speed and high-density devices. To date most of the effort has been concentrated on heterostructures based on GaAs/GaAlAs.[1-3] This heterojunction system suffers from three major problems. First, difficulty in making ohmic contacts to *n*-type GaAs causes a substantial series resistance in the

[a] Previous address: Chalmers University of Technology, S-41296 Göteborg, Sweden.

 0021-8979/89/225106-03$02.40

circuit, limiting the performance of the device. Second, small barriers for electrons in this heterojunction system lead to substantial contributions to the room-temperature current from thermally excited carriers. This current substantially reduces the peak-to-valley (P/V) current ratio observed in GaAs/AlGaAs double-barrier structures. Finally, it is difficult to obtain the high current densities that are necessary to obtain high powers from these device structures. There has been some work on InGaAs/AlAs heterostructures which addresses these problems with good results.[4,5] However, the lattice mismatch in these structures makes them difficult to fabricate.

To fix these difficulties, we have proposed the use of double barrier structures consisting of InAs/ZnTe/InAs/ZnTe/InAs.[6] This nearly lattice-matched heterojunction system has a number of advantages. First, it is very easy to make n-type, low-resistance ohmic contacts to the InAs. Second, the InAs has a high electron mobility and, consequently, can carry large currents through the requisite cladding layers. Finally, the conduction-band offset between InAs and ZnTe is estimated to be about 1.6 eV. This is in contrast to the conduction-band offset of roughly 1 eV for Γ point to Γ point GaAs/AlAs and roughly 0.2 eV for the Γ point to X point barrier in GaAs/AlAs. We projected that this structure would have substantially higher peak-to-valley current ratios at room temperature and would not suffer from some of the difficulties associated with transport through the ohmic contacts and cladding layers.

A III-V alternative in these attempts to improve performance is the near lattice-matched InAs/AlSb structure.[7] This structure has the same advantages as the ZnTe/InAs structure with low series resistance and high mobility. The Γ-point conduction-band offset is 1.8 eV; the X point is 1.2 eV. Experimentally, negative differential resistance has been observed in this structure by Lou, Beresford, and Wang.[7] They reported P/V ratios of 1.8 at room temperature and 9 at 77 K for a 168-Å InAs quantum well sandwiched between 25-Å AlSb barriers. They further point out that the small effective mass of InAs makes it possible to have thicker InAs layers and still provide substantial separation between subbands. This additional width of the quantum well should facilitate three-terminal device fabrication.[8–10]

In this communication we report results of a study of these new III-V double-barrier structures. In particular, by applying spacer techniques[11] and working with thinner barriers we have substantially improved the performance of the devices. The reason for having undoped spacer layers is the reduction of Si donors that diffuse into the barrier region during growth.[11] This reduces the impurity scattering resulting in a lower valley current. The potential drop in the undoped spacer layers also causes the peak to move to higher voltages compared to a sample with no spacer layers. We have increased the peak-to-valley current ratio to 2.9 at room temperature and to 10 at liquid-nitrogen temperature. Furthermore, we have made substantial increases in the peak currents by working with thinner barriers. The observed peak current densities are as high as 1.7×10^5 A/cm^2.

The structures were grown in a Perkin-Elmer 430 MBE system which included arsenic and antimony cracker sources. The growths were carried out using the techniques described in Ref. 12 which have been demonstrated to produce high-quality InAs and Sb-based layers. The substrates were GaAs which is subtantially lattice mismatched to InAs and AlSb. Growth commenced with a 0.5-μm-thick GaAs buffer layer at 600 °C. This buffer layer was followed by a superlattice consisting of $In_{0.7}Ga_{0.3}As$/GaAs grown at 500–520 °C. The superlattice reduces the number of strain-induced dislocations in the epilayer. The InAs/AlSb structures were grown at 500 °C. The device structure is shown in Fig. 1. A standard lift-off process followed by chemical etching was used to fabricate mesa structures (5 μm$\times$5 μm in

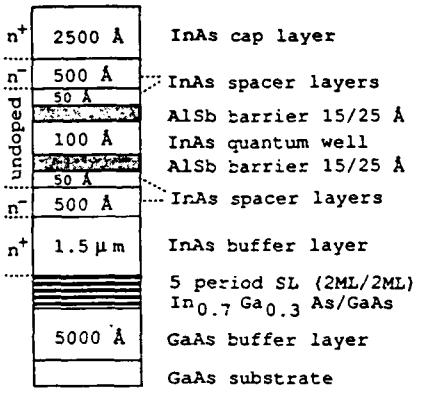

FIG. 1. Schematic diagram of a typical structure used in this study. The doping levels for the layers labeled n^- and n^+ are 2×10^{16} cm^{-3} and 2×10^{18} cm^{-3}, respectively.

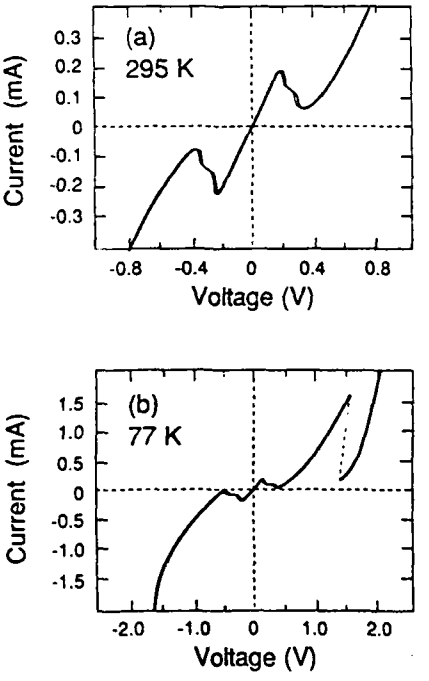

FIG. 2. The current-voltage characteristic of an InAs/AlSb/InAs/AlSb/InAs structure. The upper (lower) curve was taken at room temperature (77 K). The AlSb barriers were 25 Å thick and the InAs well was 100 Å thick.

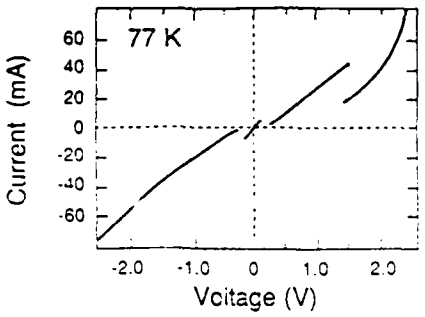

FIG. 3. The current-voltage characteristic at 77 K of InAs/AlSb/InAs/AlSb/InAs structure. The AlSb barriers were 15 Å thick and the InAs well was 100 Å thick.

size) with AuGe contacts on top. The back contact was produced by AuGe deposited on the etched InAs buffer layer.

Current-voltage (I-V) characteristics for these tunnel devices are shown in Figs. 2 and 3. The I-V characteristics shown in Fig. 2 are for a structure with 25-Å-thick AlSb barriers and an InAs well thickness of 100 Å. As can be seen from these I-V characteristics, a single peak is observed at room temperature with a peak-to-valley current (P/V) ratio of 2.9. At liquid-nitrogen temperature, two peaks are observed in forward bias and one in reverse. For the first peak, we observed a P/V ratio of 6 and for the second peak a P/V ratio of 10.

The I-V characteristic at 77 K from a second sample with 15-Å AlSb barriers and InAs well layer thickness of 100 Å is shown in Fig. 3. Again, this structure shows one peak at room temperature and two peaks at liquid-nitrogen temperature. For the second peak at liquid-nitrogen temperature, we observe a peak current density of 1.7×10^5 A/cm^2 and a P/V ratio of 2.3. This compares favorably to the previous results for InAs/AlSb structures where peak current densities less than 400 A/cm^2 were obtained.[7] Our result is also close to what has been obtained for the extensively studied GaAs/AlAs system for which peak current densities $\simeq2\times10^5$ have been reported.[13] These very large peak current densities are in the range of interest for making high speed tunnel devices.[4]

In summary, we have reported the results of a study of a new heterojunction system for double-barrier tunnel structures. By the application of some of the simple techniques of improving negative resistance, that is the addition spacer layers and the use of thinner barriers, we have substantially improved the performance over those previously reported. In particular, we have increased the peak-to-valley current ratio by roughly a factor of 2 at room temperature and have observed substantial improvements in the peak current densities. In different structures, we have been able to demonstrate very large current densities and peak-to-valley current ratios which if they could be produced in the same structure would bring them near the region of interest as defined in Ref. 4. These performance goals seem well within the range that one might hope to attain in these structures. We believe that these new device structures based on the AlSb/InAs heterojunction will be very interesting for further applications in tunneling devices.

The authors gratefully acknowledge the support of the Air Force Office of Scientific Research under Grant No. 86-0306. One of us (J.R.S.) gratefully acknowledges the support of the Sweden-America Foundation. Another (D.H.C.) gratefully acknowledges the support provided by a TRW-PAT Fellowship.

[1]R. Tsu and L. Esaki, Appl. Phys. Lett. **22**, 562 (1977).
[2]T. C. L. G. Sollner, W. D. Goodhue, P. E. Tannewald, C. Parker, and D. D. Peck, Appl. Phys. Lett. **43**, 588 (1983).
[3]A. R. Bonnefoi, R. T. Collins, T. C. McGill, and R. Burnham, Appl. Phys. Lett. **46**, 285 (1985).
[4]S. Hiyamizu, T. Fujii, S. Muto, T. Inata, Y. Nakata, Y. Sugiyama, and S. Sasa, J. Cryst. Growth **81**, 349 (1987).
[5]T. Inata, S. Muto, Y. Nakata, S.Sasa, T. Fuji, and S. Hiyamzu, Jpn. J. Appl. Phys. **26**, L1332 (1987).
[6]E. T. Yu and T.C. McGill, Appl. Phys. Lett. **53**, 60 (1988).
[7]L. F. Luo, R. Beresford, and W. I. Wang, Appl. Phys. Lett. **53**, 2320 (1988).
[8]A. R. Bonnefoi, T. C. McGill, and R. D. Burnham, IEEE Electron Device Lett. **EDL-6**, 636 (1985).
[9]A. R. Bonnefoi, D. H. Chow, and T. C. McGill, Appl. Phys. Lett. **47**, 888 (1985).
[10]J. N. Schulman and M. Waldner, J. Appl. Phys. **63**, 2859 (1988).
[11]C. I. Hwang, M. J. Paulus, C. A. Bozada, S. C. Dudley, K. R. Evans, C. E. Statz, R. L. Jones, and M. E. Cheney, Appl. Phys. Lett. **51**, 121 (1987).
[12]J. R. Söderström, D. H. Chow, and T. C. McGill, Proceedings of the Spring MRS Meeting, San Diego, California April, 1989 (to be published).
[13]S. K. Diamond, E. Ozbay, M. J. Rodwell, D. M. Bloom, Y. C. Pao, E. Wolak, and J. S. Harris, IEEE Electron Device Lett. **EDL-10**, 104 (1989).

Appendix A-6. InAs/AlSb Double Barrier Structures with Large Peak to Valley Current Ratios. A Candidate for High Frequency Microwave Devices. J. R. Soderstrom, D. H. Chow and T. C. McGill.

InAs/AlSb Double-Barrier Structure with Large Peak-to-Valley Current Ratio: A Candidate for High-Frequency Microwave Devices

J. R. SÖDERSTRÖM, D. H. CHOW, AND T. C. McGILL, MEMBER, IEEE

Abstract—We report negative differential resistance (NDR) in InAs/AlSb/InAs/AlSb/InAs double-barrier structures with peak-to-valley current (PVC) ratios as large as 11 (28) at room temperature (77 K). This is a large improvement over previous results for these materials, and also considerably better than those obtained for the extensively studied GaAs/AlGaAs material system. We have also improved the peak current density by reducing the barrier thickness and observed values exceeding 10^5 A/cm^2. These results suggest that InAs/AlSb structures are interesting alternatives to conventional GaAs/AlGaAs structures in high-frequency devices. We also report NDR in a InAs/AlSb superlattice double-barrier structure, with a lower PVC ratio than in the solid barrier case. This result indicates that valley current contributions arising from X-point tunneling are negligible in these structures, consistent with the large band offset.

SINCE the first observation of negative differential resistance (NDR) in semiconductor double-barrier structures [1], there has been much effort aimed towards improving the characteristics of these devices. The peak-to-valley current (PVC) ratio and the peak current density are often used as figures of merit. For the extensively investigated GaAs/AlGaAs material system, PVC ratios of 3.6 (21) at room temperature (77 K) have been reported [2]. The highest peak current densities observed are about $1-2 \times 10^5$ A/cm^2. However, such high current densities have only been realized in samples with much lower PVC ratios [3]. For applications such as microwave oscillators and fast digital switches, some other parameters of importance are series resistance, capacitance of the active region, quantum-well charging/discharging time, and drift time over the depletion region. In a recent study by Brown *et al.*, in which microwave oscillations at 420 GHz were reported, it was suggested that series resistance in the GaAs cladding layers and ohmic contacts were responsible for limiting the maximum frequency [4]. In an attempt to solve these inherent problems of GaAs/AlGaAs structures, we have investigated the properties of InAs/AlSb double-barrier structures. InAs has a low effective mass and hence a high mobility and low resistivity. Furthermore, a metal-InAs junction does not form a Schottky barrier (n-type InAs bows down at the interface), resulting in a very low-resistance contact. Another advantage of this structure is the large conduction-band offset: 1.35 eV for the Γ-X barrier (InAs Γ-point to AlSb X-point) and about 2 eV for the Γ-Γ barrier [5]–[7]. This is much larger than for any GaAs/AlGaAs structure and should result in lower valley currents. The first observation of NDR in InAs/AlSb double-barrier structures was reported by Luo *et al.* [8], who obtained PVC ratios of 1.8 (9.0) at room temperature (77 K) and current densities around 400 A/cm^2. In a preliminary study of these structures we were able to improve these results somewhat [9]. The InAs/AlGaSb material system has recently also been used for other NDR devices such as the single-barrier structure [10], [11] and the novel resonant interband tunneling (RIT) structure [12] with good results.

In this letter we report InAs/AlSb double-barrier structures with PVC ratios as high as 11 (28) at room temperature (77 K), which is much better than previous results for these structures and also better than what has been reported for GaAs/AlGaAs structures. We have also investigated the effect of reducing the barrier thickness and observed peak current densities as high as 2.6×10^5 A/cm^2. The larger peak current densities are achieved at the expense of lower PVC ratios. We also report the first InAs/AlSb double-barrier structure with superlattice barriers. This result provides information regarding the importance of X-point tunneling in this material system.

The samples were grown on GaAs (100) substrates in a Perkin-Elmer 430 molecular beam epitaxy (MBE) system. An As cracker and an Sb cracker were used to produce dimers instead of tetramers in the molecular beams. The details of bulk growth parameters for these materials can be found elsewhere [13]. Due to the large lattice mismatch (7.2 percent) between the GaAs substrate and the InAs epilayer, a thick buffer layer was grown. The buffer layer consisted of 2500-Å GaAs grown at 600°C, a five-period $In_{0.7}Ga_{0.3}As$/GaAs (two monolayers/two monolayers) superlattice grown at 500–520°C, and 1.0-μm InAs (heavily Si-doped) grown at 500°C. The superlattice at the GaAs/InAs interface is believed to reduce the number of strain-induced dislocations which penetrate into the InAs layer [13].

The double-barrier structure was grown at 500°C on top of the buffer layer and consisted of a 65-Å InAs quantum well sandwiched between AlSb barriers, 50-Å undoped InAs

Manuscript received September 19, 1989. This work was supported by the Air Force Office of Scientific Research under Grant 86-0306. J. R. Söderström and D. H. Chow were supported by the Sweden-America Foundation and TRW, respectively.

J. R. Söderström was with the T. J. Watson, Sr., Laboratory of Applied Physics, California Institute of Technology, Pasadena, CA. He is now with the Department of Physics, Chalmers University of Technology, S-412 96 Göteborg, Sweden.

D. H. Chow and T. C. McGill are with the T. J. Watson, Sr., Laboratory of Applied Physics, California Institute of Technology, Pasadena, CA 91125.

IEEE Log Number 8933292.

0741-3106/90/0100-0027$01.00

spacer layers, and 500-Å lightly doped ($n = 2 \times 10^{16}\ cm^{-3}$) InAs spacer layers. Finally, a 2500-Å-thick heavily doped ($n = 2 \times 10^{18}\ cm^{-3}$) InAs cap layer was grown. Five samples with AlSb barrier thickness varying from nine monolayers (ML's) to three ML's were grown. In the superlattice double-barrier sample, each barrier consisted of a three-period InAs (3 ML)/AlSb (3 ML) superlattice.

Mesa structures (area 25 μm^2) with Au/Ge contacts on top were prepared using standard photolithography, lift-off, and chemical etch techniques. Au/Ge deposited on the etched InAs buffer layer served as the "back" contact. No annealing was necessary since Au/Ge forms an ohmic contact to InAs. The mesas were probed with a thin gold wire to establish electrical contact to the devices.

Fig. 1 shows the current-voltage (I-V) curve for the sample with nine ML (27-28 Å) barriers. A distinct peak around 0.3 V corresponding to tunneling through the quantum-well ground state can be seen. The PVC ratios are 11 at room temperature and 28 at 77 K, which are much higher than previous results for these materials [8], [9]. This device also outperforms all GaAs/AlGaAs structures reported to date. We believe that this improvement is due to the higher barriers in the InAs/AlSb structure, particularly the Γ-X barrier which is about 1.35 eV compared to about 0.2 eV for GaAs/AlAs structures. The peak current density of this device is approximately $4 \times 10^3\ A/cm^2$.

To increase the peak current density, a set of samples with thinner barriers was grown. The barrier thicknesses for these four samples were seven, five, four, and three ML's, respectively. The result is shown in Fig. 2, where the PVC ratio is plotted against the measured peak current density. As the barriers become thinner the peak current densities increase at the expense of lower PVC ratios, as might be expected. The three-ML sample had a peak current density as high as $2.6 \times 10^5\ A/cm^2$ while the PVC ratio was down to 1.2 at 77 K (no NDR at room temperature). The four-ML sample had a current density of $1.6 \times 10^5\ A/cm^2$ and PVC ratios of 1.4 and 5.0 at 295 K and 77 K, respectively. The combination of high current density and relatively large PVC ratio makes this device a promising candidate for high-frequency microwave applications. It should be pointed out that these encouraging results are obtained without any effort to optimize the doping of the structure. We believe that with an asymmetric and optimized doping profile, current densities higher than $10^5\ A/cm^2$ could be obtained for five-ML or even six-ML barriers, with hence improved PVC ratios.

GaAs/AlAs superlattice double-barrier structures have previously been studied, yielding better PVC ratios than those for solid barriers [2]. The reason for this improvement is not completely understood. One explanation has been that the multiple interfaces trap impurities and imperfections in the crystal, resulting in a "cleaner" quantum well [14], and another that the superlattice reduces X-point tunneling due to an increase in the X-point effective mass [15]. By testing the superlattice barrier for the InAs/AlSb system we could help to resolve this issue. The structure used was identical to the nine-ML double-barrier structure from Fig. 1 except that each barrier was split up into three thinner barriers. In Fig. 3, the I-V curve displaying PVC ratios of 6.5 (18) at room temperature (77 K) is shown. This is worse than for the solid-barrier sample. This result is the opposite of that reported for GaAs/AlAs superlattice double-barrier structures, suggesting that the improved PVC ratios for GaAs/AlAs structures are due to the reduction of X-point tunneling. In InAs/AlSb structures, X-point tunneling can be neglected for the solid barriers due to the 1.35-eV band offset, and hence no reduction of valley current is obtained when using superlattice barriers. Moreover, the superlattice barrier increases the total barrier

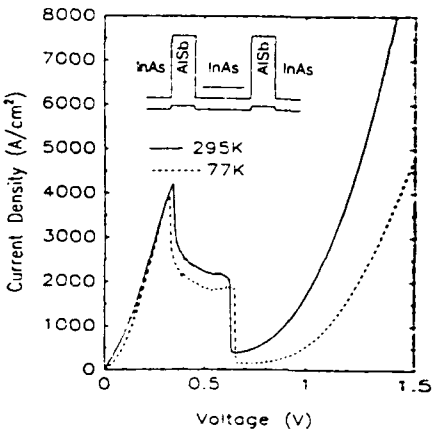

Fig. 1. Current-voltage characteristic of a double-barrier structure with nine-ML-thick AlSb barriers. The PVC ratio is 11 at room temperature and 28 at 77 K.

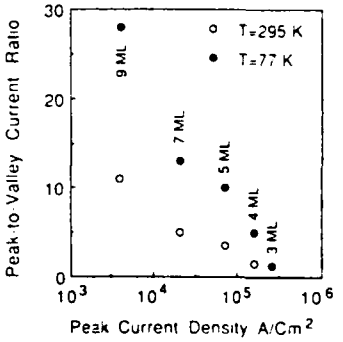

Fig. 2. PVC ratio plotted against peak current density for samples with different barrier thicknesses. The indicated barrier thicknesses correspond to the points vertically below (or above) the label.

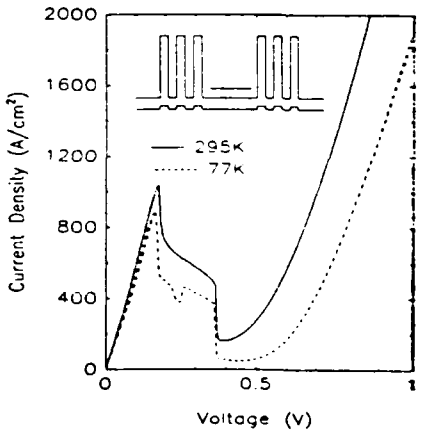

Fig. 3. Current-voltage characteristic of a superlattice double-barrier structure in which each barrier consists of three AlSb barriers (three ML thick) separated by InAs layers (three ML thick). The PVC ratio is 6.5 at room temperature and 18 at 77 K.

thickness (even though the number of AlSb layers is the same), which reduces the peak voltage to about 0.2 V. This is because a larger part of the bias is dropped across the barriers and thus less voltage is required to line up the quantum-well state with the Fermi level in the emitter contact. At these lower voltages the supply of electrons in the emitter contact is reduced, which can explain the lower peak current density ($\sim 10^3$ A/cm^2) for the superlattice barrier sample.

In summary we have studied MBE-grown InAs/AlSb double-barrier structures and obtained PVC ratios as high as 11 (28) at room temperature (77 K) for a structure with nine-ML-thick solid barriers. When the barriers are made thinner, the peak current densities increase and the PVC ratios decrease. A sample with four-ML barriers had a peak current density of 1.6×10^5 A/cm^2 and a PVC ratio of 5 at 77 K, placing this structure well into the interesting region for microwave devices. The PVC ratio was lower in a superlattice barrier sample compared to a sample with solid barriers. This result is consistent with the high Γ–X barrier in this material system, which eliminates most X-point currents in the solid barrier structure and cancels out the positive effect of the superlattice for suppression of these currents.

These results demonstrate that InAs/AlSb structures are serious competitors to the extensively studied GaAs/AlGaAs structures, particularly since they can be grown on GaAs substrates. Higher PVC ratios, higher current densities, and lower series resistance are factors which favor InAs/AlSb over GaAs/AlGaAs structures for future high-speed devices.

References

[1] L. L. Chang, L. Esaki, and R. Tsu, "Resonant tunneling in semiconductor double barriers," *Appl. Phys. Lett.*, vol. 24, pp. 593–595, 1974.

[2] C. I. Huang *et al.*, "AlGaAs/GaAs double barrier diodes with high peak-to-valley current ratio," *Appl. Phys. Lett.*, vol. 51, pp. 121–125, 1987.

[3] S. K. Diamond *et al.*, "Fabrication of 200-GHz f_{max} resonant tunneling diodes for integrated circuits and microwave applications," *IEEE Electron Device Lett.*, vol. 10, pp. 104–106, 1989.

[4] E. R. Brown, T. C. L. G. Sollner, C. D. Parker, W. D. Goodhue, and C. L. Chen, "Oscillations up to 420 GHz in GaAs/AlAs resonant-tunneling diodes," *Appl. Phys. Lett.*, vol. 55, pp. 1777–1779, 1989.

[5] A. Nakagawa, H. Kroemer, and J. H. English, "Electrical properties and band offsets of InAs/AlSb n-N isotupe heterojunctions grown on GaAs," *Appl. Phys. Lett.*, vol. 54, pp. 1893–1895, 1989.

[6] G. J. Gulatieri, G. P. Schwarz, R. G. Nuzzo, R. J. Malik, and J. F. Walker, "Determination of the (100) InAs/GaSb heterojunction valence-band discontunity by x-ray photoemission core level spectroscopy," *J. Appl. Phys.*, vol. 61, pp. 5337–5341, 1987.

[7] G. J. Gulatieri, G. P. Schwarz, R. G. Nuzzo, and W. A. Sunder, "X-ray photoemission core level determination of the GaSb/AlSb heterojunction valence-band discontinuity," *Appl. Phys. Lett.*, vol. 49, pp. 1037–1039, 1986.

[8] L. F. Luo, R. Beresford, and W. I. Wang, "Resonant tunneling in AlSb/InAl/AsSb double-barrier heterostructures," *Appl. Phys. Lett.*, vol. 53, pp. 2320–2322, 1988.

[9] J. R. Söderström, D. H. Chow, and T. C. McGill, "Observation of large peak-to-valley current ratios and large peak current densities in AlSb/InAs/AlSb double barrier structures," *J. Appl. Phys.*, vol. 66, pp. 5106–5108, 1989.

[10] R. Beresford, L. F. Luo, and W. I. Wang, "Negative differential resistance in AlGaSb/InAs single-barrier heterostructures at room temperature," *Appl. Phys. Lett.*, vol. 54, pp. 1899–1901, 1989.

[11] J. R. Söderström, D. H. Chow, and T. C. McGill, "Demonstration of large peak-to-valley current ratios in InAs/AlGaSb/InAs single barrier structures," *Appl Phys. Lett.*, vol. 55, pp. 1348–1350, 1989.

[12] J. R. Söderström, D. H. Chow, and T. C. McGill, "A new negative differential resistance device based on resonant interband tunneling," *Appl. Phys. Lett.*, vol. 55, pp. 1094–1096, 1989.

[13] J. R. Söderström, D. H. Chow, and T. C. McGill, "MBE-growth of InAs and GaSb epitaxial layers on GaAs substrates," to be published in *Proc. MRS 1989 Spring Meeting* (San Diego, CA), 1989.

[14] L. F. Luo R. Beresford, W. I. Wang, and E. E. Mendez, "Inelastic tunneling in (111) oriented AlAs/GaAs/AlAs double-barrier heterostructures," *Appl. Phys. Lett.*, vol. 54, pp. 2133–2135, 1989.

Appendix A-7. Negative Differential Resistance due to Resonant Interband Tunneling of Holes. D. H. Chow, E. T. Yu, J. R. Soderstrom, and D. Z.-Y. Ting, and T. C. McGill.

Negative differential resistance due to resonant interband tunneling of holes

D. H. Chow, E. T. Yu, J. R. Söderström,[a] D. Z. -Y. Ting, and T. C. McGill
T. J. Watson Sr. Laboratory of Applied Physics, California Institute of Technology, Pasadena, California 91125

(Received 16 April 1990; accepted for publication 11 June 1990)

The current-voltage (I-V) behavior of a GaSb(p)/AlSb/InAs/AlSb/GaSb(p) resonant interband tunneling (RIT) heterostructure is analyzed experimentally and theoretically. The structure has been successfully grown on a (100)-oriented GaAs substrate by molecular-beam epitaxy, demonstrating that more exotic lattice-matched substrates (such as InAs or GaSb) are not required for RIT devices. Theoretical simulations of I-V behavior are developed, employing a two-band tight-binding model. Experimental I-V curves show pronounced negative differential resistance, with a peak-to-valley current ratio of 8.3 at 300 K. Good agreement is observed between measured and calculated peak current densities, consistent with light-hole tunneling through the confined InAs conduction-band state.

Quantum mechanical tunneling of charge carriers in semiconductor heterostructures continues to be a subject of great interest. Much of the motivation for studying tunnel structures stems from their potential high-frequency analog and digital applications.[1,2] Many early tunneling studies were performed on GaAs/AlAs double-barrier heterostructures, in which negative differential resistance (NDR) results from resonant tunneling of electrons through a GaAs quantum well. More recently, NDR has been demonstrated in a variety of novel tunnel structures involving different materials and band alignments.[3–11] Several of these new heterostructures are superior to the best GaAs/AlAs double barriers in terms of peak current densities and/or peak-to-valley current ratios. In particular, resonant interband tunneling (RIT) devices have recently been proposed[10] and demonstrated.[9,11] In these structures, electrons or holes in one material tunnel through quasi-bound valence- or conduction-band states, respectively, in a different material. This mechanism yields a drastic suppression of valley currents due to the blocking nature of the quantum-well layer past resonance. Söderström, Chow, and McGill[9] observed peak-to-valley current ratios as large as 20:1 (88:1) at 300 K (77 K) from an InAs(n)/AlSb/GaSb/AlSb/InAs(n)(n-type InAs electrodes, AlSb barriers, and a GaSb quantum well) RIT structure. Later, Luo, Beresford, and Wang[11] reported peak-to-valley ratios as large as 13:1 (60:1) at 300 K (77 K) from a GaSb(p)/AlSb/InAs/AlSb/GaSb(p) RIT structure. However, it should be noted that Luo *et al.* obtain this peak-to-valley ratio from an extremely hysteretic I-V curve by dividing the peak current in one sweep direction by the valley current obtained in the opposite direction. Values obtained from a single sweep direction appear to be substantially lower.

In this communication, we study the current-voltage (I-V) behavior of a GaSb(p)/AlSb/InAs/AlSb/GaSb(p) heterostructure experimentally and theoretically. Growth parameters and device fabrication features have been selected to reduce the effects of parasitic series resistance in the GaSb electrodes, yielding NDR without hysteresis. Peak-to-valley current ratios are thus determined unambiguously. Theoretical simulations of I-V curves for the RIT device have been developed, based upon a two-band tight-binding model. Comparisons are made between the calculated I-V curves and those obtained experimentally.

Figure 1 contains a band-edge diagram for the heterostructure studied here. The GaSb/AlSb and GaSb/InAs valence-band offsets are taken to be 400 and 510 meV, respectively.[12,13] It is assumed that the band offsets are both transitive and commutative. The crucial feature of the diagram is that the conduction-band edge in the InAs quantum well is *lower* in energy than the valence-band edge in the GaSb electrodes. The InAs layer has been grown sufficiently thick to keep the quantum-well ground state below the GaSb valence-band maximum. Due to the strong coupling between conduction-band and light-hole states, a transmission resonance exists for light holes in the GaSb electrodes whose energies and parallel wave vectors match those of states in the two-dimensional quantum-well subband. It is straightforward to show that this resonance condition can be satisfied for small applied biases (no threshold voltage). A peak in the I-V curve is expected when the applied bias becomes large enough to lower the valence-band edge in the positively biased GaSb electrode below the ground-state energy in the InAs quantum well. Beyond this point, the tunneling probability is drastically reduced due to the blocking nature of the thick InAs layer at energies in its band gap. It should be noted that heavy holes are not expected to contribute significantly to the tunneling current because they are weakly coupled to conduction-band states.

We have developed a theoretical model to simulate the current-voltage behavior of tunnel structures in which interactions between valence- and conduction-band states are important. The simulation begins by computing the band-edge diagram throughout the heterostructure via the Pois-

[a]Present address: Chalmers University of Technology, Department of Physics, S-41296, Goteborg, Sweden.

 0021-8979/90/193744-03$03.00

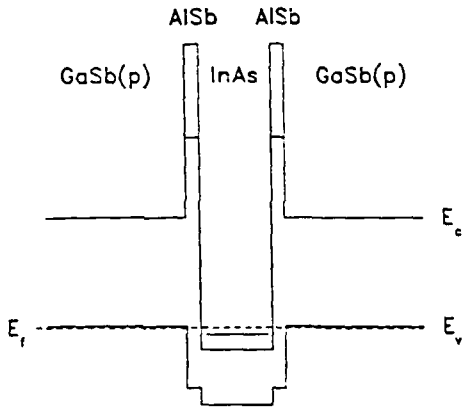

FIG. 1. Schematic band-edge diagram (energy vs position) for the GaSb(p)/AlSb/InAs/AlSb/GaSb(p) resonant interband tunneling heterostructure. The conduction-band edge, E_c, valence-band edge, E_v, and Fermi energy, E_f, are labeled. The indirect (lower) and direct (higher) conduction-band edges are both shown in the AlSb layers.

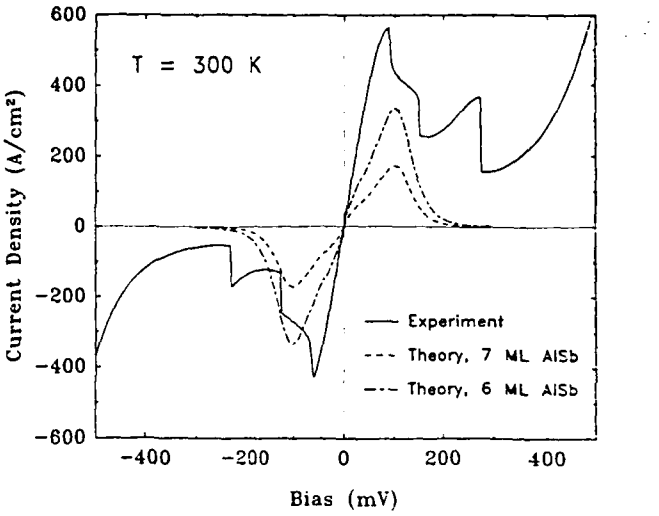

FIG. 2. Experimental current density vs voltage curve (solid), taken from a 10×10-μm device at 300 K. The forward-bias direction is taken to be when positive voltage is applied to the mesa. The curve displays peak-to-valley current ratios of 8.8 and 3.6 in the reverse- and forward-bias directions, respectively. Also plotted are theoretically calculated curves for 6 (dot-dashed) and 7 (dashed) monolayer AlSb barrier layers. The theoretical model includes only light-hole contributions to the resonant interband tunneling current.

son equation for each applied bias. In the case of the RIT structure studied here, the heavy-hole band dominates the band-bending behavior in the GaSb electrodes because its density of states is 15 times greater than that of the light-hole band. Next, localized two-band tight-binding orbitals (at each monolayer) are used to generate transfer matrices for the tunneling states. In this manner, a transmission coefficient is determined as a function of the energy (E) and parallel wave vector ($\mathbf{k}_\parallel$) of each state. In our model, only the conduction and light-hole bands are used to determine the tight-binding parameters for each material. The restriction to these two bands is effectively an assumption that only electron-light hole coupling is significant in the tunnel structure (heavy-hole tunneling is ignored). Finally, the current density is obtained by including appropriate velocities and Fermi factors and integrating over E and $\mathbf{k}_\parallel$. It should be noted that we do *not* use fitted parameters in our comparison of measured and simulated current-voltage curves.

The RIT structure was grown on a (100)-GaAs substrate by molecular-beam epitaxy (MBE) in a Perkin Elmer 430 system equipped with cracked As and Sb sources. Growth commenced with a 2500-Å undoped GaAs layer grown at 600 °C, followed by a 10-period, 1 monolayer/1 monolayer GaSb superlattice deposited at 520 °C. The substrate temperature was then lowered to 480 °C for the remainder of the growth. The bottom electrode of the RIT structure consisted of a 0.5-μm GaSb(p^+) buffer layer, a 200-Å GaSb(p) spacer, with $p=2\times10^{16}$ cm^{-3}, and a 25-Å undoped GaSb layer. Subsequently, a 100-Å undoped InAs quantum well was deposited, sandwiched between two 20-Å undoped AlSb barriers. The heterostructure was completed by 25 Å of undoped GaSb, a 200-Å GaSb(p) spacer layer (with $p=2\times10^{16}$ cm^{-3}), and a 2500-Å GaSb(p^+) cap.

X-ray diffraction has shown that the short-period superlattice at the GaAs/GaSb interface yields a strain-relaxed GaSb bottom electrode layer.[14] Cross-sectional transmission electron microscopy shows that a dense network of dislocations appears during the short-period superlattice, with the vast majority of threading dislocations confined to the first 1000 Å of the GaSb layer. The remainder of the GaSb cladding layer appears to be planar, with reasonable dislocation densities ($\approx10^9$ cm^{-2}). Reflection high-energy electron diffraction (RHEED) shows a streaky 1×3 pattern, comparable to that obtainable for homoepitaxial growth of GaSb, within the first 200 Å (2 min) of the cladding layer. p-type doping of the GaSb layer was achieved by simultaneous evaporation of Si during MBE growth. It has recently been shown that Si is a substitutional (for Sb) p-type dopant under these growth conditions, yielding controllable carrier concentrations over the range 10^{16}–5×10^{18} cm^{-3}.[15]

Rectangular 10×10 μm mesas were fabricated in the RIT structure by chemical etching in Br_2:HBR:H_2O (0.5:100:100). Au/Ge was used to make electrical contacts to the mesas and etched surface, forming a set of two-terminal devices. The device areas were sufficiently small to eliminate parasitic series resistance effects (hysteresis) arising from lateral transport of the holes through the bottom GaSb(p^+) electrode. It has recently been shown that interband tunneling devices with n-type electrodes can yield extremely high current densities ($>10^5$ A/cm^{-2}).[16] Due to the low heavy-hole mobilities, it is likely that small lateral separations and/or thicker bottom electrode layers would be needed to avoid hysteresis in p-type RIT structures with extremely high current densities.

Figure 2 displays a current density-versus-voltage curve, taken at 300 K from one of the fabricated devices. Also plotted are theoretical curves, calculated by the method described previously, for symmetric 6- and 7-monolayer (18.4 and 21.5 Å) AlSb barrier layers; the AlSb

layers in the RIT structure are nominally 20 Å thick. The experimental curve shows pronounced NDR in both bias directions, with peak-to-valley current ratios of 8.3 and 3.6 in reverse and forward bias, respectively (we take forward bias to mean positive voltage applied to the mesa). The peak current density is 430 A/cm^2 (560 A/cm^2) in reverse (forward) bias, and varied by less than 15% over ten randomly chosen devices. As is expected for RIT structures, there is no threshold voltage for the current because the interband tunneling condition is satisfied at zero bias. At 77 K, the valley current shown in Fig. 2 drops by a factor of 2, with the peak current remaining nearly constant. This temperature dependence indicates that thermally activated mechanisms are at least partially responsible for limiting the peak-to-valley ratio at room temperature, but do not make a substantial contribution to the peak current.

As shown in Fig. 2, the peak current densities predicted by the theoretical model are in good agreement with those measured experimentally. It has been suggested that the high scattering rate of heavy holes in bulk GaSb to the light hole band results in identical tunneling probabilities for the two types of carriers.[11] If this were the case, we would expect the large heavy-hole density of states to yield measured peak current densities greater than our theoretically predicted value by more than one order of magnitude. Thus, the observed agreement between the experimental and theoretical current densities suggests that heavy-hole tunneling probabilities are small. The experimental curve shown in Fig. 2 displays some asymmetry, with the forward-bias peak appearing 20 mV higher than the reverse-bias peak. This feature is probably caused by unintentional asymmetries in the doping profile of the device, introduced during growth.

It should be noted that the observed valley currents are significantly higher than the calculated values shown in Fig. 2. It has been reported that valley currents in conventional resonant tunneling structures can be dominated by elastic scattering mechanisms which result in nonconservation of the momentum parallel to the interfaces.[17] However, these mechanisms are disallowed in interband tunneling structures at high bias because the quantum-well subband does not overlap in energy with the tunneling states. Hence, the observed discrepancy between the calculated and observed valley currents suggests that transport mechanisms other than elastic tunneling dominate the current beyond resonance.

In summary, we have analyzed a GaSb(p)/AlSb/InAs/AlSb/GaSb(p) RIT heterostructure experimentally and theoretically. The resonant interband tunneling mechanism yields large peak-to-valley current ratios at 300 K due to the blocking nature of the InAs quantum well at energies in its band gap. The structure studied here was successfully grown on a (100)-oriented GaAs substrate with the assistance of a short-period superlattice buffer layer at the GaSb/GaAs interface. This result is consistent with several recent reports of successful tunnel structures with large lattice mismatches to GaAs.[4,7–9] Thus, it appears that excellent device behavior can be obtained without resorting to more exotic lattice-matched substrates such as InAs or GaSb. We have developed a theoretical model to simulate the current-voltage behavior of heterostructures in which strong interactions exist between conduction- and valence-band states. The model is a two-band tight-binding approach, in which localized orbitals are used to generate transfer matrices for the tunneling states. The observed agreement between the calculated and measured peak current densities is consistent with small interband tunneling probabilities for heavy holes.

We would like to acknowledge helpful discussions with D. A. Collins and L. R. Dawson. The support of the Office of Naval Research and the Air Force Office of Scientific research under Grant Nos. N00014-89-J-1141 and AFOSR-86-0306, respectively, has made it possible for us to carry out this program. J. R. Söderström received financial support from the Wilhelm and Martina Lundgren Foundation. E. T. Yu was supported in part by the AT&T Foundation.

[1] E. R. Brown, T. C. L. G. Sollner, C. D. Parker, W. D. Goodhue, and C. L. Chen, Appl. Phys. Lett. **55**, 1777 (1989).
[2] F. Capasso, S. Sen, A. Y. Cho, and D. L. Sivco, Appl. Phys. Lett. **53**, 1056 (1988).
[3] T. Inata, S. Muto, Y. Nakata, T. Fujii, H. Ohnishi, and S. Hiyamizu, Jpn. J. Appl. Phys. **26**, L220 (1987).
[4] D. H. Chow, T. C. McGill, I. K. Sou, J. P. Faurie, and C. W. Nieh, Appl. Phys. Lett. **52**, 54 (1988).
[5] T. P. E. Broekaert, W. Lee, and C. G. Fonstad, Appl. Phys. Lett. **53**, 1545 (1988).
[6] L. F. Luo, R. Beresford, and W. I. Wang, Appl. Phys. Lett. **53**, 2320 (1988).
[7] J. R. Söderström, D. H. Chow, and T. C. McGill, IEEE Electron. Devices Lett. **11**, 27 (1990).
[8] H. Munekata, T. P. Smith III, and L. L. Chang, Appl. Phys. Lett. **55**, 1348 (1989).
[9] J. R. Söderström, D. H. Chow, and T. C. McGill, Appl. Phys. Lett. **55**, 1094 (1989).
[10] M. Sweeney and J. Xu, Appl. Phys. Lett. **54**, 546 (1989).
[11] L. F. Luo, R. Beresford, and W. I. Wang, Appl. Phys. Lett. **55**, 2023 (1989).
[12] G. J. Gualtieri, G. P. Schwartz, R. G. Nuzzo, R. J. Malik, and J. F. Walker, J. Appl. Phys. **61**, 5337 (1987).
[13] G. J. Gualtieri, G. P. Schwartz, R. G. Nuzzo, and W. A. Sunder, Appl. Phys. Lett. **49**, 1037 (1986).
[14] D. H. Chow, R. H. Miles, J. R. Söderström, and T. C. McGill, J. Vac. Sci. Technol. B **8**, 710 (1990).
[15] T. M. Rossi, D. A. Collins, D. H. Chow, and T. C. McGill, J. Appl. Phys. (to be published).
[16] D. Z.-Y. Ting, D. A. Collins, E. T. Yu, D. H. Chow, and T. C. McGill, Appl. Phys. Lett. (to be published).
[17] P. Gueret, C. Rossel, W. Schlup, and H. P. Meier, J. Appl. Phys. **66**, 4312 (1989).

Appendix A-8. Large Peak Current Densities in Novel Resonant Interband Tunneling Heterostructures. D. Z.-Y. Ting, D. A. Collins, E. T. Yu, D. H. Chow, and T. C. McGill.

Large peak current densities in novel resonant interband tunneling heterostructures

D. Z.-Y. Ting, D. A. Collins, E. T. Yu, D. H. Chow, and T. C. McGill
Thomas J. Watson, Sr. Laboratory of Applied Physics, California Institute of Technology, Pasadena, California 91125

(Received 21 May 199[illegible]; accepted for publication 20 July 1990)

We have observed negative differential resistance (NDR) and large peak current densities in a novel resonant interband tunneling structure grown by molecular beam epitaxy in the InAs/GaSb/AlSb material system. The structure consists of a thin AlSb barrier layer displaced from an InAs(n)/GaSb(p) interface. NDR is readily observable at room temperature with peak current densities greater than 10^5 A/cm^2. The enhancement in peak current density relative to a structure with no AlSb barrier is consistent with the existence of a quasi-bound state in the region between the barrier and the InAs/GaAs interface. Furthermore, we demonstrate that by growing the AlSb layer on either the InAs or GaSb side of the interface, the quasi-bound state can be localized in either material.

The unique features of resonant tunneling diodes have been intensively studied since their original proposal[1] and demonstration.[2] The motivation has been to understand the physics of these devices as well as the possibility of using them to make electronic devices, such as high-speed digital switches and high-frequency oscillators. Recently, a new class of tunnel structures, grown in the nearly lattice-matched InAs/GaSb/AlSb material system, has been proposed[3] and demonstrated.[4,5] These resonant interband tunneling (RIT) structures produce negative differential resistance (NDR) by exploiting the broken gap band alignment of InAs and GaSb. Devices with peak-to-valley current ratios as high as 20:1 (88:1) at room temperature (77 K) have been realized. The first RIT structures consist of a GaSb (InAs) quantum well, sandwiched between two thin AlSb barrier layers and two n-type InAs (p-type GaSb) electrodes; at low applied bias, transport is dominated by electrons (holes) tunneling resonantly through the quasi-bound valence (conduction-) band state. A second class of RITs has also been demonstrated.[6,7] These devices consist of a thin GaSb layer sandwiched between two n-type InAs electrodes, resulting in a quasi-bound state in the GaSb valence band due to the mismatch of the wave functions at the InAs/GaSb interface. These structures have peak current densities greater than 10^4 A/cm^2 and, due to the weak confinement provided by InAs/GaSb interface, theoretically estimated tunneling times of ~25 fs.[8,9] NDR has also been demonstrated in interband structures without resonant states, both in an InAs(n)/AlSb/GaSb(p) heterostructure,[5] and in a device consisting of a single InAs(n)/GaSb(p) interface.[10] In both of these interband structures, the mechanism that gives rise to NDR is similar to that of a p^+-n^+ tunnel diode. However, carriers do not tunnel through through a classically forbidden region in the structure with a single InAs(n)/GaSb(p) interface.

Figure 1 shows schematic band-edge diagrams of a single InAs(n)/GaSb(a) interface structure [Fig. 1(a)], and the RITs discussed in this letter [Figs. 1(b) and 1(c)]. The InAs/GaSb and AlSb/GaSb valence-band offsets are taken to be 510 meV[11] and 400 meV,[12] respectively. The InAs/AlSb valence-band offset is taken to be 110 meV. Figure 1(b) depicts a GaSb quantum well and thin AlSb barrier sandwiched between InAs(n) and GaSb(p) electrodes. In Fig. 1(c), a thin AlSb barrier and InAs quantum well are placed between the InAs(n) and GaSb(p) electrodes. All three structures depicted in Fig. 1 are expected to display NDR when sufficient positive bias is applied to the GaSb(p) electrode to shut off elastic transport of electrons from the InAs(n) electrode into available GaSb states. In this letter, we report evidence that the formation of a quantum well layer between the InAs/GaSb interface and an AlSb barrier results in a resonant enhancement of

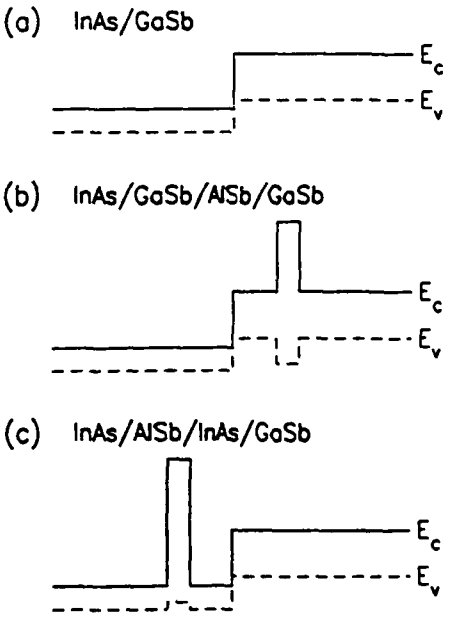

FIG. 1. Schematic band-edge diagrams (energy vs position) for (a) an InAs(n)/GaSb(p) interface, (b) an InAs(n)/GaSb/AlSb/GaSb(p) heterostructure, and (c) an InAs(n)/AlSb/InAs/GaSp(p) heterostructure. In all three diagrams, the conduction (E_c, solid) and valence (E_v, dashed) band edges are shown. The insertion of the AlSb barrier layers in (b) and (c) is hypothesized to create quasi-bound states in the regions between the barriers and the InAs/GaSb interfaces.

 0003-6951/90/381257-03$02.00

TABLE I. Layer sequences for the samples.

Sample No.	Band diagram	Layer sequence
1	Fig. 1(a)	InAs(n)/GaSb(p)
2	Fig. 1(b)	InAs(n)/GaSb(51 Å)/AlSb(12 Å)/GaSb(p)
3	Fig. 1(c)	InAs(n)//AlSb(21 Å)/InAs(120 Å)/GaSb(p)

the current density as compared to the InAs(n)/GaSb(p) interface structure depicted in Fig. 1(a). Peak current densities greater than 10^5 A/cm^2 are observed, suggested that these structures may find applications as high-frequency oscillators.

In Table I we give the layer sequences and thicknesses for the samples grown in our study. Sample 1 corresponds to the band-edge diagram in Fig. 1(a), while samples 2 and 3 correspond to Figs. 1(b) and 1(c), respectively. The samples were grown on GaAs substrates in a Perkin–Elmer molecular beam epitaxy system. Our method for growing high quality InAs, GaSb, and AlSb films on GaAs substrates has been reported elsewhere.[13] Si was used to dope the InAs electrodes n type and the GaSb electrodes p type.[14] In samples 2 and 3, the AlSb layers, quantum wells, and additional 100 Å spacer layers on the InAs sides of the active regions were undoped. There were no undoped spacer layers in sample 1. After growth, mesas 6 μm in diameter were fabricated using photolithography and a wet etch in Br_2:HBr:H_2O (0.5:100:100). Current-voltage (I-V) curves were measured at room temperature and 77 K by probing the mesas with a thin gold wire. Au/Ge was used to make ohmic contacts to the mesas and etched surfaces.

In Fig. 2 we show representative I-V curves [positive bias on the GaSb(p) electrodes] at room temperature for samples 1 (dashed) and 2 (solid). The peak current density is much larger in sample 2 ($\approx 1.6\times10^5$ A/cm^2) than in sample 1 ($\approx 0.4\times10^5$ A/cm^2). This result is consistent

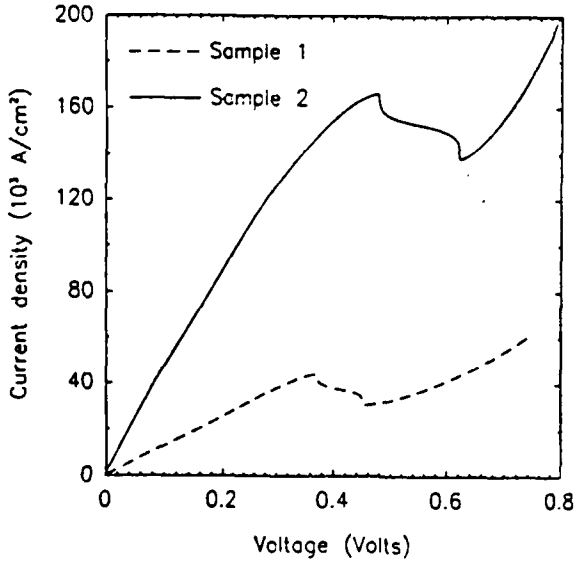

FIG. 2. Current density vs voltage curves for samples 1 (dashed) and 2 (solid). The enhanced current density in sample 2 is consistent with resonant tunneling via a quasi-bound state in the GaSb quantum well.

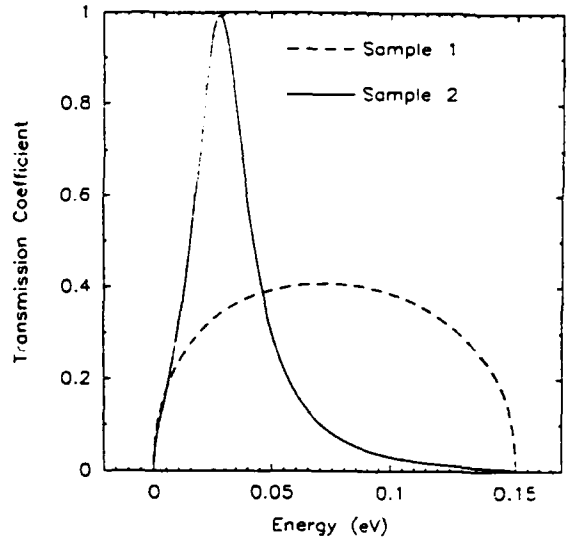

FIG. 3. Transmission coefficient for samples 1 (dashed) and 2 (solid), calculated at flatband conditions, using a two-band model which incorporates electrons and light holes. The InAs conduction-band edge is taken to be the zero of energy.

with the formation of a quasi-bound state in the region between the InAs/GaSb interface and the AlSb barrier in sample 2, leading to resonant tunneling of carriers across the structures. At resonance, the reflection coefficient for the carriers in sample 2 nearly vanishes; in contrast, significant reflection occurs at all energies for the single InAs(n)/GaSb(p) interface, due to the imperfect coupling of InAs conduction-band states to GaSb valence-band states. Figure 3 displays transmission coefficients for samples 1 (dashed) and 2 (solid), calculated at flatband conditions using a two-band model which incorporates electrons and light holes.[9] In the figure, the InAs conduction-band edge is taken to be the zero of energy. We estimate that the Fermi level in the InAs(n) electrode lies 30 meV above the conduction-band edge. Figure 3 shows that sample 2 possesses a wide transmission resonance near the estimated Fermi level, which peaks well above the maximum transmission probability for the single InAs(n)/GaSb(p) interface structure. The observed enhancement in the peak current density in sample 2 suggests that reflection coefficients at the InAs/GaSb interface are not negligible. In fact, the formation of a quasi-bound state in the quantum well of this structure is dependent upon nonnegligible reflections at the interfaces (Fabry–Perot effect).

As a further demonstration of the tunneling mechanism described above, we have grown sample 3 with a 21 Å AlSb barrier and 120 Å InAs quantum well sandwiched between InAs(n) and GaSb(p) electrodes, corresponding to the band-edge diagram of Fig. 1(c). In this sample, we expect that a quasi-bound state will be formed in the InAs quantum well due to the confinement of the AlSb barrier and the partially reflecting InAs/GaSb interface. The AlSb layer has been grown substantially thicker than that of sample 2, resulting in reduced current densities. This sample displayed NDR, with a peak-to-valley current ratio of 1.5:1 and a peak current density of 6.7×10^3 A/cm^2. This

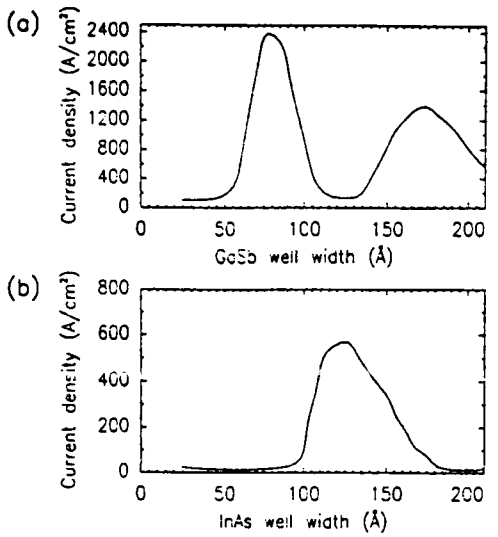

FIG. 4. Calculated current densities vs quantum well width for (a) the heterostructure depicted in Fig. 1(b), and (b) the heterostructure depicted in Fig. 1(c). Both figures show enhanced current densities corresponding to quasi-bound states in the region of overlap between the InAs conduction band and the GaSb valence band.

result demonstrates that resonant interband tunneling can be observed with the AlSb barrier placed on either side of the InAs/GaSb interface. It should be noted that placing the AlSb barrier at the InAs/GaSb interface will reduce the current carried by the device, since the addition of the AlSb layer will not cause the formation of a quasi-bound state. However, larger peak-to-valley ratios have been observed in such a structure,[5] presumably due to reduced inelastic currents across the interface.

In Figs. 4 (a) and 4(b) we show plots of the calculated peak current densities for the structures depicted in Figs. 1(b) and 1(c), respectively, as functions of quantum well width. The theoretical model used to perform the calculation has been described elsewhere.[9] The AlSb barriers have been taken to be 24 Å thick. The curves in Fig. 4 have similar shapes, with the maximum current density occurring at narrower widths for GaSb quantum wells than for InAs quantum wells, due to the difference in the effective masses of the two materials. At relatively thick GaSb layer thicknesses ($\approx$170 Å), Fig. 4(a) shows a current density enhancement due to the appearance of a second quasi-bound state. It should be noted that we have included only light holes in our theoretical model, under the assumption that electron–heavy hole coupling is weak. Due to the sensitivity of the calculation to the input parameters (such as band offset values), we have not attempted to compare the calculated current densities to those measured experimentally. However, the calculation does show that there is an optimal position for placement of the AlSb barrier. This position corresponds to a single quasi-bound state in the region of overlap between the InAs conduction band and the GaSb valence band.

The calculated transmission coefficient for sample 2 shown in Fig. 3 has a full width at half maximum of $\sim$28 meV, corresponding to a lifetime of $\sim$25 fs. This puts an intrinsic upper limit on the oscillation frequency of this structure of about 6 THz. It is almost certain that any real oscillator will roll off at a lower frequency due to series resistance, depletion capacitance, and the intrinsic response time of the materials which make up the structure. Hence, the tunneling time in these structures will not be the limiting factor in determining the maximum oscillation frequency. Furthermore, the large currents carried by these devices indicates that their output power should be large enough to be of practical interest.

In summary, we have observed NDR in two novel resonant interband tunneling devices. In these structures, a GaSb or InAs quantum well is formed between a thin AlSb barrier layer and an InAs/GaSb interface. Extremely high current densities (greater than 10^5 A/cm^2) are realized due to resonant enhancement of the transmission coefficient, relative to a single InAs(n)/GaSb(p) interface structure. Furthermore, the weak confinement provided by the InAs/GaSb interface results in a broad quasi-bound state with an intrinsic lifetime of $\sim$25 fs for a structure with a 12 Å AlSb barrier. As a result of this short lifetime and the output power implied by the large peak current densities, these structures hold promise as high-frequency oscillators.

The authors would like to thank Y. Rajakarunanayake and J. R. Söderström for helpful discussions. This work was supported by the Office of Naval Research and the Air Force Office of Scientific under grant Nos. N00014-89-J-1141 and AFOSR-86-0306, respectively. E. T. Yu was supported in part by the AT&T Foundation.

[1] R. Tsu and L. Esaki, Appl. Phys. Lett. 22, 562 (1973).
[2] L. L. Chang, L. Esaki, and R. Tsu, Appl. Phys. Lett. 24, 593 (1974).
[3] M. Sweeny and J. Xu, Appl. Phys. Lett. 54, 546 (1989).
[4] J. R. Söderström, D. H. Chow, and T. C. McGill, Appl. Phys. Lett. 55, 1094 (1989).
[5] L. F. Luo, R. Beresford, and W. I. Wang, Appl. Phys. Lett. 55, 2023 (1989).
[6] K. Taira, I. Hase, and K. Kawai, Electron. Lett. 25, 1708 (1989).
[7] D. A. Collins, D. H. Chow, and T. C. McGill (unpublished).
[8] J. R. Söderström, E. T. Yu, M. K. Jackson, Y. Rajakarunanayake, and T. C. McGill, J. Appl. Phys. 68, 1372 (1990).
[9] D. Z.-Y. Ting, E. T. Yu, D. A. Collins, D. H. Chow, and T. C. McGill, J. Vac. Sci. Technol. B 8, 810 (1990).
[10] D. A. Collins, E. T. Yu, Y. Rajakarunanayake, J. R. Söderström, D. Z.-Y. Ting, D. H. Chow, and T. C. McGill, Appl. Phys. Lett. 57, 683 (1990).
[11] G. J. Gaultieri, G. P. Schwartz, R. G. Nuzzo, R. J. Malik, and J. F. Walker, J. Appl. Phys. 61, 5337 (1987).
[12] G. J. Gaultieri, G. P. Schwartz, R. G. Nuzzo, and W. A. Sunder, Appl. Phys. Lett. 49, 1037 (1986).
[13] J. R. Söderström, D. H. Chow, and T. C. McGill, Mater. Res. Soc. Symp. Proc. 145, 409 (1989).
[14] T. M. Rossi, D. A. Collins, D. H. Chow, and T. C. McGill (unpublished).

Appendix A-9. Interband Tunneling in InAs/GaSb/AlSb Heterostructures. D. A. Collins, D. Z. Y.-Ting, D. H. Chow, and E. T. Yu.

Presented at MBE-VI Poster Session
1990

Interband Tunneling in InAs/GaSb/AlSb Heterostructures

D A. Collins, D. Z.-Y. Ting, D. H. Chow, E. T. Yu,

J.R. Söderström[a)], Y. Rajakarunanayake, and T. C. McGill

Thomas J. Watson, Sr. Laboratory of Applied Physics

California Institute of Technology

Pasadena, California 91125

Abstract

The nearly-lattice matched InAs/GaSb/AlSb material system offers a large degree of flexibility for growing tunneling heterostructures. In particular, the unique staggered band alignment of InAs/GaSb allows electrons to move between the conduction band of InAs and the valence band of GaSb making possible a new class of tunnel structures known as interband devices. We report the experimental observation of negative differential resistance (NDR) at room temperature from a structure consisting of a single InAs(n)/GaSb(p) interface. The peak current densities ranged from 4.2×10^4 A/cm^2 to 8.0×10^4 A/cm^2 depending on how the structure is doped. The mechanism that causes the NDR is similar to that of an Esaki tunnel diode. We have also observed NDR at room temperature in a second class of novel devices. These structures consist of a thin layer of AlSb displaced from a single InAs(n)/GaSb(p) interface. NDR with peak current densities greater than 1.5×10^5 A/cm^2 is seen in structures in which the AlSb barrier is placed in either the InAs or the GaSb. We attribute the increase in peak current densities with the addition of the AlSb barrier to the formation of a quasi-bound state between the AlSb layer and the InAs/GaSb interface. This quasi-bound state forms either in the conduction band of InAs or the valence band of GaSb depending on where the AlSb barrier is placed and leads to a resonat enhancement of the current in the structures. All of the devices' current-voltage characteristics show very little change when measured at 77 K indicating that thermionic currents play a negligible role in their operation.

[a)]Present address: Chalmers University of Technology, Department of Physics, S-41296 Göteborg, Sweden.

1. Introduction

Quantum mechanical tunneling in semiconductors as well as negative differential resistance (NDR) were first demonstrated in forward biased Esaki diodes[1]. An Esaki diode consists of a degenerately doped p–n diode. Because of the relative positions of the Fermi level and the conduction (valence) band of the n–type (p–type) material, under forward bias there are unoccupied states in the valence band of the p–type material with energies less than or equal to that of the quasi–Fermi level in the n–type material. As a result electrons can tunnel from the conduction band of the n–type material, across the depletion region and into the valence band of the p–type material allowing current to flow in the device. When the bias is increased to the point where the conduction band edge in the n–type material is above the valence band edge of the p–type material, interband tunneling stops because there are no available states for conduction band electrons in the n–type material to tunnel into. This sudden shutting off of the tunneling process leads to a reduction in current flow through the device and hence a region of NDR.

The discovery of NDR generated a tremendous amount of interest and research into Esaki diodes since NDR can be used to fabricate amplifiers [2] , oscillators [3] and high speed switches [4]. Although tunnel diode amplifiers have been built that operate at frequencies as high as 85 GHz, the Esaki diode has two main weaknesses: their small current densities ($\sim 10^3$ A/cm^2 [4]) limit them to much lower output powers then Gunn–effect or IMPATT diodes, and their large junction capacitance limits them to much lower frequencies than InAs/AlSb double barrier diodes which can be made to oscillate at fundamental frequencies greater than 700 GHz [5] .

In this work we report on a group of novel devices which show room temperature NDR due to a mechanism similar to that of an Esaki diode but with peak current densities of between 10^4 and 10^5 A/cm^2 (compared to $\sim 10^3$ A/cm^2 for Esaki diodes)

and which have junction capacitances which we estimate to be similar to those of double barrier diodes. These devices can be realized because of the unique staggered band alignment of InAs and GaSb in which the conduction band of InAs is 150 meV below the valence band of GaSb[6]. A schematic representation of the InAs/GaSb band alignments, which is strongly reminiscent of the band structure of an Esaki diode, is shown in Fig. 1(a). Because of this staggered band alignment a layer of GaSb(p^+) grown on InAs(n^+) should show NDR due a mechanism similar to that of an Esaki diode. Such structures, which we call heterojunction Esaki diodes (HED), have been grown and show NDR at room temperature with peak current densities ranging from 4.2×10^4 A/cm^2 to 8.0×10^4 A/cm^2 depending on how the structure is doped.

In addition we have grown a second class of novel structures, which we call resonance enhanced heterojunction Esaki diodes (REHED), which combine favorable aspects of the HED with those of double barrier diodes. The structures consist of a thin layer of AlSb (12 to 21 Å) displaced from a single InAs(n)/GaSb(p) interface. The energy band diagrams of these heterostructures are shown in Figs. 1(b) and 1(c). These devices also showed NDR at room temperature with peak current densities greater than 10^5 A/cm^2. We attribute the increase in peak current densities with the addition of a thin AlSb barrier to the formation of a quasi-bound state between the InAs/GaSb interface and the AlSb layer, which leads to a resonant enhancement of the device's current.

2. Experimental

In Table I we give the layer sequences and thicknesses for the samples grown for this study. The samples studied were grown on semi-insulating GaAs substrates in a Perkin-Elmer 430 molecular beam epitaxy system equipped with cracked Sb and As sources. The details of the crystal growth have been reported elsewhere [7]. Si was

used to dope the InAs electrodes n-type ($n \approx 2 \times 10^{17} cm^{-3}$) and the GaSb p-type ($p \approx 5 \times 10^{18}$ cm^{-3}) [8]. 100 Å undoped spacer layers were grown on each side of the InAs(n)/GaSb(p) interface in sample 1; there were no undoped spacer layers in sample 2. In samples 3 ,4 and 5, the AlSb layers, quantum wells, and additional 100 Å spacer layers on the InAs sides of the active regions were undoped.

After growth, device mesas 6 μm in diameter were fabricated using photolithography and a wet etch. The etch was stopped in the InAs epilayer so that no current flowed through the GaAs. Au/Ge was used to make ohmic contact to the individual devices. Current–voltage (I–V) curves were measured at room temperature and 77 K by probing the mesas with a thin gold wire. It is important to use devices with a small surface area due to the large current densities carried in these structures. Previous investigators studied the I–V curves of a structure consisting of an $In_{.84}Ga_{.16}As/GaSb_{.9}As_{.1}$ interface, but did not observe NDR [9]; we attribute this to the fact that the devices they fabricated had a device area over 250 times larger than the ones reported here. Because of the large current densities found in these structures (which are comparable to those measured by Sakaki *et al.*) it is essential to fabricate small area devices so that ohmic heating due to contact and parasitic series resistance does not destroy the device before it can be biased into the NDR region.

3. Results

In Figs. 2 and 3 we show representative I–V curves for HED structures (see Fig. 1(a)) with and without undoped spacer layers at the heterointerface, respectively. Both devices show NDR at room temperature with peak current densities greater than $8.2 \times 10^4 (4.0 \times 10^4)$ A/cm^2 for the structure with (without) undoped spacer layers at the heterointerface. I–V curves are shown at both 77 K and room temperature. The fact that the device's performance is virtually unchanged at the lower temperature indicates that thermionic emission plays only a minor role in the large valley current.

The observed temperature stability of these devices between 77 K and 300 K is similar to that of conventional Esaki diodes [10] .

The results for the REHED structures, whose schematic band edge diagrams are shown in Fig. 1(b) and 1(c) are more complicated. Both types of REHED structures showed NDR at room temperature with peak current densities ranging from to 6.7 $\times$ 10^3 A/cm^2 1.6 $\times$ 10^5 A/cm^2 depending on the thickness of the AlSb layer used. These structures also show a strong dependence of the peak current density on the distance between the AlSb barrier and the InAs/GaSb interface. In fact if the separation is too small NDR is observed. The qualitative behavior of both variants of the REHED can be explained by the existence of a quasi-bound state as will be shown in the discussion section.

4. Discussion

The valley currents in the HED structures are rather large considering that they should be blocked by the GaSb bandgap. However, because there is not a true barrier between the InAs conduction band and the GaSb valence band (see Fig. 1(a)) there is little to suppress inelastic processes from scattering electrons in the InAs conduction band into the GaSb valence band. It is interesting to note that in the I-V curves shown in Figs. 2 and 3 the difference between the peak current and the minimum valley current is approximately the same in both devices. The data strongly suggest that doping the device up to and through the interface reduces some of these background inelastic currents. This phenomenon will be discussed elsewhere [11].

There are some improvments that can be made to the HED if it were to be used in a high-speed application. One of the most important considerations would be to reduce the device's series resistance which will be dominated by the GaSb layer. However, the series resistance due to the GaSb layer could be greatly reduced simply by terminating the HED with a much thinner layer of GaSb. Because of the large

mass of the GaSb heavy hole and the doping densities of $p \approx 5 \times 10^{18}$ cm^{-3} the Thomas–Fermi screening length is about 20 Å which suggests that a GaSb layer as thin as 100 Å should be sufficiently thick to not adversly effect device performance. A thinner GaSb cap layer will reduce the HED's series resistance, a consideration which is important for any high speed application. Further, a thinner GaSb cap layer should improve the crystal's structural quality since there is a 0.6 % lattice mismatch between InAs and GaSb. As a result, the 2000 Å GaSb cap layer is greater than the critical thickness of GaSb grown on InAs which a Mathews–Blakesley model estimates to be a few hundred angstroms. Due to this we anticipate the formation of interfacial misfit dislocations which may degrade device performance. A GaSb cap layer below the critical thickness should reduce or even eliminate the number of these dislocations nucleated at the InAs/GaSb interface.

Because the NDR observed in HED structures is not associated with a quasi–bound state, which may have a long lifetime, they hold promise for the fabrication of high speed devices. The intrinsic upper limit of this structure's oscillation frequency will be determined by the transit time across the heterointerface and the inherent frequency response of the materials as well as the device's RC timeconstant. Furthermore, because this device can be grown without undoped spacer layers, limiting processes such as transit time delays across depleted regions which can be important in conventional double barrier heterostructures will be eliminated in this device [12].

In Fig. 4 we compare typical I–V curves for samples 2 and 3 (see table I.) The solid curve is for the REHED (see Fig. 1(b)) structure and the dashed curve is from the previously discussed HED (see Fig. 1(a)) structure. As the data show, the structure with the AlSb barrier is more conductive with a peak current density of more than $1.6 \times 10^5 A/cm^2$. This unintuitive behavior can be understood by examining the transmission coefficients of these structures. Fig. 5 displays transmission coefficients for samples 2 (dashed line) and 3 (solid line), calculated at flat band conditions us-

ing a two–band model which incorporates electrons and light holes [13]. The InAs conduction band edge is taken to be the zero of energy. The calculation shows that sample 3 possesses a broad resonance, in the region between the InAs conduction band and the GaSb valence band, which peaks well above the maximum transmission probability for the HED structure. The calculation indicates that a quasi–bound state forms in the region between the InAs/GaSb interface and the AlSb barrier in sample 3, leading to resonant tunneling of carriers across the structure at certain applied biases. At resonance, the reflection coefficient for the carriers in sample 3 nearly vanishes; in contrast, significant reflection occurs at all energies for the single InAs(n)/GaSb(p) interface, due to the imperfect coupling of InAs conduction band states to GaSb valence band states. The formation of a quasi–bound state in the REHED structure, as indicated by the calculation, is consistent with the experimentally observed enhancement in the peak current density. This also suggests that the reflection coefficients at the InAs/GaSb interface in sample 3 are not negligible. In fact, the existence of a transmission resonance in the REHED structure is dependent upon non–negligible reflections at the interfaces (a Fabry–Perot effect).

As a further demonstration of the tunneling mechanism described above, we have grown sample 4 with a 21 Å AlSb barrier and 120 Å InAs quantum well sandwiched between InAs(n) and GaSb(p) electrodes, corresponding to the band edge diagram of Fig. 1(c). In this sample, a quasi–bound state will be formed in the InAs quantum well due to the confinement of the AlSb barrier and the partially reflecting InAs/GaSb interface. The AlSb layer is thicker than that of sample 3, resulting in sharply reduced current densities. This sample displayed room temperature NDR, with a peak–to–valley current ratio of 1.5:1 and a peak current density of 6.7×10^3 A/cm^2. This result demonstrates that resonant interband tunneling can be observed with the AlSb barrier placed on either side of the InAs/GaSb interface. It should be noted that placing the AlSb barrier at the InAs/GaSb interface will reduce the current carried

by the device, since the addition of the AlSb layer will not cause the formation of a quasi-bound state. However, larger peak-to-valley ratios have been observed in such a structure [14], presumably due to suppression of inelastic transport across the interface; however, the peak current density in those structures was ≈ 10 A/cm^2.

In Fig. 6 we show I-V curves for samples 4 (solid line) and 5 (dashed line). These samples correspond to the band edge diagrams shown in Fig. 1(c) with the only difference between them being the width of the InAs well. As the figure shows for a narrow well there is no NDR present in the structure. This can be readily explained since our calculations show that for a 75 Å InAs well the confinement energy of the quasi-bound state pushes it above the valence band edge of the GaSb. As a result, this resonant level is unavailable to electrons tunneling across the structure leading to a quenching of the NDR.

The calculated transmission coefficient for sample 3 shown in Fig. 5 has a full width at half maximum of ~ 28 meV, corresponding to a lifetime of approximately 25 fsec. This puts an intrinsic upper limit on the oscillation frequency of this structure of about 6 THz. While it is almost certain that any real oscillator will roll off at a lower frequency due to series resistance, depletion capacitance and the intrinsic response time of the materials which make up the structure, the tunneling time in these structures will not be the limiting factor in determining the maximum oscillation frequency. Furthermore, the large currents carried by these devices indicates that their output power should be large enough to be of practical interest.

5. Conclusions

In conclusion we have demonstrated three novel variants of the Esaki diode: HED's which consist of a single InAs(n)/GaSb(p) interface and two types of REHED structures consisting of a thin AlSb barrier displaced from a single InAs(n)/GaSb(p) interface. The operation of these structures is dependent on the unique staggered band

alignment of InAs and GaSb as shown in Fig. 1(a). The mechanism that gives rise to NDR in these structures is similar to that of an Esaki diode. For devices consisting of a single InAs(n)/GaSb(p) interface we observed peak current densities ranging from 4.2×10^4 A/cm^2 to 8.0×10^4 A/cm^2 depending on how the structure is doped. We have also observed NDR at room temperature in devices consisting of a thin AlSb barrier displaced from an InAs/GaSb interface. In structures with the thinnest AlSb barriers we observed peak current densities of 1.6×10^5 A/cm^2 which is larger than in devices without the AlSb barrier. We also found that the device's I–V characteristics were extremely sensitive to the placement of the AlSb barrier. This sensitivity as well as the enhancement in the peak current density is consistent with the formation of a quasi–bound state in the region of the crystal bounded by the InAs/GaSb interface and the AlSb barrier layer.

6. Acknowledgments

The authors would like to thank P.C. Sercel for helpful discussions. This work was supported by the Office of Naval Research under contract No. N00014–89–J–1141 and the Air Force Office of Scientific Research under contract No. AFOSR–86–0306. E.T. Yu was supported in part by the AT & T Foundation.

References

[1] L. Esaki, Phys. Rev. **109**, p. 603 (1958).

[2] K.K.N. Chang, Proc. I.R.E. **47**, p. 1268 (1959).

[3] H.S. Sommers, Proc. I.R.E. **47**, p. 1201 (1959).

[4] H.S. Sommers, in *Selected Papers on Semiconductor Microwave Electronics* edited by S.N. Levine and R.M. Kurzrok (Dover, New York, 1964) p. 243.

[5] E.R. Brown, C.D. Parker, L.J. Mahoney, J.R. Soderstrom, andT.C. McGill, 48th Annual Device Research Conference Abstracts, IEEE Trans. Electron Devices, November 1990, in press.

[6] G.J. Gaultieri, G.P. Schwartz, R.G. Nuzzo, R.J. Malik, and J.F. Walker J. Appl. Phys. **61** p. 5337, (1987).

[7] D. A. Collins, E. T. Yu, Y. Rajakarunanayake, J.R. Söderström, D. Z.-Y. Ting, D. H. Chow,and T. C. McGill Appl. Phys. Lett. **57**, p. 683 (1990).

[8] T.M. Rossi, D.A. Collins, D.H. Chow, and T.C. McGill, to be published in Appl. Phys. Lett.

[9] H. Sakaki, L.L. Chang, R. Ludeke, Chin-An Chang, G.A. Sai-Halasz and L. Esaki Appl. Phys. Lett. **31**, 211 (1977).

[10] R.N. Hall, in *Selected Papers on Semiconductor Microwave Electronics* edited by S.N. Levine and R.M. Kurzrok (Dover, New York, 1964) p. 18.

[11] D.A. Collins and T.C. McGill, unpublished.

[12] E.R. Brown, W.D. Goodhue and T.C.L.G. Sollner, J. Appl. Phys. **64** (3), p. 1519 (1988).

[13] D.Z.-Y. Ting, E.T. Yu, D.A. Collins, D.H. Chow and T.C. McGill, to appear in J. Vac. Sci. Technol.B, July/August 1990.

[14] L. F. Luo, R. Beresford, and W. I. Wang, Appl. Phys. Lett. 55, p. 2023 (1989).

CAPTIONS

Figure 1 Schematic band edge diagrams (neglecting band bending) of the structures grown for this study.

Figure 2 Representative I–V curves for sample 1 (a HED structure.) The solid line was taken at room temperature and the dashed at 77 K.

Figure 3 Representative I–V curves for sample 2 (a HED structure.) The solid line was taken at room temperature and the dashed at 77 K.

Figure 4 I–V curves for samples 2, a HED structure (dashed line), and 3, a REHED structure (solid line.) The enhanced current density in sample 3 is consistent with resonant tunneling via a quasi–bound state in the GaSb quantum well.

Figure 5 Transmission coefficients for samples 2, a HED structure (dashed line), and 3, a REHED structure (solid line), calculated at flat band conditions, using a two–band model which incorporates electrons and light holes. The InAs conduction band edge is taken to be the zero of energy.

Figure 6 I–V curves for samples 4 and 5 showing the dramatic effect that the separation between the AlSb barrier and the InAs/GaSb has on device performance. The solid (dashed) line corresponds to a structure with a 120 Å (75 Å) InAs quantum well.

TABLE I. Layer sequences for the samples.

Sample number	Band diagram	Layer sequence
1	Fig. 2(a)	InAs(n)/undoped InAs(100 Å)/undoped GaSb(100 Å)/GaSb(p^+)
2	Fig. 2(a)	InAs(n)/GaSb(p^+)
3	Fig. 2(b)	InAs(n)/GaSb(51 Å)/AlSb(12 Å)/GaSb(p^+)
4	Fig. 2(c)	InAs(n)/AlSb(21 Å)/InAs(120 Å)/GaSb(p^+)
5	Fig. 2(c)	InAs(n)/AlSb(21 Å)/InAs(75 Å)/GaSb(p^+)

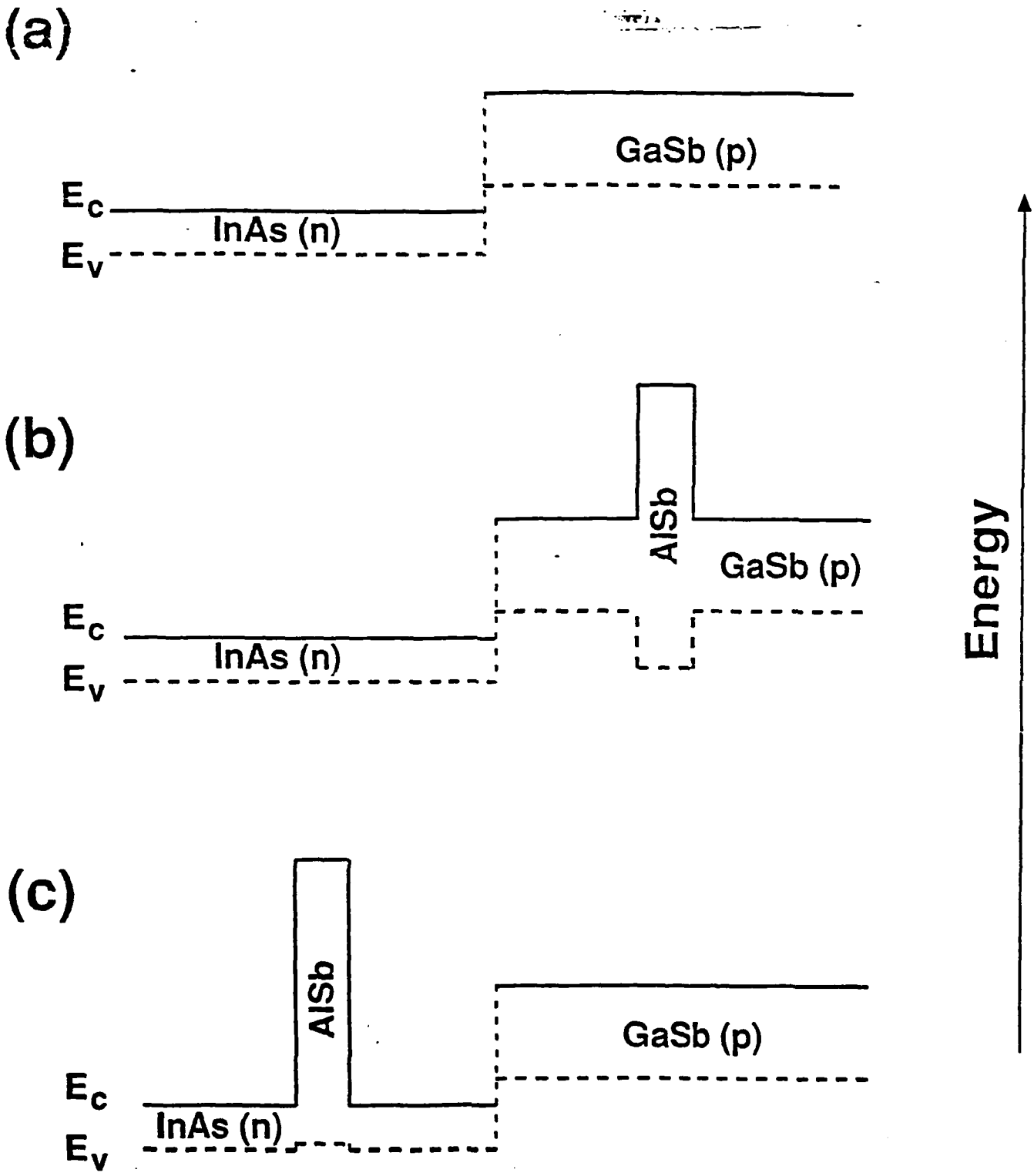
(a)
GaSb (p)
E_c
InAs (n)
E_v
(b)
AlSb
GaSb (p)
E_c
InAs (n)
E_v
(c)
AlSb
GaSb (p)
E_c
InAs (n)
E_v
Energy
Position along growth axis.

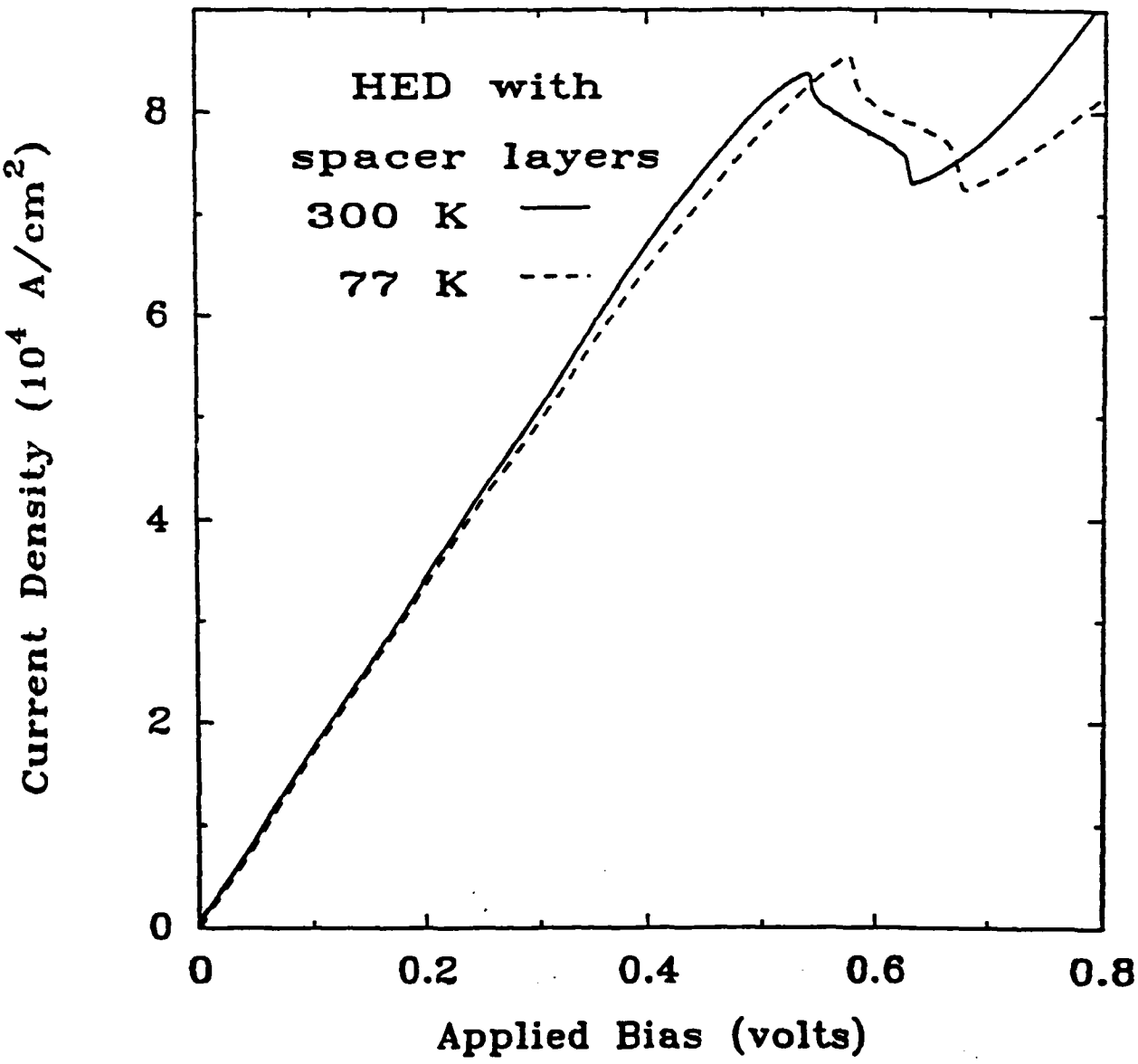
HED with
spacer layers
300 K
77 K
Current Density (10^4 A/cm^2)
0
2
4
6
8
0
0.2
0.4
0.6
0.8
Applied Bias (volts)

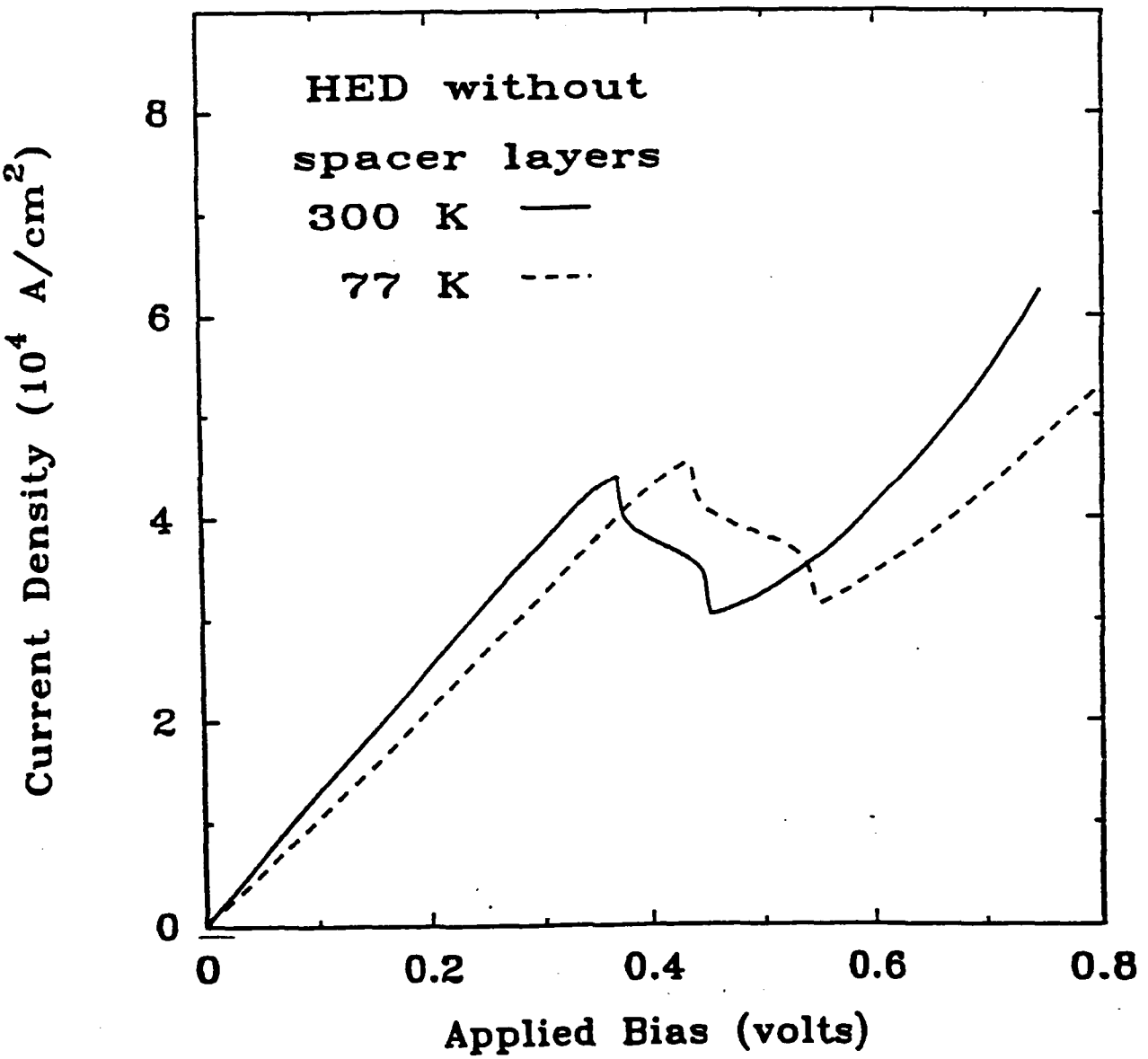
HED without
spacer layers
300 K
77 K
Current Density (10^4 A/cm^2)
0
2
4
6
8
0
0.2
0.4
0.6
0.8
Applied Bias (volts)

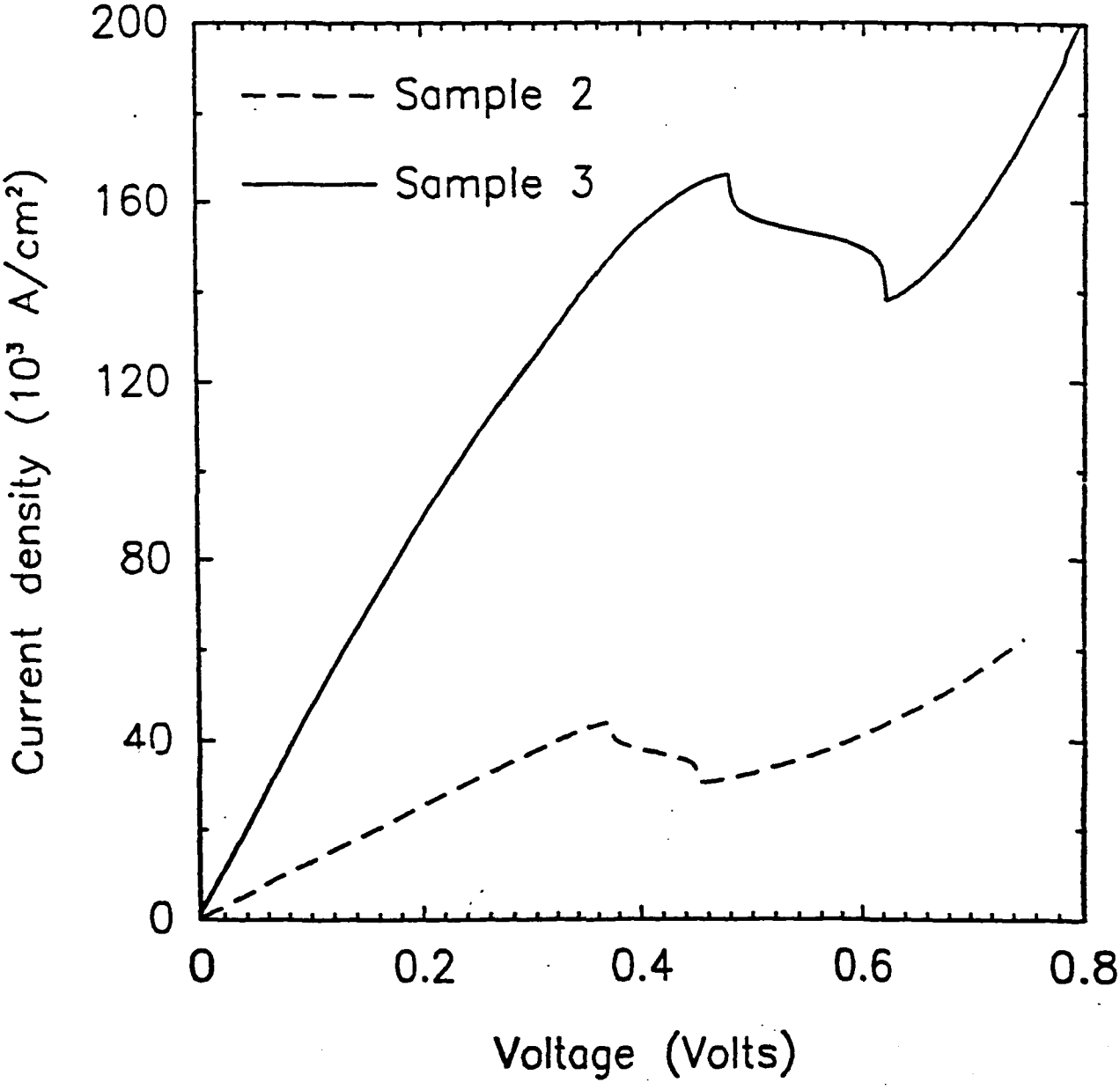
200
160
120
80
40
0
Current density (10^3 A/cm^2)
Sample 2
Sample 3
0
0.2
0.4
0.6
0.8
Voltage (Volts)

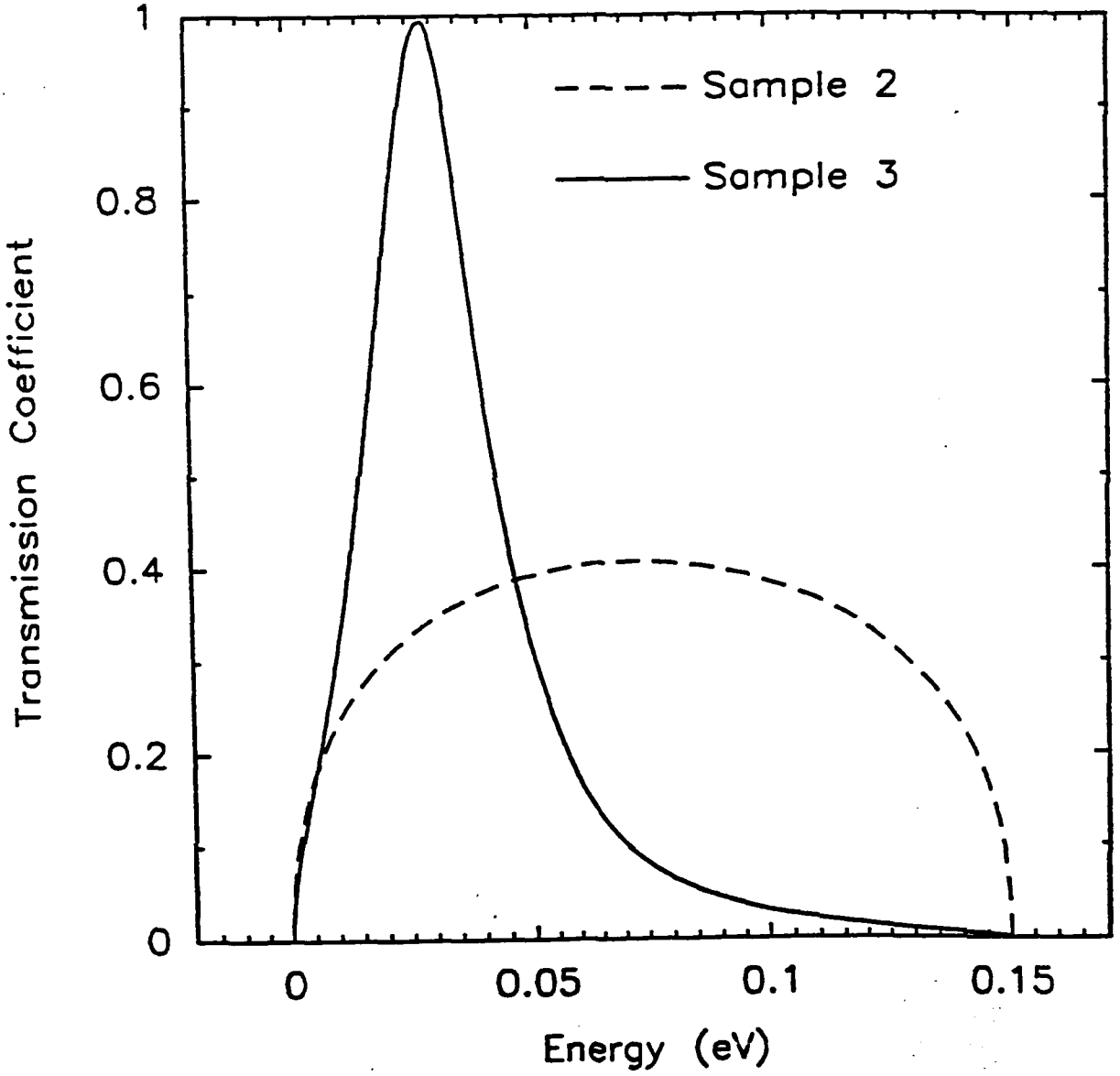
Sample 2
Sample 3
Transmission Coefficient
Energy (eV)
1
0.8
0.6
0.4
0.2
0
0
0.05
0.1
0.15

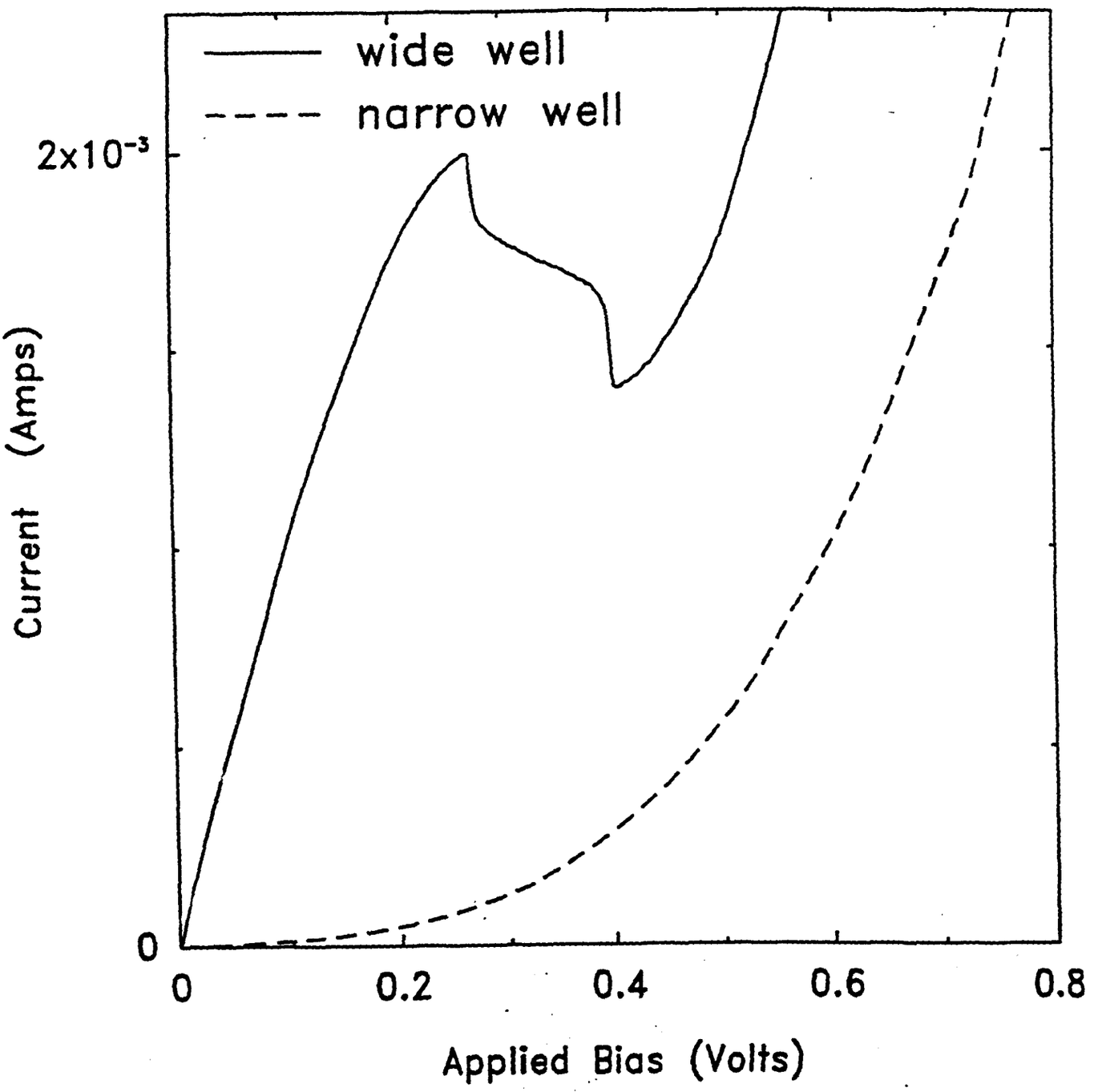
wide well
narrow well
2x10⁻³
0
Current (Amps)
0
0.2
0.4
0.6
0.8
Applied Bias (Volts)

Appendix A-10. Novel InAs/GaSb/AlSb Tunnel Structures. D. H. Chow, J. R. Soderstrom, and D. A. Collins.

Invited Paper

Novel InAs/GaSb/AlSb tunnel structures

D.H. Chow, J.R. Söderström, D.A. Collins,
D.Z.-Y. Ting, E.T. Yu and T.C. McGill

California Institute of Technology
Pasadena, California 91125

ABSTRACT

The nearly lattice–matched InAs/GaSb/AlSb system offers tremendous flexibility in designing novel heterostructures due to its wide range of band alignments. We have recently exploited this advantage to demonstrate a new class of negative differential resistance (NDR) devices based on interband tunneling. We have also studied "traditional" double barrier (resonant) and single barrier NDR tunnel structures in the InAs/GaSb/AlSb system. Several of the interband and resonant tunneling structures display excellent peak current densities (as high as 4×10^5 A/cm^2) and/or peak–to–valley current ratios (as high as 20:1 and 88:1 at 300 K and 77 K, respectively), offering great promise for high frequency and logic applications.

1. INTRODUCTION

Quantum mechanical tunneling of charge carriers in semiconductor heterostructures continues to be a subject of great interest. Much of the motivation for studying tunnel structures stems from their potential high frequency analog applications.[1] For example, a 420 GHz oscillator was recently demonstrated using a GaAs/AlAs resonant tunneling diode.[2] It has also been proposed that three terminal devices incorporating GaAs/AlAs tunnel structures could have advantages in digital applications via multiple level logic.[3]

In spite of the progress that has been made with GaAs/AlAs (and $Al_xGa_{1-x}As$) resonant tunneling structures, it has become clear that fundamental limitations exist on their performance. Maximum peak current densities of approximately 1.5×10^5 A/cm^2 can be reached only by reducing room temperature peak–to–valley ratios to 2:1 or less.[2,4] Further improvements seem unlikely because of inherently poor GaAs ohmic contacts and low indirect conduction band minima in the AlAs barriers. The nearly lattice–matched InAs/GaSb/AlSb material system would seem to be an attractive alternative to GaAs/AlAs because of its flexibility for tunnel structure design. Fig. 1 displays the band edges of the three materials, using recent band offset data.[5,6] In addition to the obvious flexibility enhancement derived from having three materials from which to choose, this material system allows for the possibility of staggered and broken–gap band alignments. Furthermore, the InAs/AlSb conduction band offset is substantially higher than that of GaAs/AlAs (referring to the indirect conduction band minima in AlSb and AlAs). Finally, InAs and GaSb are excellent materials for n–type and p–type ohmic contacts, respectively.

In this paper, we present experimental results from several InAs/GaSb/AlSb tunnel structures. Several of these new heterostructures are superior to the best GaAs/AlAs double barriers in terms of peak current densities and/or peak–to–valley current ratios. The tunnel structures can be divided into three classes, based upon the mechanisms through

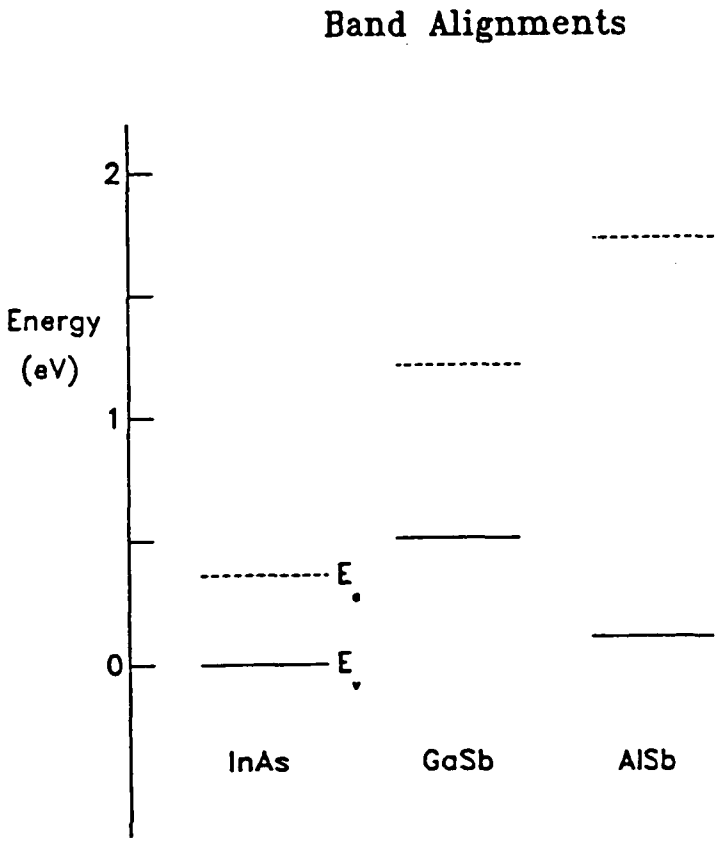

Fig. 1. Conduction (dashed) and valence (solid) band edges of InAs, GaSb, and AlSb. Band offsets values have been taken from recent x-ray photoemission reports.[5,6]

which they produce negative differential resistance (NDR): "conventional" resonant tunneling, single barrier (simple elastic) tunneling, and resonant interband tunneling. In the first category, InAs/AlSb double barrier heterostructures have been shown to yield peak current densities and peak-to-valley current ratios superior to those obtainable from GaAs/AlAs (or GaAs/$Al_zGa_{1-z}As$) double barriers. The other two categories of tunnel structures result directly from the staggered (InAs/$Ga_{1-z}Al_zSb$) and broken-gap (InAs/GaSb) band alignments afforded by this material system. In the case of the resonant interband tunneling devices, extremely high peak-to-valley curent ratios with reasonable peak current densities have been observed.

2. EXPERIMENTAL

2.1. Growth

All of the tunnel structures studied have been grown by molecular beam epitaxy (MBE) on (100)-oriented GaAs substrates. The Perkin Elmer 430 MBE system is equipped with cracked As and Sb sources, which produce dimeric molecular beams of the two materials

(As_2 and Sb_2). Substrate temperatures above 500°C were monitored with an optical pyrometer, calibrated to the GaAs oxide desorption temperature and the As-stabilized to In-stabilized transition in the surface reconstruction of InAs. A thermocouple in contact with a molybdenum block, to which the substrate was bonded with indium, was used to estimate temperatures below 500°C.

The InAs/GaSb/AlSb heterostructures were deposited on thick, strain-relaxed buffer layers of InAs or GaSb, depending upon whether InAs(n^+) or GaSb(p^+) electrodes were desired. In both cases, a short period, heavily strained superlattice was grown at the GaAs/buffer layer interface to reduce the number of threading dislocations in the buffer layer.[7,8] For InAs electrodes, growth commenced with 3000 Å of GaAs at a substrate temperature of 600°C, followed by a five period, 2 monolayer/2 monolayer, $In_{0.7}Ga_{0.3}As$/GaAs superlattice at 520°C, and a 5000 Å thick InAs(n^+) layer grown at 500°C. GaSb buffer layers consisted of 3000 Å of GaAs grown at 600°C, followed by a 1 monolayer/1 monolayer, GaAs/GaSb superlattice at 520°C, and a 5000 Å thick GaSb(p^+) layer grown at 470°C. Some structural characterization of the buffer layers has been reported elsewhere.[9] Doping of the electrodes (n-type for InAs, p-type for GaSb) was achieved by codeposition of silicon during growth. It has recently been demonstrated that GaSb can be controllably doped p-type with silicon under the growth conditions described above.[10] For some of the tunnel structures, lightly doped ($n \approx 5 \times 10^{16}$ cm^{-3} or $p \approx 5 \times 10^{16}$ cm^{-3}) and/or undoped spacer layers sandwiched the barrier and quantum well layers. Reflection high energy electron diffraction patterns observed during growth revealed a 2×4 surface reconstruction for InAs, and 1×3 reconstructions for GaSb, AlSb, and $Ga_{1-z}Al_zSb$.

2.2. Device fabrication

Conventional photolithographic and chemical etching techniques have been used to define mesas ranging in size from 2 μm diameter circles to 70×160 μm rectangles. Samples with InAs electrodes were etched in H_2SO_4:H_2O_2:H_2O (1:8:80), while Br_2:HBr:H_2O (0.5:100:100) was used to etch GaSb electrodes. In most cases, electrical contacts were formed by depositing Au/Ge on the mesas and etched surface. We have also tested Al contacts to GaSb(p^+) electrodes, and *in situ* In (prior to removal from the MBE) contacts to InAs(n^+) electrodes with good results. Current-voltage characteristics were measured with a Tektronics 577 curve tracer and/or an HP4145 analyzer, by probing the mesas with a 25 μm diameter Au wire.

3. CONVENTIONAL RESONANT TUNNELING

GaAs/AlGaAs double barrier heterostructures have been studied extensively as potential high frequency devices.[2,4] However, the performance of these GaAs/AlGaAs structures appears to be limited by poor ohmic contacts and the loss of NDR at high current densities. InAs/AlSb double barrier heterostructures are expected to have significant advantages over GaAs/AlGaAs structures because, (*i*) n-type InAs is ideal for ohmic contacts, and (*ii*) the InAs/AlSb conduction band offset (InAs Γ-point to AlSb X-point) is much larger than that of GaAs/AlAs (GaAs Γ-point to AlAs X-point) or GaAs/$Al_{0.4}Ga_{0.6}As$ (GaAs Γ-point to $Al_{0.4}Ga_{0.6}As$ Γ-point). NDR in InAs/AlSb double barrier heterostructures was first demonstrated by Luo *et al.*[11] with moderate peak-to-valley ratios and current densities. More

recently, we have observed peak–to–valley ratios of 11:1 at room temperature at a peak current density of 4×10^3 A/cm^2, as shown in Fig. 2.[12] The curve displayed in Fig. 2 was obtained from a heterostructure which consisted of a 65 Å InAs quantum well sandwiched between 28 Å AlSb barriers, 50 Å undoped InAs spacer layers, and 500 Å lightly doped ($n \approx 2 \times 10^{16}$ cm^{-3}) InAs spacer layers. The electrodes consisted of thick, heavily doped InAs layers, with $n \approx 1 \times 10^{18}$ cm^{-3}.

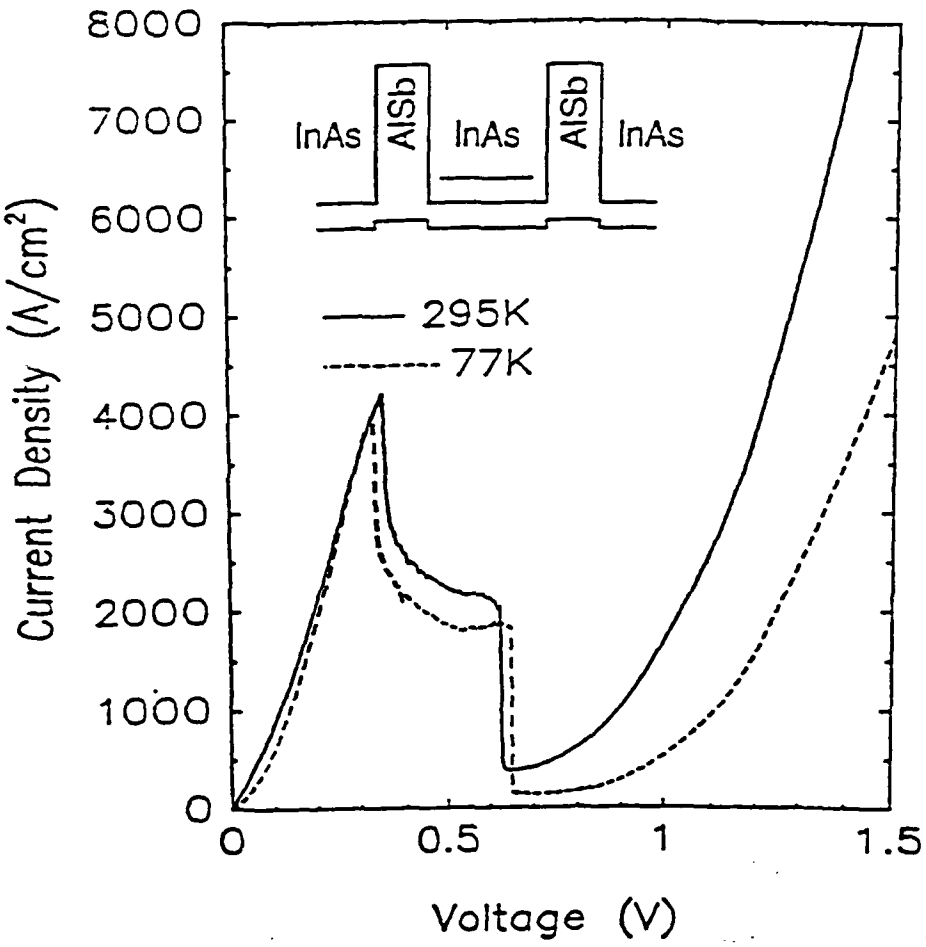

Fig. 2. Experimental current density vs. voltage curve, taken from an InAs/AlSb double barrier heterostructure with 28 Å barriers.

Although a trade–off between peak–to–valley ratios and current densities exists for InAs/AlSb resonant tunneling structures (as for GaAs/AlGaAs structures), reasonably high values for both figures of merit have been achieved. For example, we have observed a peak–current density of 4×10^5 A/cm^2 with a peak–to–valley ratio of 4:1 from a sample with 4 monolayer AlSb barriers and an asymmetric doping profile.[13] In terms of high frequency analog applications, these values are significantly better than the best GaAs/AlGaAs results reported. Thus, it is likely that InAs/AlSb resonant tunneling structures can be used as

microwave oscillators at frequencies significantly higher than 420 GHz, the highest frequency reported for GaAs/AlGaAs resonant tunneling devices.[2]

4. SINGLE BARRIER NDR

It has been proposed[14,15] and demonstrated[16-19] that single barrier tunnel structures can exhibit NDR in certain material systems. The basic requirement for observation of single barrier NDR is that tunneling electrons (holes) lie much closer in energy to the valence (conduction) band edge in the barrier material than to the conduction (valence) band edge. This requirement can be satisfied by electrons tunneling from InAs(n) electrodes into an $Al_xGa_{1-x}Sb$ barrier for $x \approx 0.4$, as depicted in Fig. 3. The single barrier structure can yield NDR because the electron tunneling probability is reduced as the valence band edge in the $Al_xGa_{1-x}Sb$ barrier is pushed to lower energies (with respect to the tunneling electrons) by an increasing applied voltage.

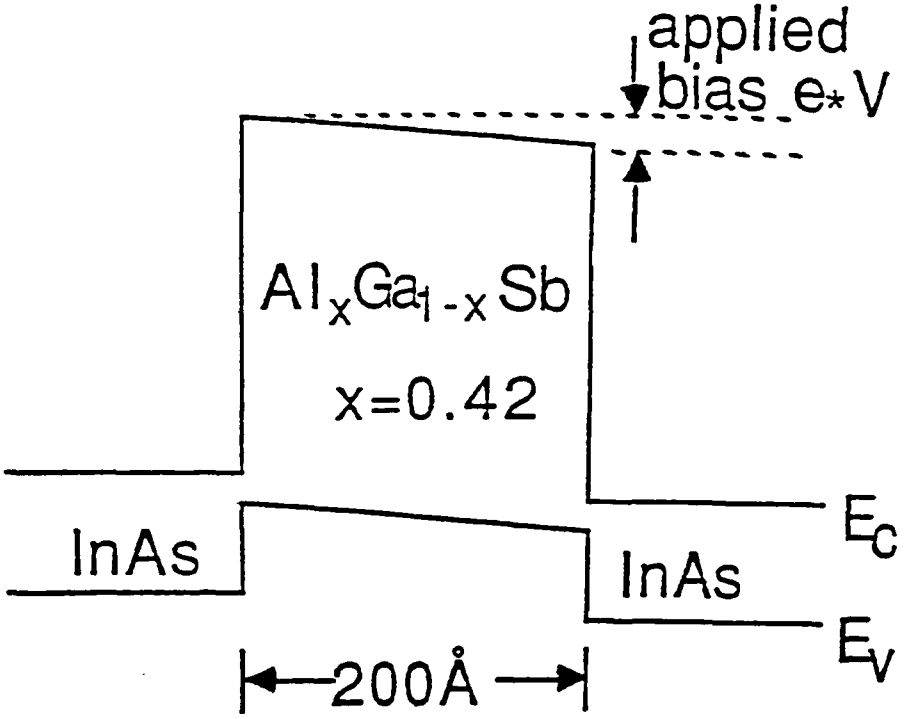

Fig. 3. Band-edge diagram for an InAs(n)/$Al_{0.42}Ga_{0.58}Sb$ single barrier heterostructure under an applied bias.

Fig. 4 contains room temperature and 77 K current density vs. voltage (J–V) curves from a single barrier InAs/$Al_{0.42}Ga_{0.58}Sb$ heterostructure. A room temperature (77 K) peak-to-valley current ratio of 1.2 (3.4) is observed in reverse bias (negative voltage on the mesa), at a modest current density ($\approx$ 25 A/cm^2). The J–V curves were taken from a structure which consisted of a 200 Å $Al_{0.42}Ga_{0.58}Sb$ barrier sandwiched between 100 Å undoped InAs spacer

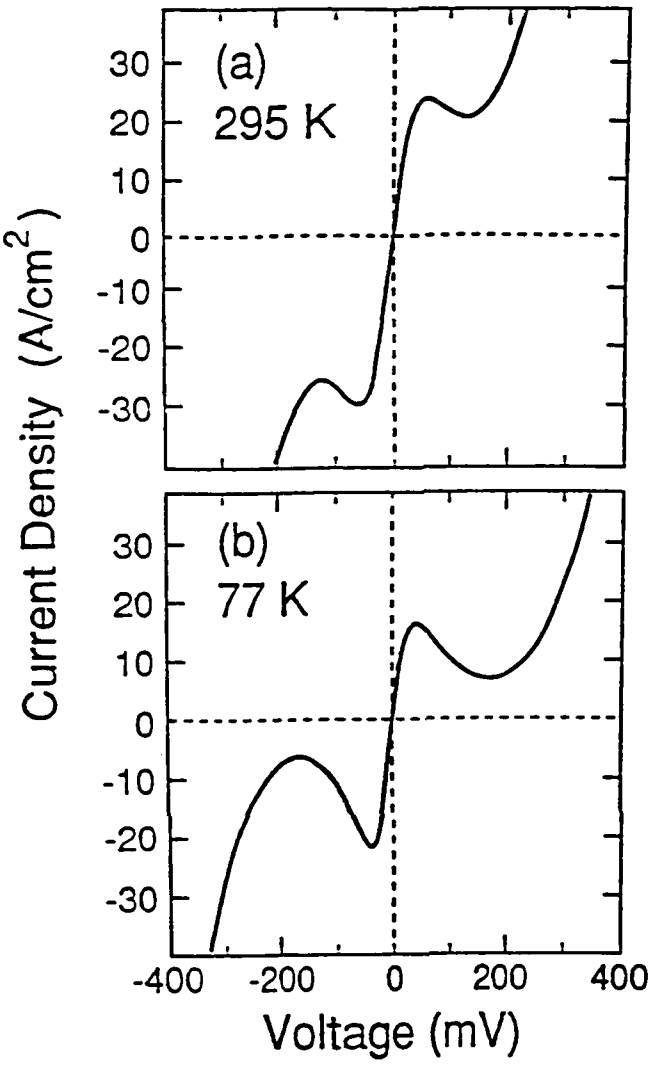

Fig. 4. Experimental current density vs. voltage curve at (a) room temperature and (b) 77 K for an InAs(n)/$Al_{0.42}Ga_{0.58}Sb$ single barrier heterostructure.

layers, and 500 Å lightly doped ($n \approx 2 \times 10^{16}$ cm^{-3}) spacer layers. The electrodes consisted of thick, heavily doped InAs layers, with $n \approx 1 \times 10^{18}$ cm^{-3}.

It is interesting to note that the J–V curves shown in Fig. 4 do not display threshold voltages for tunneling because single barrier elastic tunneling is allowed at any applied bias (in contrast to resonant tunneling). The peak in the J–V curve occurs when additional incident electrons in the negatively biased electrode are no longer generated by an increasing bias (approximately when the voltage surpasses the Fermi level in the spacer layers). We have also demonstrated NDR in this material system for single $Al_xGa_{1-x}Sb$ barrier compositions of $x = 0.38$, 0.40, and 0.44.[19]

5. RESONANT INTERBAND TUNNELING

Resonant interband tunneling (RIT) structures have recently been proposed[20] and demonstrated[21,22]. In these structures, electrons (holes) in one material tunnel through a quasi-bound valence (conduction) band state in a different material. This mechanism yields a drastic suppression of valley currents due to the blocking nature of the quantum well layer past resonance. We have observed peak-to-valley current ratios as large as 20:1 (88:1) at 300 K (77 K) from an InAs(n)/AlSb/GaSb/AlSb/InAs(n) (n-type InAs electrodes, AlSb barriers, and a GaSb quantum well) RIT structure.[21]

We report here an experimental and theoretical study of the current-voltage behavior of a GaSb(p)/AlSb/InAs/AlSb/GaSb(p) heterostructure. Fig. 5 contains a band-edge diagram for the heterostructure. The crucial feature of the diagram is that the conduction band edge in the InAs quantum well is *lower* in energy than the valence band edge in the GaSb electrodes. The InAs layer has been grown sufficiently thick to keep the quantum well ground state below the GaSb valence band maximum. Due to the strong coupling between conduction band and light hole states, a transmission resonance exists for light holes in the GaSb electrodes whose energies and parallel wavevectors match those of states in the two dimensional quantum well subband. It is straightforward to show that this resonance condition can be satisfied for small applied biases (no threshold voltage). A peak in the I–V curve is expected when the applied bias becomes large enough to lower the valence band edge in the positively biased GaSb electrode below the ground state energy in the InAs quantum well. Beyond this point, the tunneling probability is drastically reduced due to the blocking nature of the thick InAs layer at energies in its band gap. It should be noted that heavy holes are not expected to contribute significantly to the tunneling current because they are weakly coupled to conduction band states.

We have developed a theoretical model to simulate the current-voltage behavior of tunnel structures in which interactions between valence and conduction band states are important. The simulation begins by computing the band edge diagram throughout the heterostructure via the Poisson equation for each applied bias. In the case of the RIT structure studied here, the heavy hole band dominates the band bending behavior in the GaSb electrodes because its density of states is fifteen times greater than that of the light hole band. Next, localized two-band tight-binding orbitals are used to generate transfer matrices for the tunneling states. In this manner, a transmission coefficient is determined as a function of the energy and parallel wavevector of each state. In our model, only the conduction and light hole bands are used to determine the tight-binding parameters for each material. The restriction to these two bands is effectively an assumption that only electron-light hole coupling is significant in the tunnel structure (heavy hole tunneling is ignored). Finally, the current density is obtained by including appropriate velocities and Fermi factors and integrating over all energies and parallel wavevectors.

MBE growth and device fabrication have been performed as described in Section 2. The active region of the structure consisted of a 100 Å InAs quantum well, sandwiched between 20 Å AlSb barriers, 25 Å undoped GaSb spacer layers, and 200 Å lightly doped ($p \approx 2 \times 10^{16}$ cm^{-3}) GaSb spacer layers. The electrodes consisted of thick, heavily doped GaSb layers, with $p \approx 5 \times 10^{18}$ cm^{-3}.

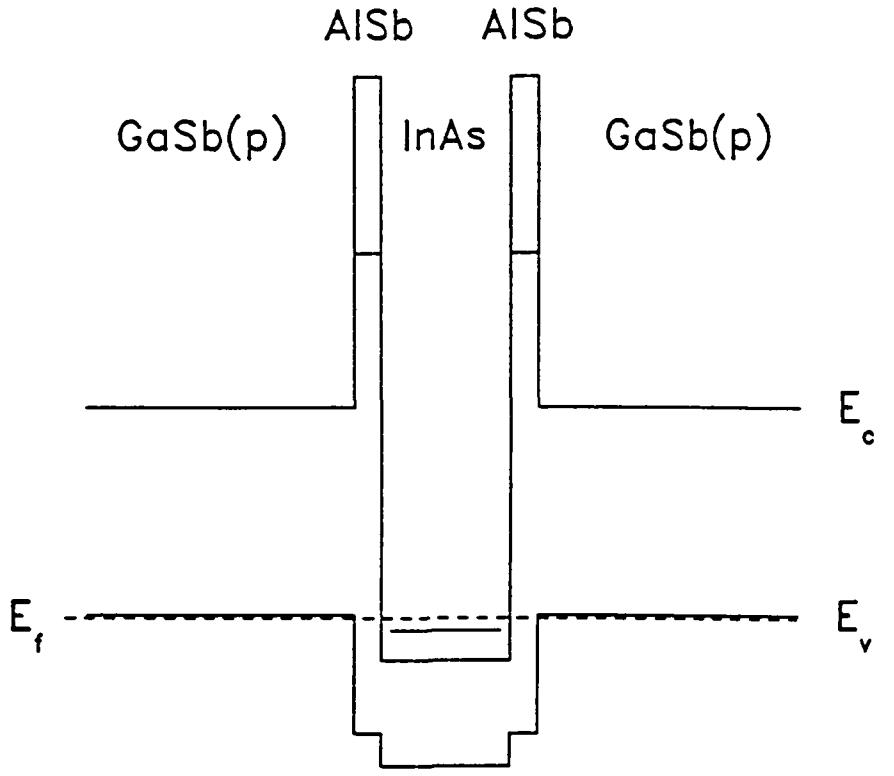

Fig. 5. Schematic band–edge diagram (energy vs. position) for the GaSb(p)/AlSb/InAs/AlSb/GaSb(p) RIT heterostructure. The conduction band edge, E_c, valence band edge, E_v, and Fermi energy, E_f, are labeled. The indirect (lower) and direct (higher) conduction band edges are both shown in the AlSb layers. The position of the quasi–bound state in the InAs quantum well is also shown.

Fig. 6 displays a current density vs. voltage curve taken at 300 K from one of the fabricated devices. Also plotted are theoretical curves, calculated by the method described previously, for symmetric 6 and 7 monolayer (18.4 and 21.5 Å) AlSb barrier layers. The experimental curve shows pronounced NDR in both bias directions, with peak–to–valley current ratios of 8.3 and 3.6 in reverse and forward bias, respectively (we take forward bias to mean positive voltage applied to the mesa). The peak current density is 430 A/cm^2 (560 A/cm^2) in reverse (forward) bias, and varied by less than 15% over ten randomly chosen devices.

As shown in Fig. 6, the peak current densities predicted by the theoretical model are in good agreement with those measured experimentally. It has been suggested that the high scattering rate of heavy holes in bulk GaSb to the light hole band results in identical tunneling probabilities for the two types of carriers.[22] If this were the case, we would expect the large heavy hole density of states to yield measured peak current densities greater than our theoretically predicted value by more than one order of magnitude. Thus, the observed agreement between the experimental and theoretical current densities suggests that heavy

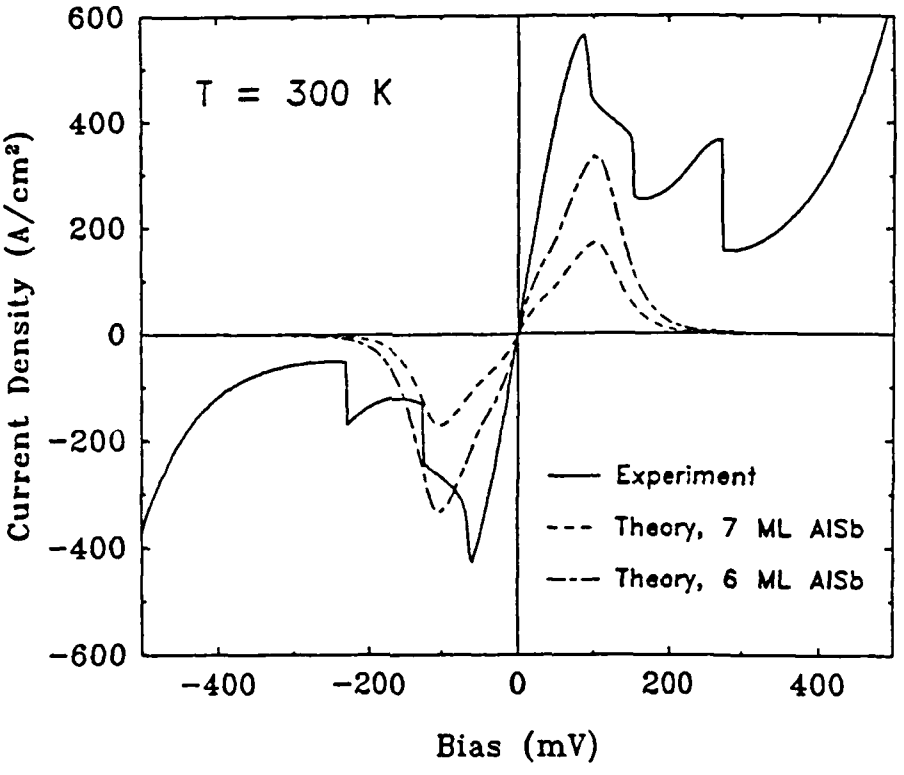

Fig. 6. Experimental current density vs. voltage curve taken from the GaSb(p)/AlSb/InAs/AlSb/GaSb(p) RIT device. Also displayed are theoretically simulated curves, calculated for 6 and 7 monolayer (ML) AlSb barrier layers. The theoretical model includes only light hole contributions to the resonant interband tunneling current.

hole tunneling probabilities are small. The experimental curve shown in Fig. 6 displays some asymmetry, with the forward bias peak appearing 20 mV higher than the reverse bias peak. This feature is probably caused by unintentional asymmetries in the doping profile of the device, introduced during growth. It should be noted that the observed valley currents are significantly higher than the calculated values, suggesting that transport mechanisms other than elastic tunneling dominate the current at high bias.

In addition to the demonstration of high peak-to-valley current ratios in RIT devices, we have recently explored interband tunneling devices designed to yield high peak current densities. Each of these heterostructures consists of an undoped GaSb quantum well ($\approx$ 150 Å thick) sandwiched between heavily doped InAs(n^+) electrodes.[23] The major difference between this structure and the RIT's described previously is the absence of AlSb barriers. Nevertheless, a quasi-bound state is formed in the GaSb quantum well due to non-negligible reflections of the free carrier wavefunctions at the InAs/GaSb interfaces. This quantum well state results in a transmission resonance for electrons in the InAs electrodes whose energies and parallel wavevectors match those of states in the two dimensional quantum well subband.

We have observed peak current densities in excess of 2×10^4 A/cm^2 from these structures, with peak-to-valley current ratios of 2:1.[23] These results suggest that interband tunneling devices may be suitable for high frequency applications. Furthermore, the quasi-bound states in the barrierless RIT's are extremely broad, due to the extremely weak confinement. As a result, the tunneling time in these structures, as defined by the uncertainty principle relating the energy width of the resonanance to the lifetime of the quasi-bound state, is very short ($\approx$ 50 fs), and should not be the limiting factor in the frequency of operation.

6. CONCLUSIONS

In summary, we have studied several novel InAs/GaSb/AlSb tunnel structures. This material system offers several advantages over GaAs/AlGaAs for tunnel structure design: (*i*) enhanced flexibility from *three* nearly-lattice matched materials, (*ii*) the possibility of staggered and broken-gap band alignments, (*iii*) large conduction band offsets, and (*iv*) excellent ohmic contacts. We have studied three distinct mechanisms for achieving negative differential resistance from InAs/GaSb/AlSb structures: conventional resonant tunneling, single barrier tunneling, and resonant interband tunneling. Several of the structures show extremely high peak current densities and/or peak-to-valley current ratios. These results suggest that the InAs/GaSb/AlSb material system is ideal for fabrication of high frequency oscillators and mixers.

7. ACKNOWLEDGEMENTS

The authors gratefully acknowledge helpful discussions with Y. Rajakarunanayake, M.K. Jackson, and E.R. Brown. The support of the Office of Naval Research and the Air Force Office of Scientific Research under Grant Nos. N00014-89-J-1141 and AFOSR-86-0306, respectively, have made it possible for us to carry out this program. J.R. Söderström received financial support from the Wilhelm and Martina Lundgren Foundation. E.T. Yu was supported in part by the AT& T Foundation. D.H. Chow was supported in part by Caltech's Program in Advanced Technologies, sponsored by Aerojet General, General Motors, and TRW.

8. REFERENCES

1. K.A. Lee and M.A. Frerking, "Experimental results of a high Q quasioptical reflection cavity," Int. Journal of Infrared and Millimeter Waves, vol. 10, no. 7, pp. 789–802, 1989.
2. E.R. Brown, T.C.L.G. Sollner, C.D. Parker, W.D. Goodhue, and C.L. Chen, "Oscillations up to 420 GHz in GaAs/AlAs resonant tunneling diodes," Appl. Phys. Lett., vol. 55, no. 17, pp. 1777–1779, 1989.
3. F. Capasso, S.Sen, A.Y. Cho, and D.L. Sivco, "Multiple negative transconductance and differential conductance in a bipolar transistor by sequential quenching of resonant tunneling," Appl. Phys. Lett., vol. 53, no. 12, pp. 1056–1058, 1988.
4. S.K. Diamond, E. Özbay, M.J.W. Rodwell, D.M. Bloom, E. Wolak, and J.S. Harris, "Fabrication of 200-GHz f_{max} resonant-tunneling diodes for integrated circuit and microwave applications," IEEE Elec. Dev. Lett., vol. 10, no. 3, pp. 104–106, 1989.

5. G.J. Gualtieri, G.P. Schwartz, R.G. Nuzzo, R.J. Malik, and J.F. Walker, "Determination of the (100) InAs/GaSb heterojunction valence–band discontinuity by x–ray photoemission core level spectroscopy," J. Appl. Phys., vol. 61, no. 12, pp. 5337–5341, 1987.
6. G.J. Gualtieri, G.P. Schwartz, R.G. Nuzzo, and W.A. Sunder, "X–ray photoemission core level determination of the GaSb/AlSb heterojunction valence–band discontinuity,"Appl. Phys. Lett., vol. 49, no. 16, pp. 1037–1039, 1986.
7. S. Kalem, J.I. Chyi, H. Morkoc, R. Bean, and K. Zanio, "Growth and transport properties of InAs epilayers on GaAs," Appl. Phys. Lett., vol. 53, no. 17, pp. 1647–1649, 1988.
8. J.R. Söderström, D.H. Chow, and T.C. McGill, "MBE–growth of InAs and GaSb epitaxial layers on GaAs substrates," Mat. Res. Soc. Symp. Proc., vol. 145, pp. 409–414, 1989.
9. D.H. Chow, R.H. Miles, J.R. Söderström, and T.C. McGill, "InAs/$Ga_{1-z}In_zSb$ strained–layer superlattices grown by molecular beam epitaxy," to appear in *J. Vac. Sci. and Technol. B*, July/August 1990.
10. T.M. Rossi, D.A. Collins, D.H. Chow, and T.C. McGill, "P–type doping of gallium antimonide grown by molecular beam epitaxy using silicon," unpublished.
11. L.F. Luo, R. Beresford, and W.I. Wang, "Resonant tunneling in AlSb/InAs/AlSb double–barrier heterostructures," Appl. Phys. Lett. vol. 53, no. 23, pp. 2320–2322, 1988.
12. J.R. Söderström, D.H. Chow, and T.C. McGill, "InAs/AlSb double–barrier structure with large peak–to–valley current ratio: a candidate for high–frequency microwave devices," IEEE Elec. Dev. Lett., vol. 11, no. 1, pp. 27–29 1990.
13. J.R. Söderström, T.C. McGill, and E.R. Brown, unpublished.
14. G.A. Sai–Halasz, R. Tsu, and L. Esaki, "A new semiconductor superlattice," Appl.Phys.Lett., vol. 30, no. 12, pp. 651–653, 1977.
15. D.H. Chow and T.C. McGill, "Negative differential resistances from $Hg_{1-z}Cd_zTe$ single quantum barrier heterostructures," Appl. Phys. Lett., vol. 48, no. 21. pp. 1485–1487, 1986.
16. D.H. Chow, T.C. McGill, I.K. Sou, J.P. Faurie, and C.W. Nieh, "Observation of negative differential resistance from a single barrier heterostructure," Appl. Phys. Lett., vol. 52, no. 1, pp. 54–56, 1988.
17. H. Munekata, T.P. Smith III, and L.L. Chang, "Growth and transport properties of (Ga,Al)Sb barriers on InAs," J. Vac. Sci. Technol. B, vol. 7, pp. 324–326, 1989.
18. R. Beresford, L.F. Luo, W.I. Wang, "Negative differential resistance in AlGaSb/InAs single barrier heterostructures at room temperature," Appl. Phys. Lett., vol. 54, no. 19, pp. 1899–1901, 1989.
19. J.R. Söderström, D.H. Chow, and T.C. McGill, "Demonstration of large peak–to–valley current ratios in InAs/AlGaSb/InAs single–barrier heterostructures," Appl. Phys. Lett., vol. 55, no. 13, pp. 1348–1350 1989.
20. M. Sweeny and J. Xu, "Resonant interband tunnel diodes," Appl. Phys. Lett., vol. 54, no. 6, pp. 546–548, 1989.
21. J.R. Söderström, D.H. Chow, and T.C. McGill, "New negative differential resistance device based on resonant interband tunneling," Appl. Phys. Lett., vol. 55, no. 11, pp. 1094–1096, 1989.

22. L.F. Luo, R. Beresford, and W.I. Wang, "Interband tunneling in polytype GaSb/AlSb/InAs heterostructures," Appl. Phys. Lett., vol. 55, no. 19, pp. 2023–2025, 1989.
23. D.A. Collins, D.H. Chow, and T.C. McGill, "Observation of negative differential resistance in a broken-gap resonant interband tunneling structure," unpublished.

Appendix A-11. InAs/GaSb/AlSb: The Material System of Choice for Novel Tunneling Devices.

Presented at NATO-ARW Workshop,
El Escorial, Spain May 14, 1990

InAs/GaSb/AlSb: The Material System of Choice for Novel Tunneling Devices

D. A. Collins, D. H. Chow, E. T. Yu, D. Z.-Y. Ting,
J. R. Söderström*, Y. Rajakarunanayake, and T. C. McGill

T. J. Watson, Sr., Laboratory of Applied Physics
California Institute of Technology
Pasadena, California 91125

Abstract

The nearly lattice–matched InAs/GaSb/AlSb system offers tremendous flexibility in designing novel heterostructures due to the wide range of available band alignments. We have recently exploited this advantage to demonstrate several different devices exhibiting negative differential resistance (NDR) based on interband tunneling. These devices show a wide range of different characteristics including very high peak current densities (1.6×10^5 A/cm^2) or peak to valley current ratios (20:1 at 300K and 88:1 at 77K). We have also studied "traditional" double barrier (resonant) tunneling in the InAs/GaSb/AlSb system. In particular, extremely high peak current densities in InAs/AlSb double barrier devices have been exploited to fabricate oscillators operating at the highest frequencies yet reported. Two and three terminal tunneling devices in this material system show great promise for use in high frequency analog and digital applications.

INTRODUCTION

The InAs/GaSb/AlSb material system is a nearly lattice–matched system in which Type I, Type II and Type II broken–gap band alignments are obtainable. Figure 1 shows the currently accepted energy positions of the conduction and valence band edges for InAs, GaSb and AlSb.[1,2,3] As shown in this figure, the band offset between InAs and GaSb is such that the conduction band edge of InAs lies below the valence band edge of GaSb, leading to a Type II broken–gap heterojunction. The band offset between GaSb and AlSb is of the Type I variety, with the conduction and valence band edges of GaSb

* Current address:Department of Physics, Chalmers University, Götebörg, Sweden

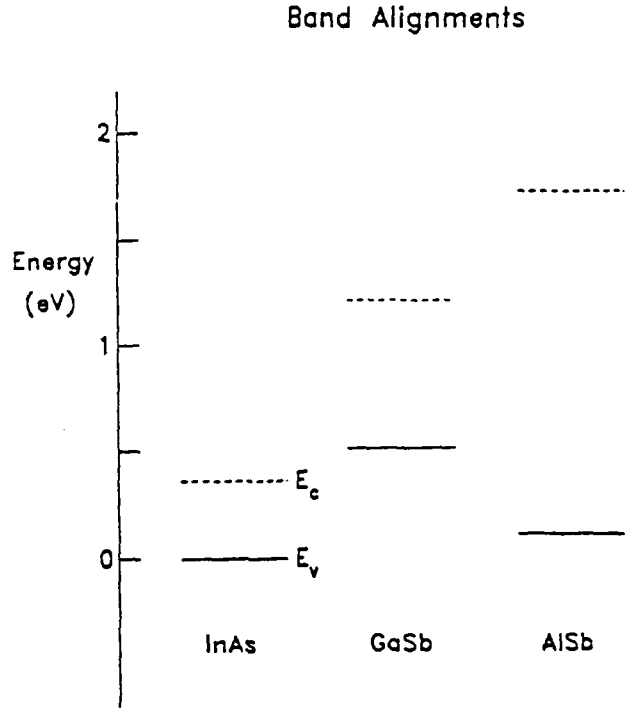

Fig. 1. Conduction (dashed) and valence (solid) band edges for the InAs/GaSb/AlSb material system. The energy gaps and band offsets allow the possibility of Type I, Type II, and Type II broken–gap band alignments. The indirect conduction band minimum is shown for AlSb.

falling in the band gap of AlSb. Finally, the InAs/AlSb heterojunction exhibits a Type II band alignment, with the conduction band of InAs lying well below the conduction band edge of AlSb (a high barrier for electrons) but above the valence band edge of AlSb, and with the valence band of InAs lying below that of AlSb.

The electrical properties of InAs and GaSb also make these materials extremely attractive as electrodes for tunneling devices. InAs can be made n-type with very low resistivity, and forms an ohmic contact for electrons to metals. GaSb can be made p-type with relatively low resistivity,[4] and the small p-type Schottky barrier for GaSb facilitates the formation of p-type ohmic contacts to GaSb. Hence, parasitic series resistance can be minimized for metal contacts to n-type InAs layers and p-type GaSb layers. Furthermore, contacts to thin layers of n-InAs and p-GaSb are relatively easy to make due to the lack of surface depletion. Finally, the small effective mass of InAs compared to that of GaAs enhances quantum effects (quantum confinement energies vary inversely with effective mass), so that subband spacings will be larger in InAs than in GaAs, and limitations in lithographic resolution, for example, should be less important for InAs than for GaAs.

To illustrate the tremendous variety of device structures with NDR that can be realized in this material system, we have shown schematically ten such structures in Fig. 2. Table I contains a summary of measured peak current densities and peak to valley current ratios for these devices. The device in Figure 2(A) is a standard InAs/AlSb

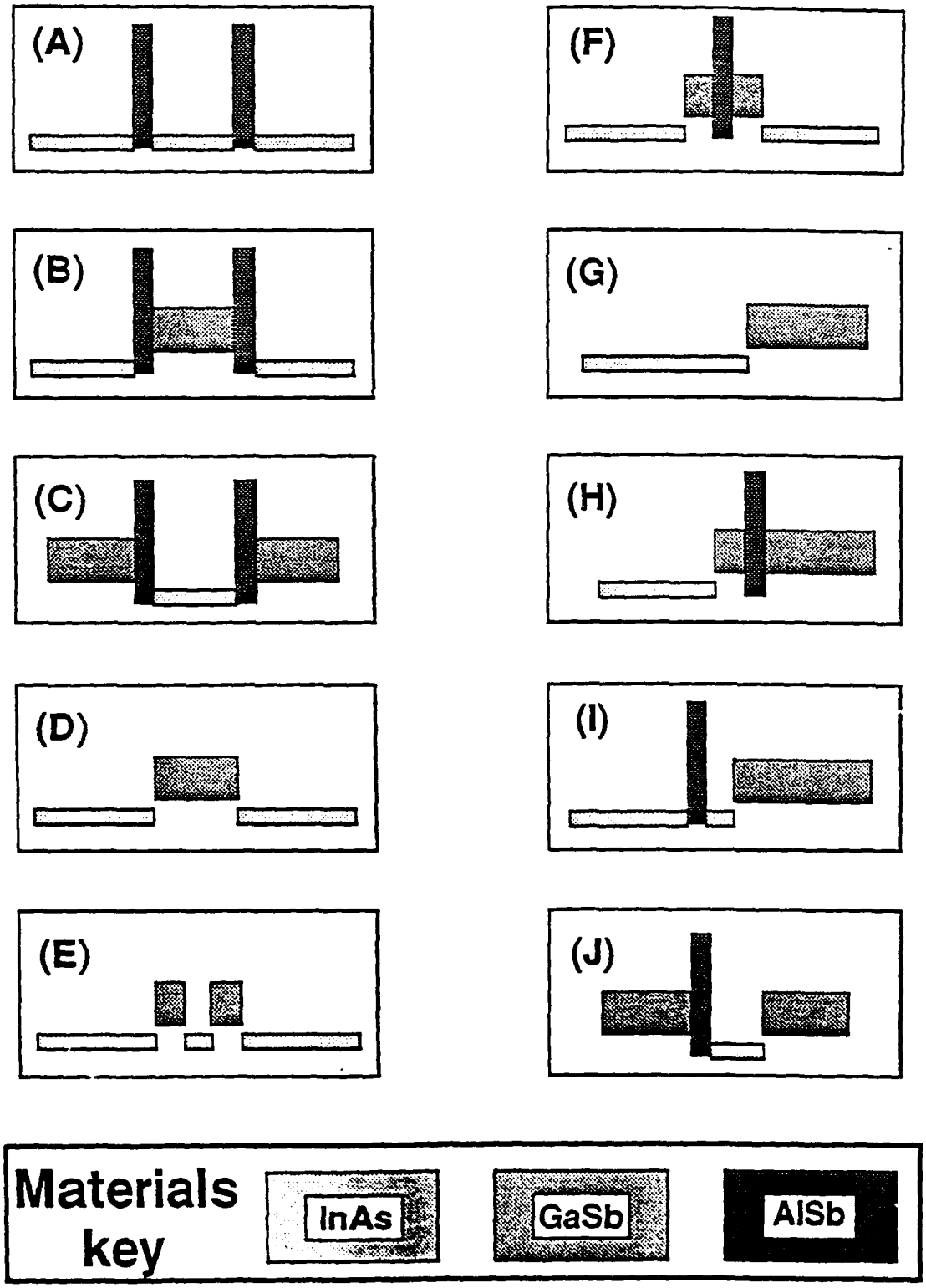

Fig. 2. Schematic energy band diagrams (energy vs. position) for ten different tunnel structures realized in the InAs/GaSb/AlSb material system. Energy gaps for each material are shaded, so that the top (bottom) of each shaded region represents the conduction (valence) band edge in the heterostructure.

TABLE I. Summary of two-terminal device performance.

Material sequence	Temperature (K)	Peak-to-valley current ratio	Peak current density (A/cm^2)
InAs(n)/AlSb/InAs/AlSb/InAs(n)	300	4.0	3.7×10^5
	300	13.0	4.0×10^3
InAs(n)/AlSb/GaSb/AlSb/InAs(n)	300	12.0	950
	300	21.0	50
	77	60.0	1.7×10^3
	77	88.0	90
GaSb(p)/AlSb/InAs/AlSb/GaSb(p)	300	8.0 – 10.0	450 – 500
	77	16.0	450 – 500
InAs(n)/GaSb/InAs(n)	300	2.2	5.1×10^3
	300	1.2	1.2×10^5
InAs(n)/GaSb/InAs/GaSb/InAs(n)	300	2.2	1.2×10^4
InAs(n)/GaSb/AlSb/GaSb/InAs(n)	300	3.5	1.4×10^4
InAs(n)/GaSb(p)	300	1.7	4.2×10^4
	300	1.2	8.4×10^4
InAs(n)/GaSb/AlSb/GaSb(p)	300	1.5 – 1.8	1.6×10^5
	300	1.5 – 1.8	3.5×10^4
InAs(n)/AlSb/InAs/GaSb(p)	300	1.5 – 1.7	3.1×10^3
InAs(n)/AlSb/GaSb/InAs(n)	300	15.0 – 18.0[a]	2.7×10^3[a]
		1.6 – 2.2[b]	1.52×10^4[b]

[a]Reverse bias, *i.e.*, negative voltage applied to electrode next to AlSb barrier.
[b]Forward bias, *i.e.*, positive voltage applied to electrode next to AlSb barrier.

double barrier structure.[5,6,7] The first of the interband devices, which has been named the resonant interband tunneling device (RIT),[8,9] is shown in Figure 2(B), with the p-type analog of this device[10] shown in Figure 2(C). In Figure 2(J), we have shown a device structure that is the basis of our efforts to fabricate three-terminal devices; a contact to the central InAs layer, which can be made quite thick in this structure without the loss of NDR, would allow the fabrication of either Stark effect transistors[11] or the more standard tunneling transistor.[12,13]

Each of the device structures shown in Figure 2 has been grown, fabricated, and characterized in our laboratories. We have also developed theoretical simulations of the electrical behavior of these structures which have allowed us to explore a wide range of device parameter space relatively efficiently, and have also provided insight into the transport mechanisms that are important in these devices. In Sections 2 and 3 we present experimental and theoretical results for several of the devices shown in Figure 2. Further details of the growth and fabrication can be found in Ref. 14.

InAs/AlSb/InAs/AlSb/InAs DOUBLE BARRIER TUNNEL DEVICES

Until very recently, the standard double barrier tunnel structure has been the principal subject of research in the field of semiconductor tunneling heterostructures; research

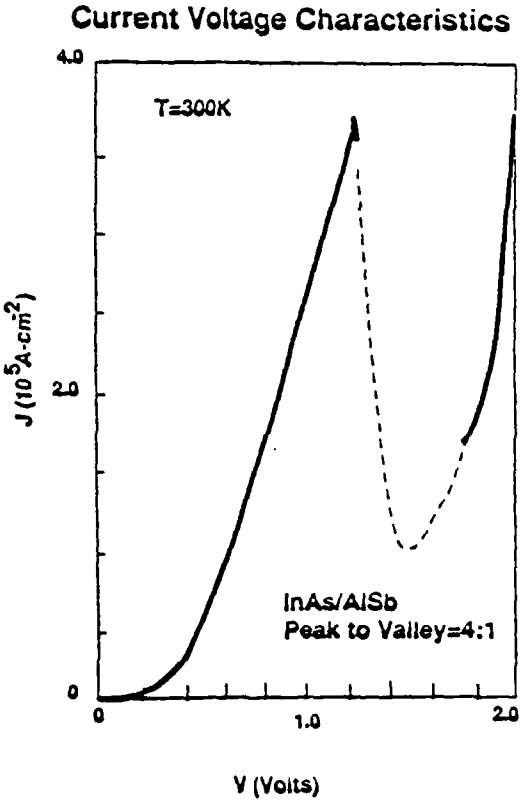

Fig. 3. Current–voltage characteristics for an InAs/AlSb double barrier heterostructure. The structure was grown at Caltech and characterized at Lincoln Laboratories by E.R. Brown.

activities have focused primarily on GaAs/AlGaAs and InGaAs/InAlAs structures. In spite of the progress that has been made with GaAs/AlAs (and $Al_xGa_{1-x}As$) resonant tunneling structures, it has become clear that fundamental limitations exist on their performance. For example, maximum peak current densities of approximately 1.5×10^5 A/cm^2 can be reached only by reducing room temperature peak–to–valley current ratios to 2:1 or less.[15,16]

Recently, InAs/AlSb structures grown at Caltech and characterized at Lincoln Laboratories have shown the highest peak current densities of any double barrier devices reported to date, while maintaining peak–to–valley ratios of 3.7:1. Figure 3 shows the current–voltage characteristic for an InAs/AlSb device. At Lincoln Laboratories, this InAs/AlSb structure has been used in oscillator circuits which demonstrate power and frequency characteristics that significantly exceed those obtained from other devices.[17]

INTERBAND DEVICES

Interband tunneling devices are made possible by the unusual Type II broken–gap band alignment in the InAs/GaSb heterojunction. Because the valence band edge of GaSb is higher in energy than the conduction band edge of InAs, it is possible to produce devices in which conduction band states in InAs interact with valence band states in GaSb. Devices exploiting this feature have been found, in many cases, to

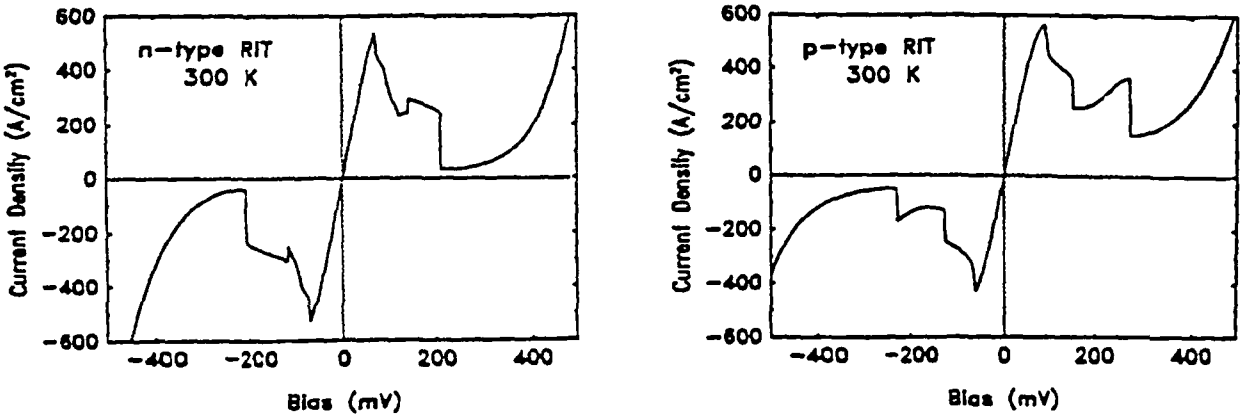

Fig. 4. Current-voltage characteristics for n-type and p-type resonant interband tunnel (RIT) structures. Schematic energy band diagrams for these structures are shown in Figures 2(B) and 2(C), respectively.

exhibit performance markedly superior to that of more conventional structures.

Resonant Interband Tunneling (RIT) Devices

The first device of this type studied experimentally was the resonant interband tunneling (RIT) device. Two varieties of this device have been studied, one in which electrons tunnel through valence-band states in a quantum well (the n-type RIT, shown in Figure 2(B)), and the other in which holes tunnel through conduction-band states in a quantum well (the p-type RIT, shown in Figure 2(C)). Current–voltage characteristics for an n-type RIT and a p-type RIT are shown in Fig. 4. As discussed in Ref. 9, these devices typically exhibit extremely high peak–to–valley current ratios — as high as 20:1 and 88:1 at 300 K and 77 K for n-type RIT's, respectively. At low bias, resonant tunneling of electrons (holes) occurs in the n–type (p–type) RIT via the quasi–bound valence (conduction) band state in the quantum well. As the bias is increased beyond the resonance in these devices, the carriers are required to tunnel through not only the AlSb barrier layers, but also through the band gaps in the quantum well layers. This leads to a strong suppression of the valley current, resulting in extremely high peak-to-valley current ratios.

Barrierless Resonant Interband Tunneling (BRIT) Devices

To date, RIT structures have displayed relatively low peak current densities, a disadvantage for high frequency analog applications. Because the peak current density depends strongly on the AlSb barrier widths, we have investigated a RIT-like device structure, shown in Figure 2(D), in which the AlSb barriers have been removed. The current transport mechanism in this device has been claimed by some investigators[18] to be simply ohmic conduction from one InAs electrode to the other through the GaSb valence band. Our studies have shown, however, that this interpretation is incorrect, and that resonant tunneling in these devices occurs via a quasi–bound state in the GaSb valence band that exists despite the absence of confinement by classically forbidden barrier

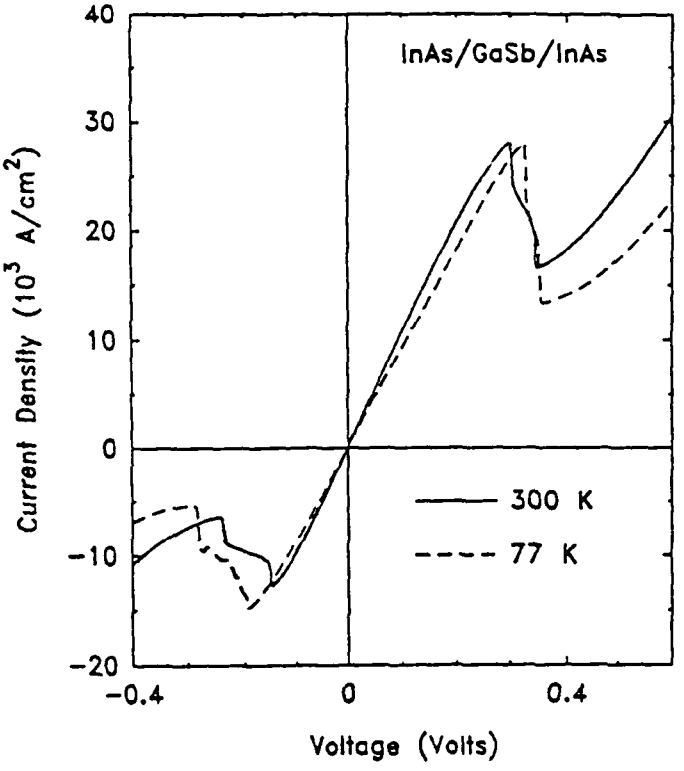

Fig. 5. Current voltage characteristics at 300 K and 77 K for a barrierless resonant interband tunneling (BRIT) device. A schematic energy band diagram for this structure is shown in Figure 2(D).

regions. Current-voltage characteristics for a barrierless resonant interband tunneling (BRIT) device are shown in Fig. 5. As expected, the peak current densities for this structure are far higher than those obtained from the RIT device — (few)$\times 10^2$ A/cm^2 for a typical RIT compared to (few)$\times 10^4$ A/cm^2 for the BRIT.

A theoretical analysis of this device reveals a number of interesting features. Because interband tunneling devices involve both conduction and valence band states, any theoretical model for these structures must include both conduction and valence bands, and must also correctly account for the interactions between these bands. We have implemented a simple two-band tight-binding model that satisfies these requirements.[19] This model, in conjunction with realistic band bending calculations, allows us to simulate the current-voltage behavior of a wide variety of interband tunneling devices.

Simulations of BRIT structures with varying GaSb layer widths and subsequent experimental measurements for these devices have provided strong evidence that the current transport mechanism responsible for NDR is indeed resonant. Figure 6 shows transmission coefficients for BRIT structures with three different well widths. The main feature of interest is that, despite the absence of any classically forbidden barrier regions, transmission resonances are formed due solely to the imperfect matching of InAs conduction band and GaSb valence band wave functions at the InAs/GaSb interfaces. For the 15 monolayer (ML) GaSb well (Figure 6(a)), the confinement energy moves

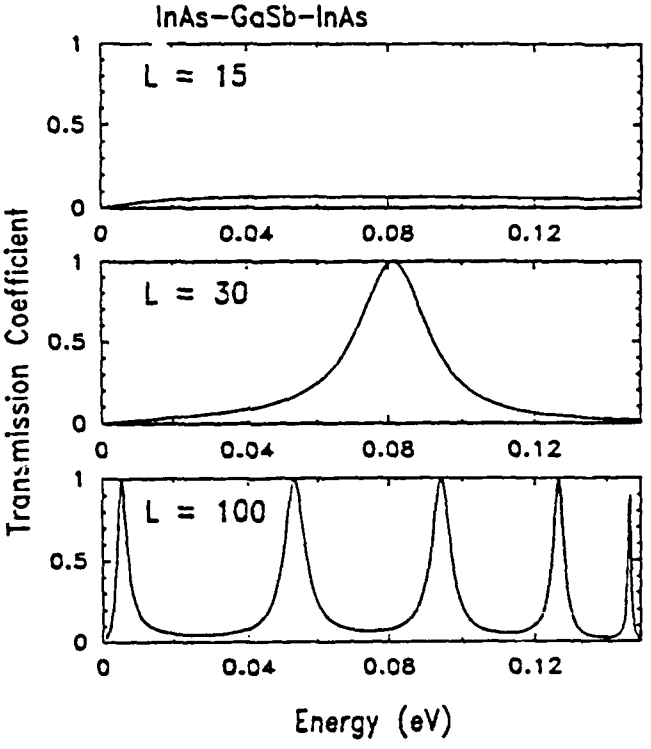

Fig. 6. Theoretical transmissions coefficients for the barrierless resonant interband tunneling (BRIT) device (the structure depicted in Fig. 2(D)). The energy range shown is from the valence band edge of the GaSb to the conduction band edge of the InAs. Transmission coefficients for three different widths (in monolayers) of the GaSb layer are presented.

the quantum well state below the InAs conduction band edge; in this case, resonant transport cannot occur. For the 30 ML GaSb well (Figure 6(b)), a single broad resonance is present in the transmission coefficient, and for the 100 ML GaSb well (Figure 6(c)) a large number of resonances occur in the energy range between the InAs conduction band edge and the GaSb valence band edge. This variation in the transmission coefficient with the width of the GaSb layer leads to a nonintuitive variation in the peak current density. The absence of a resonance should lead to a small peak current for a device with a thin GaSb layer; BRIT devices with intermediate GaSb layer widths should exhibit much higher peak current densities, due to the presence of the single broad resonance. For wide GaSb layers, however, the peak current density should decrease since the resonances, although more numerous, are significantly narrower than for GaSb layers of intermediate width and therefore allow less of the incoming electron distribution to be transmitted across the GaSb layer.

As shown in Figure 7, this qualitative dependence of peak current density on GaSb layer width is exhibited both experimentally and theoretically. Figure 7(a) shows the theoretically calculated peak current density as a function of GaSb layer width; calculated valley currents for these devices are extremely small compared to the peak currents. Figure 7(b) shows the difference between the peak and valley current densities measured experimentally for devices with varying GaSb layer widths. The difference

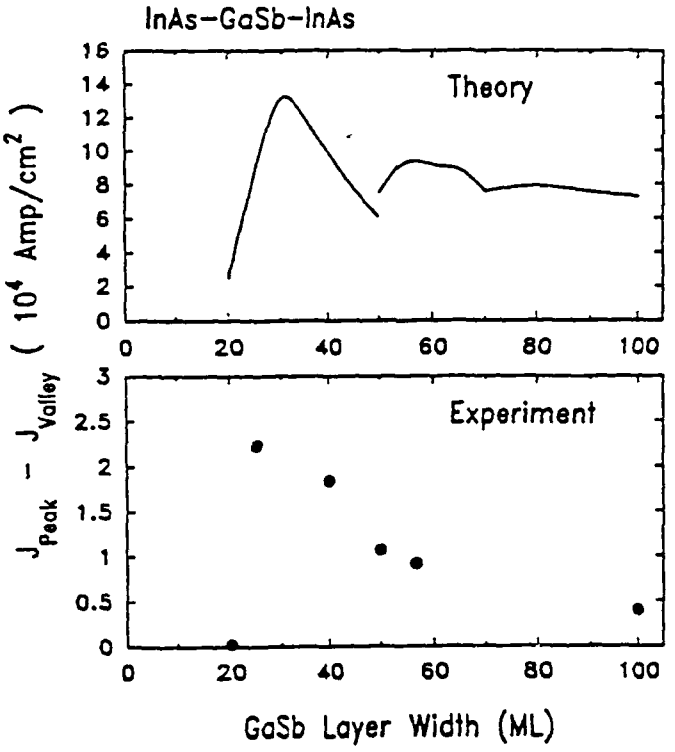

Fig. 7. (a)Theoretical calculations and (b)experimental values for the difference between the peak and valley curent density for the BRIT device (shown in Fig. 2(D)) as a function of GaSb layer width. The discontinuity in the theoretical curve is due to the presence of two widely separated transmission resonances that lead to two separate peaks in the calculated current-voltage characteristic.

between the peak and valley current densities, rather than simply the peak current density, has been used in order to eliminate contributions to the peak current density from inelastic transport mechanisms, which have not been included in our calculations. Both the experimental and theoretical curves show the qualitative dependence on GaSb layer width expected from our analysis of the transmission coefficients; in particular, the sharp drop in the resonant current for narrow GaSb layers is strong evidence that NDR in these devices is due to transport through a light-hole-like resonance in the GaSb well, rather than simple ohmic conduction through the GaSb valence band that is eventually blocked by the GaSb band gap.

Another attractive feature of the BRIT device structure is the broadness of the transmission resonances. The width of a typical transmission resonance for a BRIT device corresponds to a quasi-bound state lifetime of a few tens of femtoseconds, compared to typical quasi-bound state lifetimes (i.e., tunneling times) of picoseconds or longer for typical double barrier structures.[19] These shorter lifetimes in BRIT structures suggest that limitations on device speed due to quantum well charging effects should be much less stringent for BRIT's than for conventional double barrier structures.

Variations of the BRIT structure in which intermediate layers of InAs or AlSb have been inserted in the GaSb layers, as shown in Figures 2(E) and 2(F), have also been

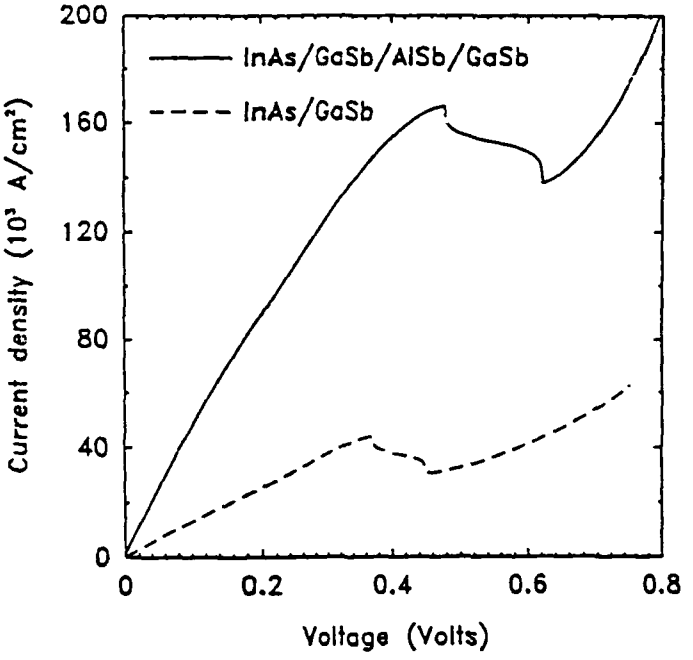

Fig. 8. Current-voltage characteristics for the structures shown in Fig. 2(G) (dashed line) and Fig. 2(H) (solid line).

studied both theoretically and experimentally. Results of this work will be reported elsewhere.[20]

n-InAs/p-GaSb Devices

The possibility of interband tunneling in the InAs/GaSb/AlSb material system leads very naturally to the device structure shown in Figure 2(G), which consists simply of an interface between n-type InAs and p-type GaSb, and which can be thought of as a heterojunction Esaki diode. This device, which works only in forward bias (i.e., positive voltage applied to the p-type GaSb layer), has yielded very respectable peak current densities (up to 8.4×10^4 A/cm^2 at 300 K) with peak-to-valley current ratios of 1.2 to 1.7. One advantage of this device structure is that, because a quasi-bound state resonance is not formed, speed limitations due to finite resonance lifetimes are eliminated.

InAs/GaSb/AlSb/GaSb and InAs/AlSb/InAs/GaSb Devices

A substantial improvement in the performance of the heterojunction Esaki diode can be achieved by inserting a thin AlSb barrier layer on either side of the InAs/GaSb interface. The AlSb barrier induces a resonance in either the GaSb valence band (for the structure in Figure 2(H)) or the InAs conduction band (Figure 2(I)). Because resonant transport in this structure requires that the InAs electron Fermi sea, the transmission resonance, and the GaSb hole Fermi sea all be aligned in energy, the performance of these devices is quite sensitive to the exact distance between the AlSb barrier and the InAs/GaSb interface. Simulations of these device structures have allowed us to achieve

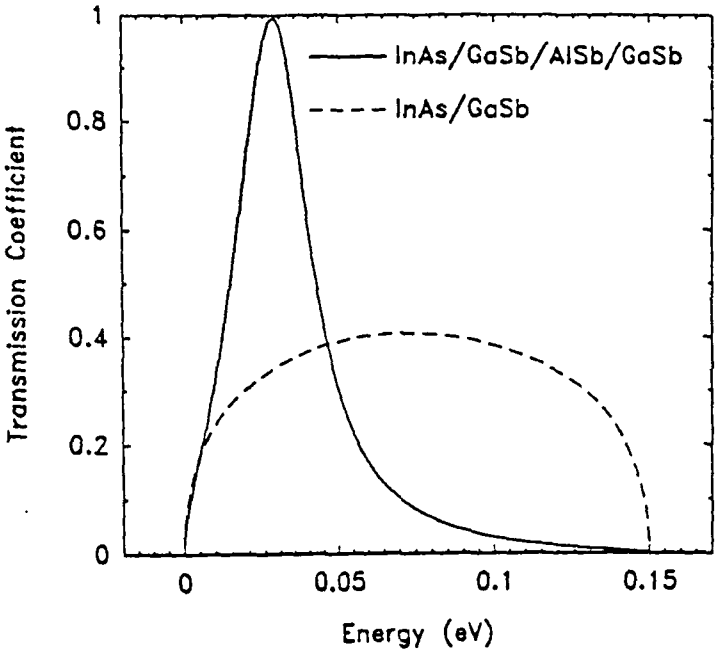

Fig. 9. Theoretical transmission coefficients for an InAs/GaSb/AlSb/GaSb structure (solid line) and for an InAs/GaSb structure (dashed line).

an approximate optimization of the peak current density as a function of the InAs or GaSb quantum well width. Figure 8 shows current–voltage characteristics for an InAs/GaSb/AlSb/GaSb structure and for a simple InAs/GaSb device. As shown in this figure, the introduction of the AlSb barrier layer increases the peak current density dramatically.

This effect can be understood if one examines the transmission coefficients for these two structures, shown in Figure 9. The smooth transmission coefficient for the n-InAs/p-GaSb structure is replaced by a broad resonance in the GaSb quantum well; this resonance is due to confinement from the AlSb barrier and from imperfect matching of GaSb valence band and InAs conduction band wave functions at the InAs/GaSb interface. Because of the finite widths of the Fermi seas of electrons in InAs and of holes in GaSb, the resonance in the InAs/GaSb/AlSb/GaSb structure is much more effective in allowing carriers to be transmitted across the device. Peak current densities as high as $1.6 \times 10^5 \mathrm{A/cm^2}$ have been achieved using the InAs/GaSb/AlSb/GaSb structure.

Three-Terminal Devices

Although two-terminal tunnel devices have been demonstrated in a number of applications, most notably high-frequency analog circuits,[15,17,21] a great deal of flexibility would be gained if three-terminal tunnel devices were available, and considerable effort has been expended in this area. Historically, the efforts to make three-terminal tunnel devices date to the pioneering work of Mead in the 1960's.[12] However, these devices were plagued with high base currents and low collector efficiencies. Based on these previously noted short comings, Bonnefoi and co-workers proposed inverting the gate

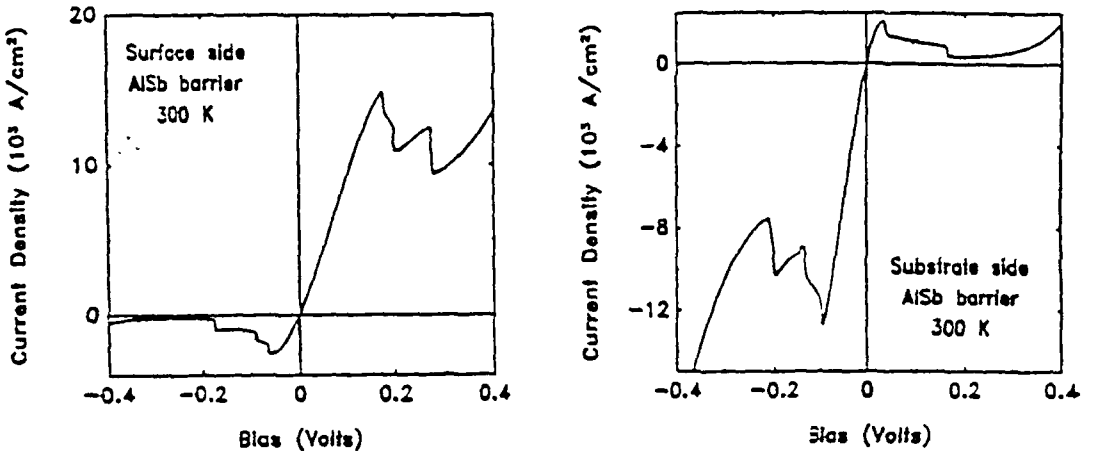

Fig. 10. Current-voltage characteristics for an InAs/AlSb/GaSb/InAs tunnel structure. Characteristics are shown for samples with (a) the AlSb barrier grown on top of the GaSb quantum well, and (b) the GaSb quantum well grown on top of the AlSb barrier.

and collector positions and using electric fields from the gate to modulate the emitter-collector current.[11] More recently, Mead's original structure has been revived by Schulman and Waldner,[13] with the additional concept of establishing two distributions of carriers in separated subbands — one to apply the potential and the other to carry the resonant current. We plan to pursue both of these concepts in the InAs/GaSb/AlSb material system. A basic device structure is shown in Figure 2(J). Our initial efforts involved studying the current-voltage characteristics of this structure as a standard two-terminal device. Typical current-voltage characteristics are shown in Figs. 10(a) and 10(b). A particularly notable aspect of these structures is the marked asymmetry in the current-voltage behavior between forward and reverse bias. The reproducibility of this asymmetry for samples with the AlSb barrier grown above and below the GaSb quantum well demonstrates that this phenomenon is an inherent feature of this device structure, and does not depend on growth sequence.

Three-terminal devices like that shown in Fig. 11, based on the structure in Figure 2(J), have also been fabricated. Preliminary results show that modulation of the emitter-collector current can be achieved by changing the bias on the base electrode. The prospects for fabricating three terminal devices in the InAs/GaSb/AlSb material system thus appear to be quite encouraging.

CONCLUSIONS

We have presented recent results for several different tunneling devices based on the InAs/GaSb/AlSb material system. These devices exhibit a wide range of peak current densities and peak-to-valley current ratios. Table I summarizes the results we have obtained from each structure. In addition, the InAs/AlSb double barrier structure has been shown to be capable of oscillation at the highest frequencies yet reported,

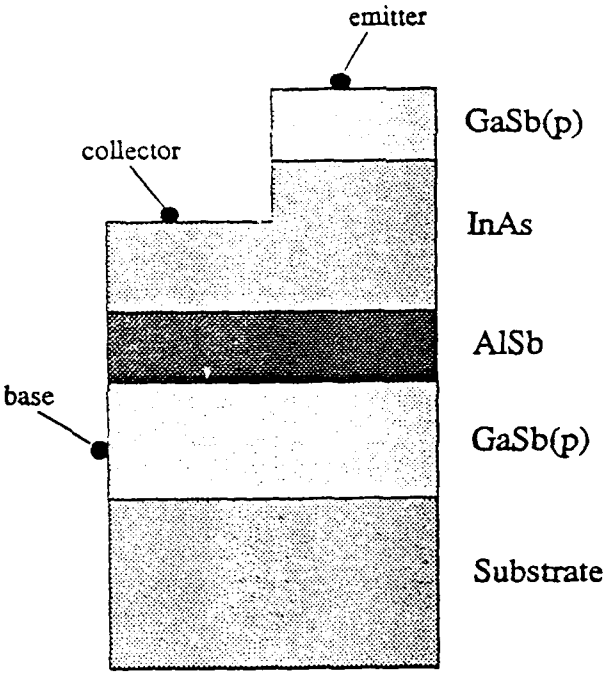

Fig. 11. A schematic layer diagram for a three terminal device. The ability to modulate the emitter-collector current through the bias on the base electrode has recently been demonstrated.

and several other device structures we have studied are expected, based on calculated resonance lifetimes, to be capable of operation at even higher frequencies. Preliminary results also suggest that this material system is extremely promising for the fabrication of three terminal tunnel devices.

ACKNOWLEDGEMENTS

The authors gratefully acknowledge helpful discussions with M. K. Jackson. Fabrication of the device structures and measurement of the DC and high-frequency behavior of the InAs/AlSb double barrier structures were carried out at Lincoln Laboratories by E. R. Brown. The support of the Office of Naval Research and the Air Force Office of Scientific Research under Grant Nos. N00014-89-J-1141 and AFOSR-86-0306, respectively, have made it possible for us to carry out this program. J.R. Söderström received financial support from The Sweden-America Foundation. E.T. Yu was supported in part by the AT& T Foundation. D.H. Chow was supported in part by Caltech's Program in Advanced Technologies, sponsored by Aerojet General, General Motors, and TRW.

REFERENCES

1. G.J. Gualtieri, G.P. Schwartz, R.G. Nuzzo, R.J. Malik, and J.F. Walker, "Determination of the (100) InAs/GaSb heterojunction valence–band discontinuity by x–ray photoemission core level spectroscopy," J. Appl. Phys., vol. 61, no. 12, pp. 5337–5341, 1987.
2. G.J. Gualtieri, G.P. Schwartz, R.G. Nuzzo, and W.A. Sunder, "X–ray photoemission core level determination of the GaSb/AlSb heterojunction valence–band discontinuity,"Appl. Phys. Lett., vol. 49, no. 16, pp. 1037–1039, 1986.
3. The value of the band offsets between InAs and AlSb have been derived using the transivity of the band offsets.
4. T.M. Rossi, D.A. Collins, D.H. Chow, and T.C. McGill, "P–type doping of gallium antimonide grown by molecular beam epitaxy using silicon," unpublished.
5. L.F. Luo, R. Beresford, and W.I. Wang, "Resonant tunneling in AlSb/InAs/AlSb double–barrier heterostructures," Appl. Phys. Lett. vol. 53, no. 23, pp. 2320–2322, 1988.
6. J.R. Söderström, D.H. Chow, and T.C. McGill, "InAs/AlSb double–barrier structure with large peak–to–valley current ratio: a candidate for high–frequency microwave devices," IEEE Elec. Dev. Lett., vol. 11, no. 1, pp. 27–29 1990.
7. J.R. Söderström, T.C. McGill, and E.R. Brown, unpublished.
8. M. Sweeny and J. Xu, "Resonant interband tunnel diodes," Appl. Phys. Lett., vol. 54, no. 6, pp. 546–548, 1989.
9. J.R. Söderström, D.H. Chow, and T.C. McGill, "New negative differential resistance device based on resonant interband tunneling," Appl. Phys. Lett., vol. 55, no. 11, pp. 1094–1096, 1989.
10. L.F. Luo, R. Beresford, and W.I. Wang, "Interband tunneling in polytype GaSb/AlSb/InAs heterostructures," Appl. Phys. Lett., vol. 55, no. 19, pp. 2023–2025, 1989.
11. A.R. Bonnefoi, D.H. Chow, and T.C. McGill, "Inverted base–collector tunnel transistors," Appl. Phys. Lett. 47, 888 (1985).
12. C.A. Mead, *IRE* 48, 359 (1960).
13. J. N. Schulman and M. Waldner, "Analysis of second level resonant tunneling diodes and transistors," J. Appl. Phys., vol. 63., pp. 2859 (1988).
14. D.H. Chow, J.R. Söderström, D.A. Collins, D.Z.-Y. Ting, E.T. Yu, and T.C. McGill, "Novel InAs/GaSb/AlSb tunnel structures," to appear in Proc. IEEE SPIE meeting, March 1990.
15. E.R. Brown, T.C.L.G. Sollner, C.D. Parker, W.D. Goodhue, and C.L. Chen, "Oscillations up to 420 GHz in GaAs/AlAs resonant tunneling diodes," Appl. Phys. Lett., vol. 55, no. 17, pp. 1777–1779, 1989.
16. S.K. Diamond, E. Özbay, M.J.W. Rodwell, D.M. Bloom, E. Wolak, and J.S. Harris,

"Fabrication of 200–GHz f_{max} resonant–tunneling diodes for integrated circuit and microwave applications," IEEE Elec. Dev. Lett., vol. 10, no. 3, pp. 104–106, 1989.

17. E. R. Brown, J. Söderström, and T. C. McGill, unpublished.
18. K. Taira, I. Hase, and H. Kawai, *Electronics Letters* **25**, 1708 (1989).
19. D.Z.-Y. Ting, E.T. Yu, D.A. Collins, D.H. Chow, and T.C. McGill, "Modeling of novel heterojunction tunnel structures," to appear in J. Vac. Sci. Technol., July/August 1990.
20. D. A. Collins and T.C. McGill, unpublished.
21. S.K. Diamond, E. Özbay, M.J.W. Rodwell, D.M. Bloom, Y.C. Pao, and J.S. Harris, "Resonant tunneling diodes for switching applications," Appl. Phys. Lett. **54**, 153 (1989).